

PHENOMENOLOGY OF EXTRA
DIMENSIONS

By

CORNELIU MARIUS RUJOIU

Bachelor of Science
Bucharest University
Bucharest, Romania
1997

Master of Science
Bucharest University
Bucharest, Romania
1998

Submitted to the Faculty of the
Graduate College of the
Oklahoma State University
in partial fulfillment of
the requirements for
the Degree of
DOCTOR OF PHILOSOPHY
July, 2006

PHENOMENOLOGY OF EXTRA DIMENSIONS

Thesis Approved:

Dr. S. Nandi

Thesis Advisor

Dr. K. S. Babu

Member

Dr. J. Mintmire

Member

Dr. J. Chandler

Outside Member

Dr. G. Emslie

Dean of the Graduate College

ACKNOWLEDGMENTS

I wish to express my gratitude to my advisor Prof. S. Nandi and to my collaborator and friend Dr. C. Macesanu for all the guidance, encouragement and patience shown while I was a Ph.D. student.

I would also like to extend my gratitude to my other committee members Prof. K. S. Babu, Prof. J. Mintmire, Prof. J. Chandler and Prof. B. Binengar, to the rest of the the members of the High Energy Physics group, to the Physics Department.

I want to thank also to the US Department of Energy for providing part of my financial support.

And last but by no means the least, many, many thanks to my family and friends from home for their support when I needed it the most.

TABLE OF CONTENTS

Chapter	Page
1. INTRODUCTION	1
2. STANDARD MODEL AND BEYOND	6
2.1. The Standard Model	6
2.2. Extra Dimensions	9
3. SINGLE KK PRODUCTION	14
3.1. Single KK production mediated by gravitons	14
3.1.1. Parton Processes and Amplitudes	15
3.1.2. Summed Propagator	18
3.1.3. Results	19
3.2. Single KK plus graviton production	27
3.2.1. Parton Processes and Amplitudes	28
3.2.2. Results	33
4. LEPTONS AND EXTRA DIMENSIONS	39
4.1. Current situation in lepton physics	39
4.2. Leptons in UED with fat branes	40
4.2.1. The Model	40
4.2.2. Results	48
5. CONCLUSIONS	51
BIBLIOGRAPHY	53
APPENDICES	56
APPENDIX A—Standard Model and Extra Dimensions	57
A.1. Standard Model particle content	57
A.2. Feynman rules for matter-gravity interactions	58
APPENDIX B—Single KK production	61

Chapter	Page
B.1. FORM program listing.....	61
B.2. Isajet code listing	66
B.3. Amplitudes squared and mediated for KK graviton plus a KK excitation production	67

LIST OF TABLES

Table	Page
A.1. Particle content of the Standard Model (SM).	57
A.2. Standard Model (SM) particle masses and electrical charges.....	58
A.3. The bilinear terms of the matter energy-momentum tensor in momentum representation.	59

LIST OF FIGURES

Figure	Page
2.1. The general matter-gravity interaction vertex.....	12
3.1. Proton-proton collisions creating KK plus SM as primary particles which in turn create two jets plus missing energy.....	15
3.2. Sub-processes creating a two jets plus missing energy signal.	16
3.3. Ratio of values for exact propagator versus analytic approximation, for $n = 6$ extra dimensions. Here $M_D = 10 \text{ TeV}$. Lines correspond to values for M of 1 TeV (straight) 2 TeV (dashed) and 5 TeV (dotted line). On the horizontal axis is $x = \text{sign}(s)\sqrt{ s }$	19
3.4. Production cross-sections at LHC (right) and Tevatron RunII (left) for $N = 2$ (straight line), 4 (dashed line) and 6 (dotted line) extra dimensions.	20
3.5. Cross section as function of cuts on the minimum p_T of jets (left) and missing energy \cancel{E}_T in an event (right). Straight and dashed line correspond to $M = 3 \text{ TeV}$ ($N = 2$ and $N = 6$ respectively) while dotted and dash-dotted lines correspond to $M = 5 \text{ TeV}$ (again, for $N = 2$ and $N = 6$).	21
3.6. Signal (left) and background (right) as a function of p_T^{cut} . The solid line corresponds to $n = 1$, the dashed one to $n = 2$ and the dotted one to $n = 3$. The rapidity and jet separation cuts are the ones mentioned in the text.	22
3.7. LHC reach for 20 and 100 signal events (straight and dotted lines corresponds to $N = 6$, and dashed and dot-dashed line correspond to $N = 2$, respectively). The cuts are the ones described in the text....	23
3.8. The production cross section for LHC using the following combined cuts: 1 TeV cut for the p_T of the two jets, 1 TeV for the \cancel{E}_T and a 10 TeV fundamental scale for gravity.....	24

Figure	Page
3.9. The production cross section for LHC using the following combined cuts: 1 <i>TeV</i> cut for the p_T of the two jets, 1 <i>TeV</i> for the \cancel{E}_T , 1 <i>TeV</i> for the invariant mass of the two jets and a 10 <i>TeV</i> fundamental scale for gravity.	25
3.10. The production cross section for LHC using the following combined cuts: 1 <i>TeV</i> cut for the p_T of the two jets, 1 <i>TeV</i> for the \cancel{E}_T , 1 <i>TeV</i> for the invariant mass of the two jets and a 5 <i>TeV</i> fundamental scale for gravity.	26
3.11. Proton-proton collisions creating KK plus graviton as primary particles which in turn create a jet plus a lot of missing energy.	27
3.12. Feynman diagrams contributing to the production of a g^* and a graviton KK excitation (either $h_{\mu\nu}$, $A_{\mu i}$ or Φ_{ij}) at hadron colliders.	28
3.13. The jet+ missing energy cross section from graviton and SM quark or gluon production at Tevatron Run II (left panel) and LHC (right panel). The solid, dashed and dotted lines correspond to $N = 2, 4$ and 6 extra dimensions.	34
3.14. Left panel: the jet+ missing energy cross section from graviton and KK quark or gluon production at LHC. The solid line corresponds to $N = 2$, while the dashed line corresponds to $N = 4$. Right panel: the distribution of the cross-section as a function of the cut imposed on the jet transverse momentum, for production of SM particle (solid line), and production of KK excitations with $m_{KK} = 2$ <i>TeV</i> (dashed line) and $m_{KK} = 3$ <i>TeV</i> (dotted line). M_D is taken 5 <i>TeV</i> for both panels.	35
3.15. Solid lines: the 5σ discovery reach at the LHC in the photon + \cancel{E}_T channel for $N = 2$ (left panel) and $N = 4$ (right panel). For values of $M_D, 1/R$ below the dashed lines, the KK quarks and gluons decay first to the LKP.	37
3.16. Left panel: the 5σ discovery reach at the LHC in the photon + \cancel{E}_T channel for $N = 6$. Right panel: the SM photon + \cancel{E}_T cross-section at the Tevatron Run II, with $p_T > 100$ <i>GeV</i> (solid, dashed and dotted lines correspond to $n = 2, 4$ and 6 extra dimensions respectively).	37

CHAPTER 1

INTRODUCTION

The appearance of the notion of extra dimensions in the high energy physics was motivated by the attempt to unify all the elementary particle interactions. Indeed, after the electricity and magnetism unification realized by Maxwell toward the end of the 19th century, together with the recognition of its special relativistic invariance observed later on, a quest for unifying the new found electromagnetism with the gravity started. After some early attempts [1] and after the publication of Einstein's general relativity, it came the turn of Theodor Kaluza to propose a unified theory based on a five-dimensional gravitational Einstein action [2]. The same theory was rediscovered independently five years later by Oskar Klein [3].

Then, for many years, the extra dimensions were abandoned in favor of the more successful four-dimensional theories which culminated with the appearance of the Standard Model (SM) of elementary particles [4]. To further hinder the development of the theories with more than four space-time dimensions was the impressive experimental confirmation of the SM predictions.

Although successful, SM leaves also a lot of questions unanswered. Why are the strengths of the gauge interactions so different at low energy scales? Why is the number of generations three? Where do the fermion masses come from? Why is the CP invariance broken? And those are only few of the questions SM fails to address. All the hints point to the fact that SM is just an effective theory valid at lower energies up to 246 *GeV*. Above that a more fundamental theory comes into place. Attempts to answer some of the above questions materialized in the appearance of the Grand Unified Theories (GUT). But GUTs too were formulated in a four-dimensional framework.

It was only recently realized, triggered by the appearance of the string theories, the true potential of the $4+N$ dimensional* description of the physical phenomena. As a parenthesis, we note that the recent theories (for example M-theory) require up to seven extra dimensions to consistently describe all the four known fundamental forces. Nowadays, along with the development of the theories including extra dimensions, phenomenological studies try to shed more light on what influence the existence of extra dimensions might have on the physics directly accessible to our experiments. One such study constitutes this thesis. It is worth mentioning that, although most of the phenomenological studies are based on simplified models of theories yet to be established, their main advantage is the fact that they investigate different ways to incorporate the idea of extra dimensions into some predictive models allowing for quantitative estimates. This in turn, allows for the planning of different discovery strategies of the extra dimensions.

Once one allows for the existence of extra dimensions, the next obvious question is how big those extra dimensions are? Here, mostly because of the lack of a compelling theory, there are several scenarios one can choose to follow. There are the possibilities that the extra dimensions are infinite in size [5], or that they have finite large sizes [6] and not all of them are equal [7].

Whether or not the extra dimensions are infinite or finite, flat [8] or compactified, the scenarios involving them have some common features. The ordinary four dimensional space is embedded in a higher dimensional $4+N$ space known as the "bulk". From the higher dimensional point of view then, our universe would appear as a four dimensional "brane" (in short, a 4D-brane). The higher dimensional brane is just an extension of the two dimensional notion of "membrane". Now, the brane itself can be infinitely thin or can be endowed with some thickness [9].

It is apparent now that as a function of what fields one allows to propagate in the bulk, the scenarios mentioned above give (if at all) different experimental signatures.

In the simplest case, the ADD scenario [5], only gravity propagates in the extra dimensions. Our universe is viewed as a 4D-brane embedded in the bigger $4+N$

*Here N stands for the number of extra dimensions one considers.

dimensional space. In this picture, matter fields and gauge bosons are confined to the 4D-brane, gravity is naturally weak because it is propagating in N extra compact dimensions, and the hierarchy problem is resolved by bringing the fundamental scale of gravity close to the electroweak scale according to the formula:

$$M_{Pl}^2 = M_D^{N+2} \left(\frac{R}{2\pi} \right)^N . \quad (1.1)$$

Here $M_{Pl} \simeq 10^{19} \text{ GeV}$ is the Plank scale in four dimensions, while M_D is the new fundamental scale of gravity in $4+N$ dimensions. One can see that with M_D of order TeV , one would obtain R as large as eV^{-1} (for $N = 2$) up to MeV^{-1} (for $N = 6$). A general feature of this type of models is the existence of the so called Kaluza-Klein (KK) towers of excited states of the graviton. We will introduce in a more appropriate way the KK excitations in the next chapter. For now suffice to say that the mass splitting between levels (KK excitations) is proportional to the inverse of the compactification radius $\Delta m \sim 1/R$.

Of course, one can construct extensions of the ADD model where matter fields are also allowed to propagate in extra dimensions [10]. Then ordinary matter will also have KK excitations with masses of order $1/R$. But no such excitations have been seen at colliders. So, one might conclude that R should be at least of inverse TeV order. However, we have to change our picture about gravity, then, by assuming either that the extra dimensions are asymmetrical (some of order inverse eV , in which only gravity propagate, and some of order inverse TeV , in which matter can also propagate) or, if we keep all compact dimensions of TeV^{-1} size, reintroducing some hierarchy between the gravity and electroweak scale. A better scenario is obtained if all matter fields are allowed to propagate small distances in extra dimensions*. One obtains then the universal extra dimensions (UED) [11] plus fat branes scenario. Precisely this is the model we used in this thesis. While in the standard UED scenario the first level of KK excitations is stable (due to KK number conservation and degeneracy at tree level), which means that they can be only pair-produced, adding the fat

*This is the equivalent of saying that the branes have now finite thickness with respect to the extra dimensions. Hence the name used in literature: "fat branes".

branes to UED allows, through matter-gravity interactions which break the KK number conservation, for the gravitational decay of the first level KK particles. Another interesting consequence is that in UED plus fat branes, gravitons can now mediate the production of single KK excitations. Associated with the single KK production comes the advantage of a bigger reach in mass for the experiments at present and future colliders. But there is also a disadvantage: the scale of the higher dimensional gravity should be low (order 10 TeV).

Now one can pause and wonder how is possible to even compare the gravitational interactions with the other three much stronger fundamental forces. Indeed, when one considers only the effect of an individual graviton, the effects are negligible compared to the other forces. But one must not forget that there is a large number of gravitons with increasing masses (eV to MeV spaced) contributing to the interactions below the typical TeV scale. And it is precisely this big number which ensures that the gravitational decay width is big enough so that the KK excitations will decay inside the detector. This is very important for the relevance of the results given in chapter three.

The present thesis contains five chapters; chapters three and four are based on the materials presented in three publications [12], [13], [14]. The second chapter is provided as a brief review on the Standard Model of the elementary particles. It also introduces the fundamental concepts and relations related to the extra dimensions. In the third chapter we will describe two different methods to search for extra dimensions at the present and future colliders. Both methods are applied in the context of the UED with fat branes. The first method correlates the the existence of the extra dimensions via gravity mediated processes with the characteristics of the two-jet plus missing energy signals. The second method analyzes the monojet plus missing energy signals coming from the production of a single KK excitation plus a graviton. The fourth chapter provides another method for testing the existence of the extra dimensions. This method is based on a variation of the model used in the third chapter and which allows for different generations of SM fermions to be localized on branes of different thickness. Although the phenomenological implications are

broader than that, this model is applied mostly to neutrino physics. The last chapter is reserved for conclusions.

CHAPTER 2

STANDARD MODEL AND BEYOND

This chapter is provided as a brief review of the Standard Model (SM) of the elementary particle physics. It is also meant to introduce the key concepts of the theories with extra dimensions.

2.1 The Standard Model

The Standard Model (SM) of elementary particle physics successfully describes the physics beyond atomic scales up to about 10^{-18} m. It is a non-abelian gauge theory based on the gauge group [15]

$$SU(3)_C \times SU(2)_L \times U(1)_Y,$$

where $SU(3)_C$ is the color gauge group describing strong interactions and $SU(2)_L \times U(1)_Y$ is the electroweak gauge group describing weak and electromagnetic interactions. The field content, the transformation properties under the gauge symmetries and the corresponding masses and charges [16] are shown in Table A.1 and Table A.2.

The $SU(3)_C$ gauge group of the strong interactions (also known as Quantum Chromodynamics, in short QCD) details the interaction between "colored"* quarks, antiquarks, and gluons. The QCD is a flavor-blind symmetry based on the following Lagrangian

*Please keep in mind that the term "color" denotes a quantum number, not an actual color although traditionally, the three fundamental "colors" for the quarks are taken to be "red", "green" and "blue". Regardless of the names one chooses to use, the three possible states form the fundamental representation of the $SU(3)_C$ symmetry group.

$$\mathcal{L}_{QCD} = -\frac{1}{4}F_{\mu\nu}^{(a)}F^{(a)\mu\nu} + \imath \sum_q \bar{\Psi}_q^i \gamma^\mu (D_\mu)_{ij} \Psi_q^j - \sum_q m_q \bar{\Psi}_q^i \Psi_{qi}, \quad (2.1)$$

$$F_{\mu\nu}^{(a)} = \partial_\mu A_\nu^a - \partial_\nu A_\mu^a - g_s f_{abc} A_\mu^b A_\nu^c, \quad (2.2)$$

$$(D_\mu)_{ij} = \delta_{ij} \partial_\mu + \imath g_s \sum_a \frac{\lambda_{i,j}^a}{2} A_\mu^a, \quad (2.3)$$

with g_s the strong coupling*, f_{abc} the structure constants, $\Psi_q^i(x)$ a 4-component Dirac spinor of color $i = 1 - 3$ and flavor $q = 1 - 6$, A_μ^a the Yang-Mills gluon field in the adjoint representation of the $SU(3)_C$ gauge group with $a = 1 - 8$. To the best of our knowledge, the color symmetry is an exact symmetry in nature. This means that the 8 gluons are massless. It worth mentioning that so far, all the experimentally observed hadrons are quark-antiquark (mesons) or three-quark (baryons) combinations in a color singlet configuration.

The electroweak interaction on the other hand, based on the gauge group $SU(2)_L \times U(1)_Y$, is not an exact symmetry of the nature. The electroweak gauge group is spontaneously broken down to $U(1)_{em}$. The Lagrangian describing this for the fermion fields is

$$\begin{aligned} \mathcal{L}_F &= \sum_i \bar{\Psi}_i \left(i\not{\partial} - m_i - \frac{gm_i H}{2M_W} \right) \Psi_i \\ &- \frac{g}{2\sqrt{2}} \sum_i \bar{\Psi}_i \gamma^\mu (1 - \gamma^5) (T^+ W_\mu^+ + T^- W_\mu^-) \Psi_i \\ &- e \sum_i \bar{\Psi}_i \gamma^\mu \Psi_i A_\mu \\ &- \frac{g}{2 \cos \theta_W} \sum_i \bar{\Psi}_i \gamma^\mu (g_V^i - g_A^i \gamma^5) \Psi_i Z_\mu, \end{aligned} \quad (2.4)$$

where $\Psi_i = \begin{pmatrix} \nu_i \\ l_i^- \end{pmatrix}, \begin{pmatrix} u_i \\ d_i' \end{pmatrix}$ is the left-handed fermionic field with $d' \equiv \sum_j V_{ij} d_j$ and V the Cabibbo-Kobayashi-Maskawa (CKM) matrix, $\theta_W \equiv \tan^{-1}(g'/g)$ is the weak

*The strong coupling g_s is dependent of the momentum transferred in the interaction process. In fact, all the SM gauge couplings depend on the momentum scale. Due to the nature of the gauge group, the strong coupling decreases as the momentum transferred increases; this phenomenon is the well known "asymptotic freedom" of the strong interaction.

angle, $e = g \sin \theta_W$ the positron charge, $A = B \cos \theta_W + W^3 \sin \theta_W$ the massless photon (B_μ is the gauge boson for $U(1)$ and W_μ^3 is one of the three gauge bosons for $SU(2)$). The rest of the fields in (2.4) are the massive charged $W^\pm \equiv (W^1 \mp iW^2)/\sqrt{2}$ and neutral $Z \equiv -B \sin \theta_W + W^3 \cos \theta_W$ weak bosons, and H is the physical neutral Higgs. T^+ and T^- are the weak isospin raising and lowering operators, g_V^i and g_A^i are the vector and axial-vector coupling

$$g_V^i \equiv t_{3L}(i) - 2q_i \sin^2 \theta_W, \quad (2.5)$$

$$g_A^i \equiv t_{3L}(i), \quad (2.6)$$

with $t_{3L}(i)$ the weak isospin and q_i the charge of the fermion i .

The electric charge Q_{em} , the $U(1)_Y$ hypercharge and the third component of weak isospin T_{3L} are related by

$$Q_{em} = T_{3L} + \frac{Y}{2}. \quad (2.7)$$

One important thing about the electroweak interactions is that the left and the right handed components of the fermions are in different representations (doublets and singlets respectively) of the weak gauge group $SU(2)_L$ giving a chiral structure to the SM. This will prove to be an important constrain for any theory involving extra dimensions because the $4 + N$ dimensional theories, where N is odd, have an inherent vector-like character. If one is to start with a multi-dimensional theory or model, one must make sure that, after dimensional reduction, the remaining effective 4-dimensional theory is chiral.

The rest of the SM Lagrangian describes the interactions of the Higgs boson with the fermions (Yukawa) and the gauge bosons.

The Yukawa part of the SM Lagrangian is given by

$$\mathcal{L}_{Yukawa} = Y_{\alpha\beta}^\ell \ell_\alpha e_\beta^c \tilde{\phi} + Y_{\alpha\beta}^d Q_\alpha d_\beta^c \tilde{\phi} + Y_{\alpha\beta}^u Q_\alpha u_\beta^c \phi + \text{h.c.}, \quad (2.8)$$

where $\phi = \begin{pmatrix} \phi^+ \\ \phi^0 \end{pmatrix}$ is the scalar Higgs doublet responsible for the spontaneous symmetry breaking of $SU(2)_L \times U(1)_Y \rightarrow U(1)_{em}$, $\tilde{\phi} = i\sigma^2 \phi^* = \begin{pmatrix} \bar{\phi}^0 \\ -\phi^- \end{pmatrix}$, $\alpha, \beta = \overline{1, 3}$ the

generation indices and Y 's the Yukawa matrices. Note that there is no mass for the neutrinos in the SM due to the absence of the corresponding right-handed singlets.

After symmetry breaking and from the Yukawa interactions in (2.8), the fermions acquire masses

$$M_u = Y_u v, \quad M_d = Y_d v, \quad M_\ell = Y_\ell v. \quad (2.9)$$

Here $Y_{u,d,\ell}$ are arbitrary 3×3 complex matrices in generation space. Note that the mass terms for the fermions in (2.4) comes from this spontaneous symmetry breaking.

The Lagrangian for the gauge-Higgs interactions is

$$\mathcal{L}_{gauge-Higgs} = \left| \partial_\mu \phi - \frac{ig}{2} \vec{\tau} \cdot \vec{W}_\mu \phi - \frac{ig'}{2} B_\mu \phi \right|^2. \quad (2.10)$$

If one chooses the vacuum expectation value (vev) for the Higgs field of the form

$$\langle \phi_0 \rangle = \frac{1}{\sqrt{2}} \begin{pmatrix} 0 \\ v \end{pmatrix}. \quad (2.11)$$

then the masses for the weak gauge bosons from (2.4) are

$$M_W = \frac{gv}{2}, \quad M_Z = \frac{M_W}{\cos \theta_W}, \quad M_A = 0, \quad (2.12)$$

where A is the photon field, g is the $SU(2)_L$ gauge coupling strength, $\tan \theta_W = g'/g$ and g' is the $U(1)_Y$ gauge coupling constant.

After this brief review of the SM, it is now time to introduce the formalism related to extra dimensions. We will achieve this in the next section.

2.2 Extra Dimensions

As mentioned before, the universal treatment based on the non-abelian gauge theory $SU(3)_C \times SU(2)_L \times U(1)_Y$, for the strong, electromagnetic and weak forces provided by the SM of elementary particles is quite successful. It is only natural to try to incorporate the notion of extra dimensions into it first. So let us first define the theoretical framework used in this thesis. In the scenario envisioned in this thesis,

matter (the SM content) propagates in one* extra dimension compactified in an S_1/Z_2 orbifold† of radius R of order inverse TeV .

In general, with respect to the compact extra dimension, one can write the following Fourier expansions for the SM fields (fermions, scalars and gauge bosons) correct up to a normalization constant:

$$\begin{aligned}
Q &= Q_L + \sum_{n=1}^{\infty} \left[Q_L^n \cos\left(\frac{ny}{R}\right) + Q_L^n \sin\left(\frac{ny}{R}\right) \right] \\
&+ Q_R + \sum_{n=1}^{\infty} \left[Q_R^n \cos\left(\frac{ny}{R}\right) + Q_R^n \sin\left(\frac{ny}{R}\right) \right], \\
q &= q_L + \sum_{n=1}^{\infty} \left[q_L^n \cos\left(\frac{ny}{R}\right) + q_L^n \sin\left(\frac{ny}{R}\right) \right] \\
&+ q_R + \sum_{n=1}^{\infty} \left[q_R^n \cos\left(\frac{ny}{R}\right) + q_R^n \sin\left(\frac{ny}{R}\right) \right], \\
(\Phi, B_\mu^a) &= (\Phi_0, B_{\mu,0}^a) + \sum_{n=1}^{\infty} \left[(\Phi_n, B_{\mu,n}^a) \cos\left(\frac{ny}{R}\right) + (\Phi_n, B_{\mu,n}^a) \sin\left(\frac{ny}{R}\right) \right]. \quad (2.13)
\end{aligned}$$

Here $Q(q)$ is the 5D fermionic doublet(singlet) under $SU(2)$ whose zero mode is the usual SM fermionic doublet(singlet); Φ is the scalar field (Higgs) and B_μ^a are the vector (gauge) fields. We work in a gauge where $B_5^a = 0$ [17, 18]. Assigning the following parities under the $Z_2(y \rightarrow -y)$ symmetry for the fields in (2.13):

$$Q_L(x, y) = Q_L(x, -y), \quad Q_R(x, y) = -Q_R(x, -y), \quad B_\mu^a(x, y) = B_\mu^a(x, -y), \quad (2.14)$$

one remains with the correct chiral content for the SM zero modes particles. The expansions from (2.13) will then become (this time, the normalized wave functions are given) [19]:

$$\begin{aligned}
Q &= \frac{1}{\sqrt{\pi R}} \left\{ Q_L + \sqrt{2} \sum_{n=1}^{\infty} \left[Q_L^n \cos\left(\frac{ny}{R}\right) + Q_R^n \sin\left(\frac{ny}{R}\right) \right] \right\}, \\
q &= \frac{1}{\sqrt{\pi R}} \left\{ q_R + \sqrt{2} \sum_{n=1}^{\infty} \left[q_R^n \cos\left(\frac{ny}{R}\right) + q_L^n \sin\left(\frac{ny}{R}\right) \right] \right\},
\end{aligned}$$

*The extrapolation of our results to more than one extra dimension, although straightforward, is more involved.

†An approximate definition for orbifold is: a topologically smooth space with some singularities(edges and sharp points).

$$(\Phi, B_\mu^a) = \frac{1}{\sqrt{\pi R}} \left[(\Phi_0, B_{\mu,0}^a) + \sqrt{2} \sum_{n=1}^{\infty} (\Phi_n, B_{\mu,n}^a) \cos\left(\frac{ny}{R}\right) \right]. \quad (2.15)$$

Note that we obtain two towers of KK excitations for each fermion of any flavor and that the spacing between adjacent levels is indeed of order $1/R$. Gravity, on the other hand, is not affected in any way by orbifolding. So the following expansion over the N extra dimensions in which only gravity propagates holds true:

$$\hat{h}_{\hat{\mu}\hat{\nu}}(x, y) = \sum_{\vec{n}} \hat{h}_{\hat{\mu}\hat{\nu}}^{\vec{n}}(x) \exp\left(i \frac{2\pi \vec{n} \cdot \vec{y}}{r}\right). \quad (2.16)$$

We assume that the N extra dimensions can have radii r as large as eV^{-1} ; the radius r of these extra dimensions is given in terms of the fundamental Plank scale M_D by the ADD relation (1.1).

The ‘hat’ denotes quantities which live in $4+N$ dimensions: $\hat{\mu}, \hat{\nu} = 0, \dots, 3, \dots, 4+N$, while $\mu, \nu = 0, \dots, 3$. At each KK level we have the decomposition of the $\hat{h}_{\hat{\mu}\hat{\nu}}$ field ($(N+2)(N+3)/2 - 1$ d.o.f.) into 4D tensor $h_{\mu\nu}$ (5 d.o.f), vector $A_{\mu i}$ ($3 * (N-1)$ d.o.f.) and scalar ϕ_{ij} ($N(N-1)/2$ d.o.f) components by:

$$\hat{h}_{\hat{\mu}\hat{\nu}}^{\vec{n}} = V_N^{-1/2} \begin{pmatrix} h_{\mu\nu}^{\vec{n}} + \eta_{\mu\nu} \phi^{\vec{n}} & A_{\mu i}^{\vec{n}} \\ A_{\nu j}^{\vec{n}} & 2\phi_{ij}^{\vec{n}} \end{pmatrix} \quad (2.17)$$

where $V_N = (2\pi r)^N$ is the volume of the N -dimensional torus.

For completion, we mention here that the fields in (2.17) obey also the following relations:

$$\partial^{\hat{\mu}} \left(\hat{h}_{\hat{\mu}\hat{\nu}} - \frac{1}{2} \hat{\eta}_{\hat{\mu}\hat{\nu}} \hat{h} \right) = 0, \quad n_i A_{\mu i}^{\vec{n}} = 0, \quad n_i \phi_{ij}^{\vec{n}} = 0. \quad (2.18)$$

The above relations take care of the extra internal degrees of freedom of the $4+N$ dimensional graviton. Having introduced the main ingredients of our model, the matter and the gravity, it is time now to describe the way they interact.

In general, one can write the following N dimensional action describing the fact that matter propagates only a limited distance in the fifth dimension while gravity propagates in all N extra dimensions without restrictions [20]:

$$\mathcal{S}_{int} = -\frac{\hat{\kappa}}{2} \int d^5 x \delta(x^6) \dots \delta(x^N) \hat{h}^{\hat{\mu}\hat{\nu}} T_{\hat{\mu}\hat{\nu}}, \quad (2.19)$$

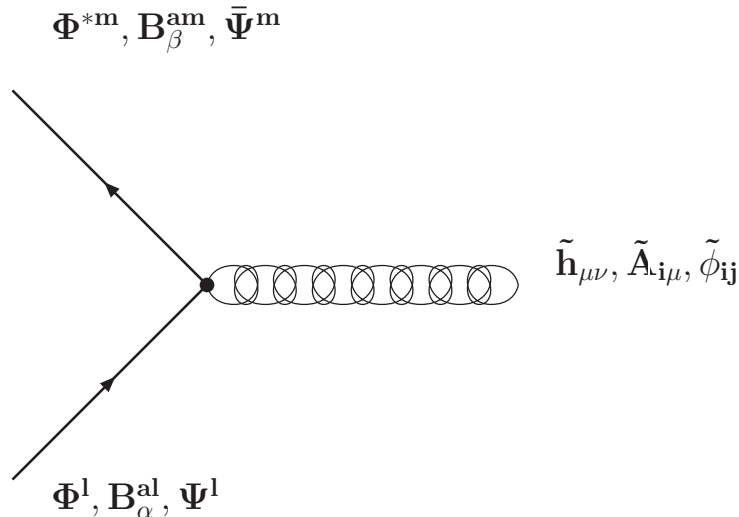


Figure 2.1. The general matter-gravity interaction vertex.

with $T_{\hat{\mu}\hat{\nu}}$ the energy-momentum tensor of the 5D matter and $\hat{\kappa}$ the strength of the $4 + N$ gravitational coupling (related to the 4D one by $\kappa = \hat{\kappa}V_N^{-1/2}$).

From (2.16), (2.17) and (2.19) one then obtains*:

$$\mathcal{S}_{int} = -\frac{\hat{\kappa}}{2} \int d^4x \int_0^{\pi R} dy \sum_{\vec{n}} [(h_{\mu\nu}^{\vec{n}} + \eta_{\mu\nu}\phi^{\vec{n}}) T_{\mu\nu} - 2A_{\mu 5}^{\vec{n}} T_5^{\mu} + 2\phi_{55}^{\vec{n}} T_{55}] e^{\frac{2\pi i(n_5 y)}{r}}. \quad (2.20)$$

Assuming a decomposition of the following from for the energy-momentum tensor

$$T^{\mu\nu}(x, y) = \sum_{l,m} T_{lm}^{\mu\nu}(x) (\cos, \sin)\left(\frac{ly}{R}\right) (\cos, \sin)\left(\frac{my}{R}\right) \quad (2.21)$$

with respect to the fifth dimension, the Feynman rules [21] are similar to those for matter propagating in four dimensions only [20]. However, the vertex is multiplied by a form-factor [19, 22] which will prove important for some of our results :

$$\mathcal{F}_{lm|n}^{(c,s)} \sim \frac{1}{\pi R} \int_0^{\pi R} dy (\cos, \sin)\left(\frac{ly}{R}\right) (\cos, \sin)\left(\frac{my}{R}\right) \exp\left(2\pi i \frac{ny}{r}\right) \quad (2.22)$$

The form factor from (2.22) reflects the overlap of the graviton and matter wave functions in the fifth dimension. It is just an example meant to illustrate the change

*Note that we neglected so far any brane effects. That will no longer be the case for the results obtained in section 3.2

from the model in [20]. To understand its origin, consider the general vertex depicted in Fig. 2.1 involving the l^{th} level of an incoming KK excitation radiating a graviton and thus becoming an m^{th} level outgoing KK excitation.

The first factor under the integral (2.22) is coming precisely from the KK expansion of the incoming field. The second is due to the KK expansion of the outgoing field. Finally, the last term originated from the expansion of the graviton field. A short summary of the Feynman rules is given in Appendix A.2 following the notation conventions from [21].

Having briefly reviewed the basic notions we will use in the next chapters, it is time now to present the results we obtained when using the UED plus fat branes scenario.

CHAPTER 3

SINGLE KK PRODUCTION

This chapter is dedicated to the possible production of single KK excitations at the hadron colliders experiments. We analyze the production of single KK excitations at the present and future hadron colliders. The big advantage in doing this, when compared to pair production of KK excited states, is the bigger reach in mass. But, there is also a disadvantage. The scale of the higher dimensional gravity should be low (order 10 TeV)*.

At the time this thesis was written, recent results gave as lower limits for the $1/R$ of one extra dimension (in the UED scenario) values ranging from 400 to 600 GeV depending on the assumed values for m_t and m_H [23]. The quoted values are already within the reach of the Tevatron.

In this chapter, the quantity of interest for us is the cross-section. We compute it in the usual way according to the formula:

$$\sigma_{AB} = \sum_{ab} \int f_{a/A}(x_1, Q^2) \cdot f_{b/B}(x_2, Q^2) \cdot \hat{\sigma}_{ab} \cdot dx_1 dx_2. \quad (3.1)$$

The small letters (a, b) designate the partons and the capital ones (A, B) the parent protons (LHC) or the parent proton and anti-proton (Tevatron).

3.1 Single KK production mediated by gravitons

The big advantage of the UED plus fat brane scenario resides in the possibility for the KK excitations to decay to SM particles by radiating gravitons. The KK number-conservation is broken by the interactions between matter and gravity.

*As we will show later on, the cross section is proportional to M_D^{-10} .

Because we have a big number of gravitons with masses smaller than a TeV , the gravitational decay width is big enough to ensure that the decay happens in the detector. Thus, the experimental signature of a decaying KK excitation would be a jet plus missing energy carried away by the graviton escaping detection. In Fig. 3.1 is schematically depicted such a process [12].

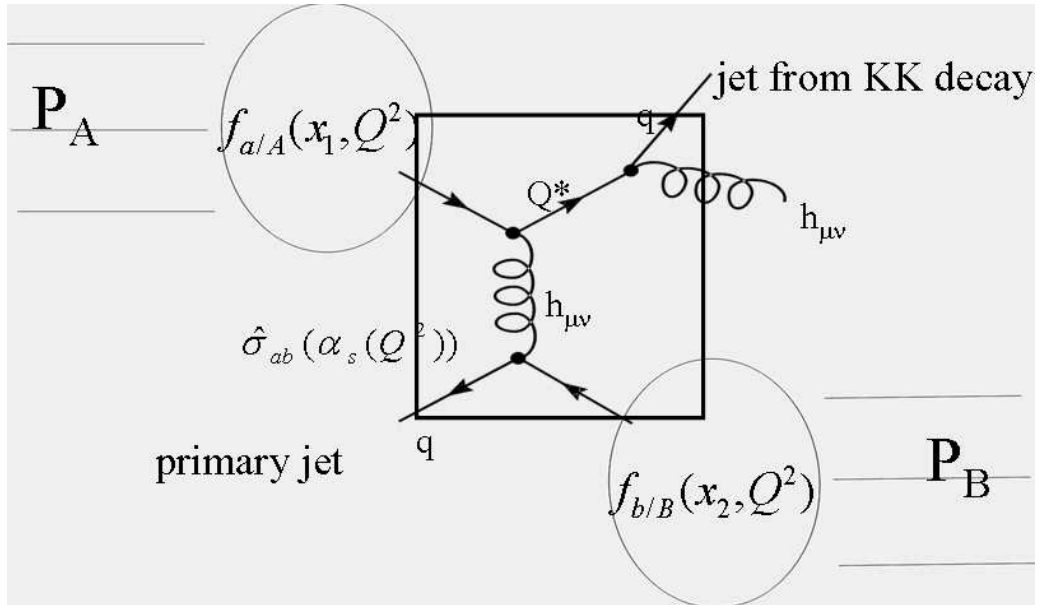


Figure 3.1. Proton-proton collisions creating KK plus SM as primary particles which in turn create two jets plus missing energy.

Since in this section we discuss the production of KK plus SM particle, the experimental signature of this process would be two jets plus missing energy.

In the following subsections we discuss some of the details of the computations.

3.1.1 Parton Processes and Amplitudes

The partonic processes (classified by the initial state) contributing to the desired experimental signal are given in Fig. 3.2.

Notice that there are no gravitons on the external lines. In all, there are 22 diagrams considered.

In order to compute the squared matrix elements for the sub-processes from Fig. 3.2, we used the Jos Vermaseren's FORM [24]. FORM is a symbolic computation

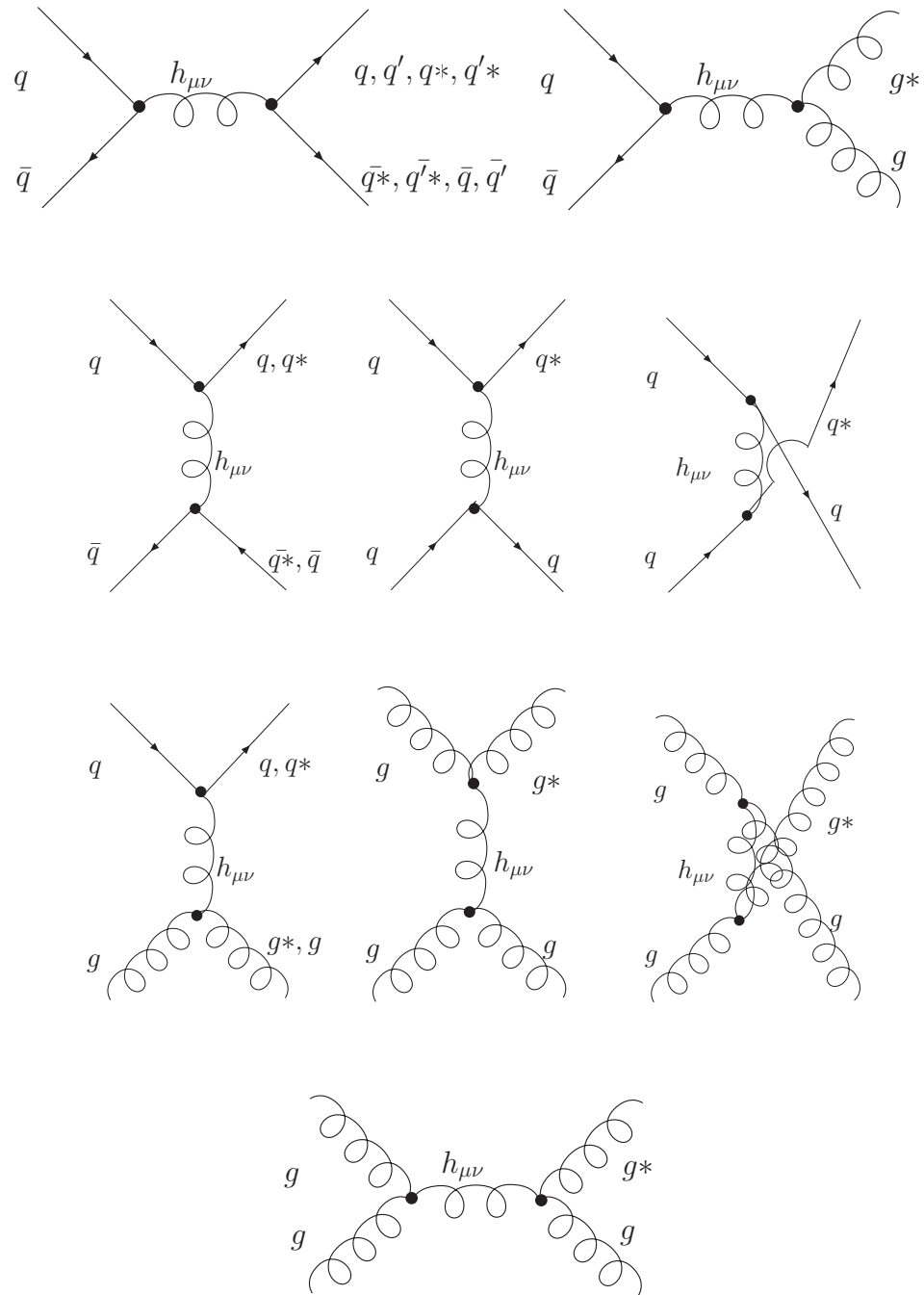


Figure 3.2. Sub-processes creating a two jets plus missing energy signal.

program optimized for handling huge computations in reasonably short time intervals. Pre-compiled binaries are available free from the web. In the appendix we give as an example a listing of such a program.

We use modified Mandelstam variables as follows:

$$s = 2p_1p_2, \quad t = -2p_1p_3, \quad u = -2p_1p_4$$

with p_1, p_2 the momenta of the initial state partons and p_3, p_4 for the momenta of the final state ones. We also use the notation $D(s), D(t)$ and $D(u)$ for the summed graviton propagators (see next section) in the s, t and u channels. A "*" will denote the KK excitation. With the notations above, the matrix elements squared are:

1. for $q\bar{q} \rightarrow g^*g$ (s channel only):

$$\sum_{\bar{}} |M(q\bar{q} \rightarrow g^*g)|^2 = \frac{1}{3}tu(t^2 + u^2) * Ds^2$$

2. for $gg \rightarrow g^*g$ (s, t and u channels):

$$\sum_{\bar{}} |M(gg \rightarrow g^*g)|^2 = \frac{1}{18}[(t^4 + u^4) * Ds^2 + (s^4 + u^4) * Dt^2 + (s^4 + t^4) * Du^2 + 2u^4 * Ds * Dt + 2t^4 * Ds * Du + 2s^4 * Du * Dt]$$

3. for $qg \rightarrow qg^*$ and $\bar{q}g \rightarrow \bar{q}g^*$ (t channel only):

$$\sum_{\bar{}} |M(qg \rightarrow qg^*)|^2 = -\frac{1}{12}su(s^2 + u^2) * Dt^2$$

4. for $gg \rightarrow q^*\bar{q}$ (s channel):

$$\sum_{\bar{}} |M(gg \rightarrow q^*\bar{q})|^2 = \frac{1}{96}tu(t^2 + u^2) * Ds^2$$

5. for $q\bar{q} \rightarrow q^*\bar{q}$ and $q\bar{q} \rightarrow q\bar{q}^*$:

$$\sum_{\bar{}} |M(q\bar{q} \rightarrow q^*\bar{q})|^2 = \frac{1}{256}[(s^4 - 10s^2tu + 32t^2u^2) * Ds^2 + (t^4 - 10t^2su + 32s^2u^2) * Dt^2 - 2u^2(4u^2 + 9st) * Ds * Dt]$$

6. for $qq \rightarrow q^*q$ and $\bar{q}\bar{q} \rightarrow \bar{q}^*\bar{q}$:

$$\sum_{\bar{}} |M(qq \rightarrow q^*q)|^2 = \frac{1}{256}[(t^4 - 10t^2su + 32s^2u^2) * Dt^2 + (u^4 - 10u^2st + 32s^2t^2) * Du^2 - 2s^2(4s^2 + 9tu) * Dt * Du]$$

7. for $qg \rightarrow q^*g$:

$$\sum_{\bar{}} |M(qg \rightarrow q^*g)|^2 = -\frac{1}{24}su(s^2 + u^2) * Dt^2$$

The averaged squared matrix elements for scattering processes involving different flavor quarks in the initial state ($q\bar{q}' \rightarrow q^*\bar{q}'$ and $qq' \rightarrow q^*q'$) are given by the t channel contributions only from the corresponding expressions (5) and (6) above.

3.1.2 Summed Propagator

The effective propagator for gravity mediated KK production is obtained by summing over all graviton excitations up to a cut-off M_D . Thus,

$$D(s) = \kappa^2 \sum_{\vec{n}} F_{00|n_5} \frac{i}{s - m_{\vec{n}}^2} (F_{10|n_5}^c)^*, \quad (3.2)$$

where $\kappa = \sqrt{16\pi/M_{Pl}^2}$ is the 4D gravitational coupling constant, and $F_{00|n_5}$ and $F_{10|n_5}^c$ are form factors describing the interaction of the gravitons with the matter excitations on the brane [21]. Note that terms in numerator of the propagator for a single graviton proportional to p^μ, p^ν [20] drop out due to the fact that one end of the propagator couples always to two massless fermions*. Hence the Lorenz structure of the propagator for the spin 2 massive graviton is simply:

$$B(k)_{\mu\nu,\rho\sigma} = \left(\eta_{\mu\rho}\eta_{\nu\sigma} + \eta_{\mu\sigma}\eta_{\nu\rho} - \frac{2}{3}\eta_{\mu\nu}\eta_{\rho\sigma} \right) D(k^2) .$$

In the limit where $s, M \ll M_D$, the sum (3.2) has been evaluated in [21]:

$$D(s) \simeq V_{N-1} \frac{16}{N-3} \frac{M}{M_D^5} \frac{2\sqrt{2}}{\pi^2} \int_0^{\pi M_s/M} \frac{\sin x}{1 - x^2/\pi^2} dx . \quad (3.3)$$

In the computations of this chapter, (3.2) was evaluated numerically for each value of s and M_D and it turned out that the approximate result (3.3) is reasonably accurate, except for the cases $N = 2, 3$ (when it is not applicable).

In Fig. 3.3 we print the ratio between the exact summed propagator (obtained by numerical integration) and the analytic approximation (3.3); negative values of s are applicable for the case of t and u channel scattering.

As an example, in the following formulas i will give the expressions for the exact summed propagator we integrated. We considered matter propagating in one extra dimension and gravity propagating in two. For the case $m_5^2 < s$ we have:

$$I_1(m_5^2 < s) = \int_0^{\sqrt{s}-\epsilon} dm_5 \frac{\sqrt{2}t \sin(\pi m_5/M)}{\pi^2 [1 - (m_5/M)^2]} \frac{\ln\left(\frac{\sqrt{M_s^2 - m_5^2} + \sqrt{s - m_5^2}}{\sqrt{M_s^2 - m_5^2} - \sqrt{s - m_5^2}}\right)}{\sqrt{s - m_5^2}}, \quad (3.4)$$

while for $m_5^2 > s$ we have:

*The amplitude is proportional to $T_{00}^{\mu\nu} B_{\mu\nu,\rho\sigma} T_{10}^{\rho\sigma}$.

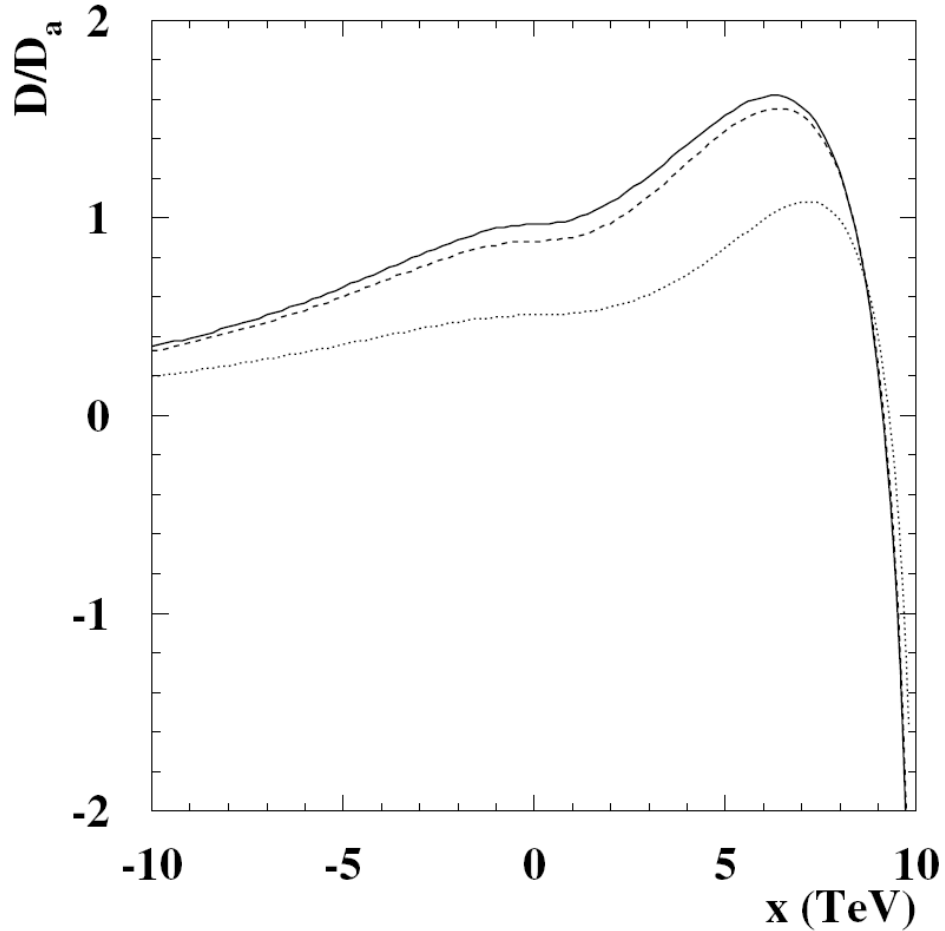


Figure 3.3. Ratio of values for exact propagator versus analytic approximation, for $n = 6$ extra dimensions. Here $M_D = 10 \text{ TeV}$. Lines correspond to values for M of 1 TeV (straight) 2 TeV (dashed) and 5 TeV (dotted line). On the horizontal axis is $x = \text{sign}(s)\sqrt{|s|}$.

$$I_2(m_5^2 > s) = \int_{\sqrt{s+\epsilon}}^{M_s} dm_5 \frac{\sqrt{2}t \sin(\pi m_5/M) \arctan\left(\frac{\sqrt{M_s^2 - m_5^2}}{\sqrt{m_5^2 - s}}\right)}{\pi^2 [1 - (m_5/M)^2] \sqrt{m_5^2 - s}}, \quad (3.5)$$

Having clarified the details related to the summed propagator, we will now move to presenting the results of our computations.

3.1.3 Results

The model under investigation has only three parameters: the fundamental Plank scale M_D , the mass of the KK excitation and the number of extra dimensions

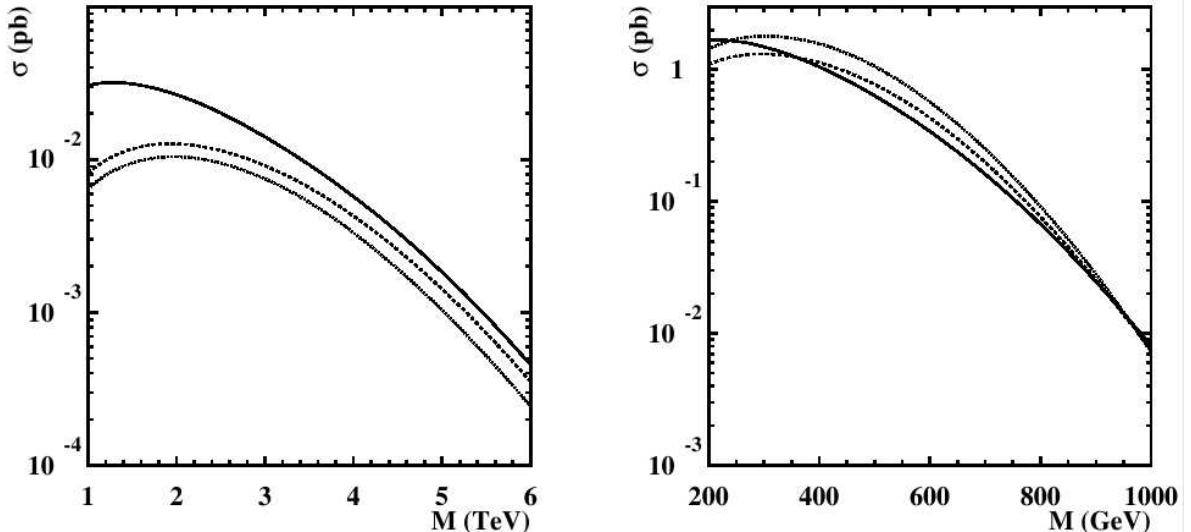


Figure 3.4. Production cross-sections at LHC (right) and Tevatron RunII (left) for $N = 2$ (straight line), 4 (dashed line) and 6 (dotted line) extra dimensions.

N . From the approximate relation (3.3) one can see that the cross-section is very sensitive to the value one uses for M_D and it scales roughly as $1/M_D^{10}$. In Fig. 3.4 we give the gravity mediated production cross-sections for a KK excitation assuming a fundamental Planck scale $M_D = 10 \text{ TeV}$ for LHC and $M_D = 1.5 \text{ TeV}$ for Tevatron.

The SM background of this process is given by events like $Z + 2$ jets processes (where Z decays to $\nu\bar{\nu}$ or $\tau\bar{\tau}$ pairs), $W + 2$ jets (with the lepton from the W decay unidentifiable), $t\bar{t}$ production, with one top decaying to $b\bar{\nu}l$ and unidentified lepton and jets, and QCD multijet production with mismeasured \cancel{E}_T . To eliminate this background, one must impose cuts on the jets. The effect of such cuts on the signal of interest is given in Fig. 3.5. Due to the large mass of the produced KK particle, the transverse momentum of the jets is quite large.

By requiring a large transverse momentum for the two jets ($p_{1T}, p_{2T} > p_T^{cut}$) and a large transverse missing energy ($\cancel{E}_T > np_T^{cut}, n = 1, 2, \dots$) one can then obtain presumably a good signal over the background. In our computations we analyzed also the effect of some other cuts over the signal. Included in our results is a rapidity cut of $|y| < 4$ and a requirement that the two observed jets are separated by a cone

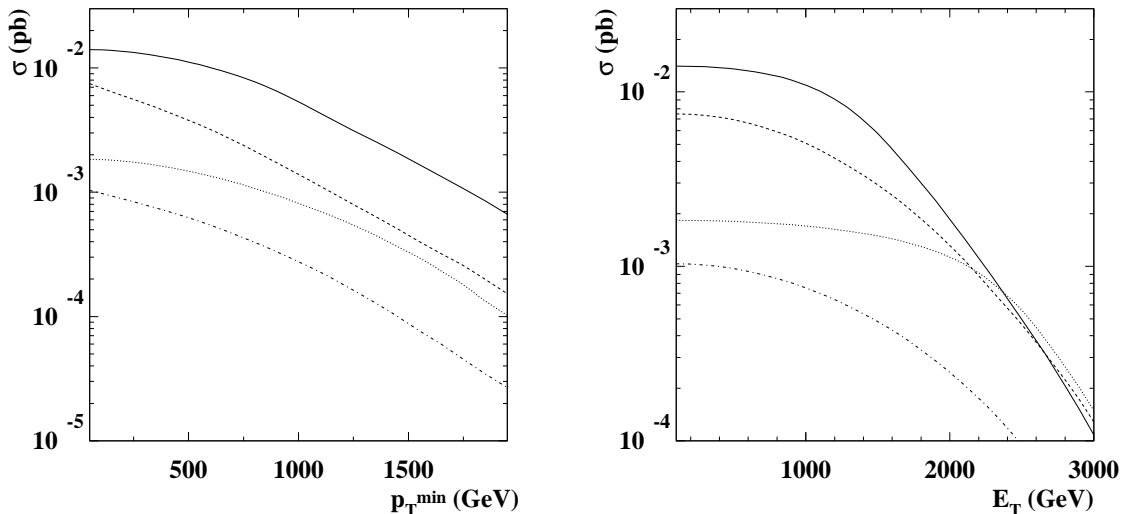


Figure 3.5. Cross section as function of cuts on the minimum p_T of jets (left) and missing energy \cancel{E}_T in an event (right). Straight and dashed line correspond to $M = 3 \text{ TeV}$ ($N = 2$ and $N = 6$ respectively) while dotted and dash-dotted lines correspond to $M = 5 \text{ TeV}$ (again, for $N = 2$ and $N = 6$).

with $R = \sqrt{\Delta\phi^2 + \Delta\eta^2} > 0.4$. As a function of the transverse momentum and taking $M = 3 \text{ TeV}$, $M_D = 10 \text{ TeV}$ and $N = 6$, one then obtains the results from Fig. 3.6 (left).

It is shown in literature [25] for example that for $n = 1$ and $p_T^{cut} > 400 \text{ GeV}$ the main backgrounds coming from $Z + 2$ jets and from mismeasured QCD processes are about the same. But one expects that as the cuts get harder, the QCD background of mismeasured events will decrease faster than the one from $Z + 2$ jets [26]. That being the case, for high enough p_T cuts, we will effectively have only the background given by the $Z + 2$ jets events. This background can be evaluated at parton level using for example MadEvent generator [27]. In Fig. 3.6 (right) we give the dependence of this background on the p_T^{cut} . From the figure, one can see that by demanding a number of 10 events for the background, for an LHC integrated luminosity of 100 fb^{-1} , there are two possible sets of cuts satisfying the requirements. We will use those cuts in the next figure.

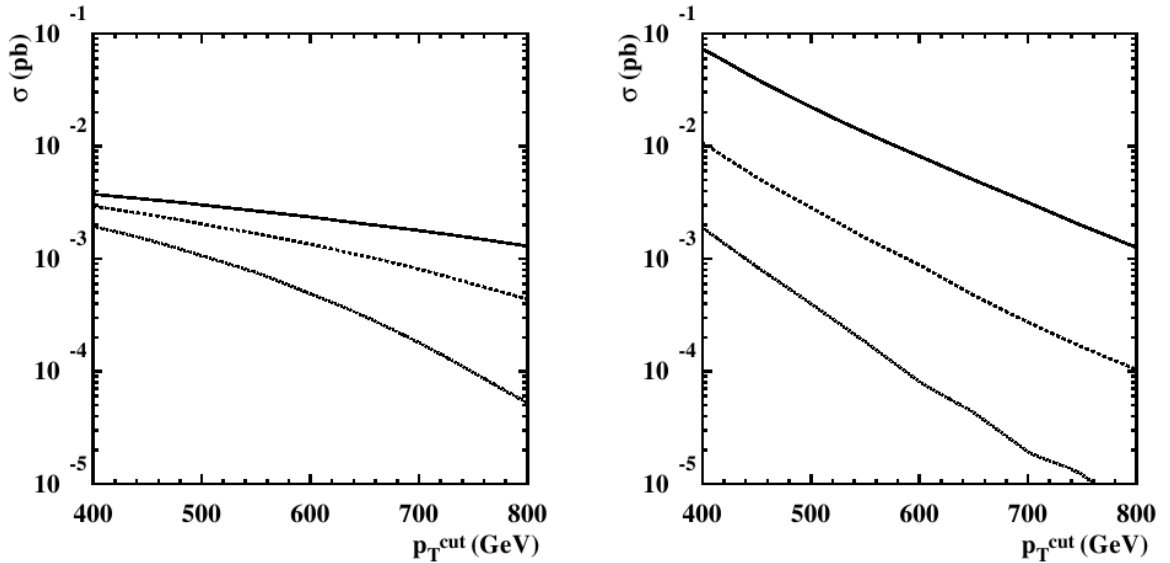


Figure 3.6. Signal (left) and background (right) as a function of p_T^{cut} . The solid line corresponds to $n = 1$, the dashed one to $n = 2$ and the dotted one to $n = 3$. The rapidity and jet separation cuts are the ones mentioned in the text.

In Fig. 3.7 we give the contour lines in the $M - M_D$ plane corresponding to the signal being 20 events (straight line for $N = 6$ and dashed line for $N = 2$) and 100 events (dotted line for $N = 6$ and dot-dashed line for $N = 2$) at the same luminosity. The left plot in the figure was obtained using $p_T^{cut} = 600 \text{ GeV}$ and $n = 3$, while the right plot was obtained using $p_T^{cut} = 800 \text{ GeV}$ and $n = 2$. As noted before, the reach in M can be large ($\sim 6 \text{ TeV}$) for low values of M_D , but it drops quite fast as M_D decreases. We see from this plot that the most favorable case corresponds to $N = 2$, due to the fact that the production cross-section is larger, and also that the transverse momenta of the jets are stronger in this case.

In the next three figures 3.8, 3.9, 3.10 we illustrate the effect of different cuts on the cross section. It can be seen that the invariant mass of the two jets might prove itself as a useful cut, if possible to implement. The color code for the figures is as follows: black are the curves for two extra dimensions; red are the curves for four extra dimensions and green are the curves for 6 extra dimensions. The horizontal line is the background ($Z + 2$ jets, with Z decaying invisibly) obtained this time using the Isajet input given in the appendix B. So far, we have seen that the two jet plus

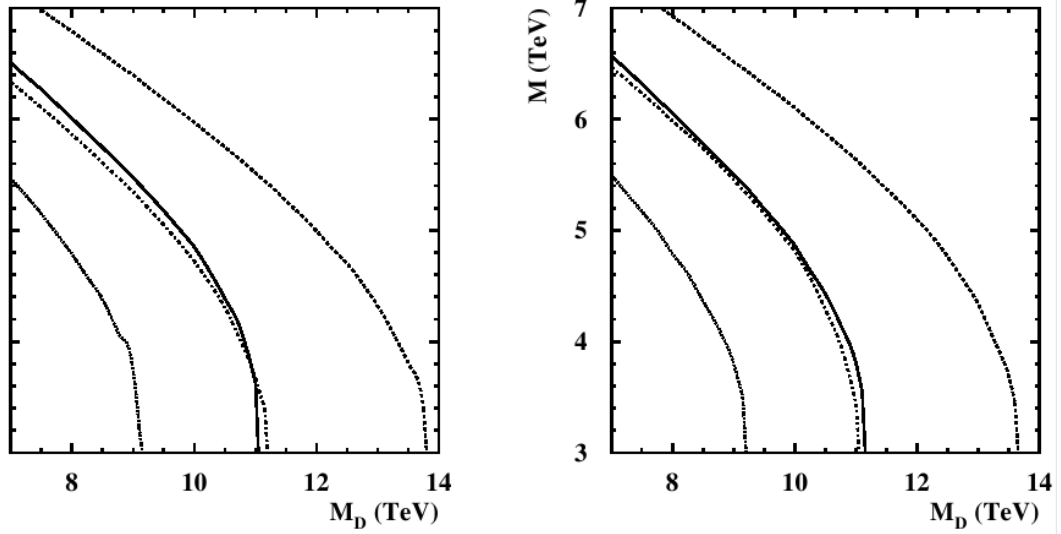


Figure 3.7. LHC reach for 20 and 100 signal events (straight and dotted lines corresponds to $N = 6$, and dashed and dot-dashed line correspond to $N = 2$, respectively). The cuts are the ones described in the text.

missing energy signal is a good candidate for the discovery of the existence of extra dimensions. In the next section we will investigate another possible discovery channel.

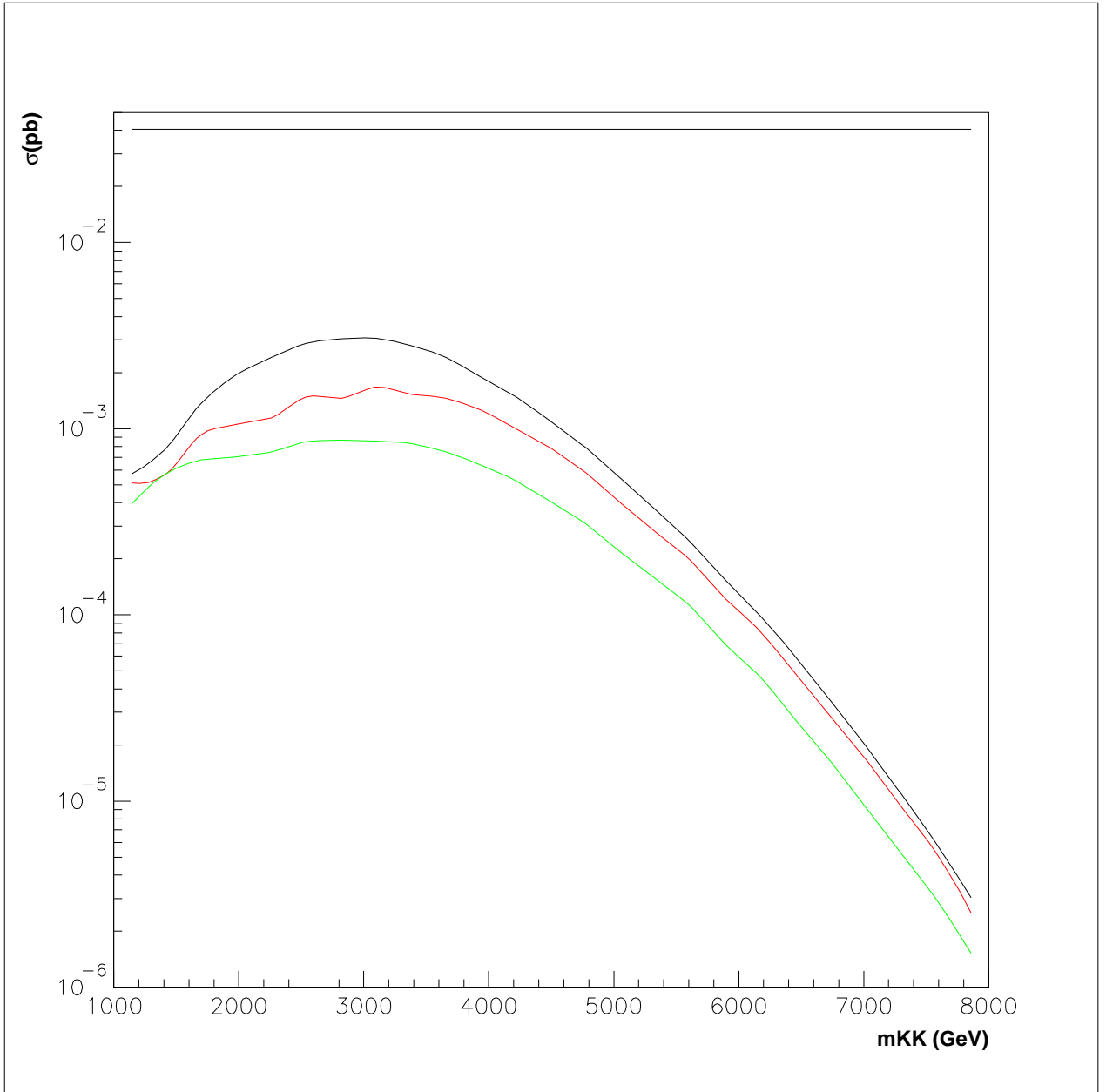


Figure 3.8. The production cross section for LHC using the following combined cuts: 1 TeV cut for the p_T of the two jets, 1 TeV for the \cancel{E}_T and a 10 TeV fundamental scale for gravity.

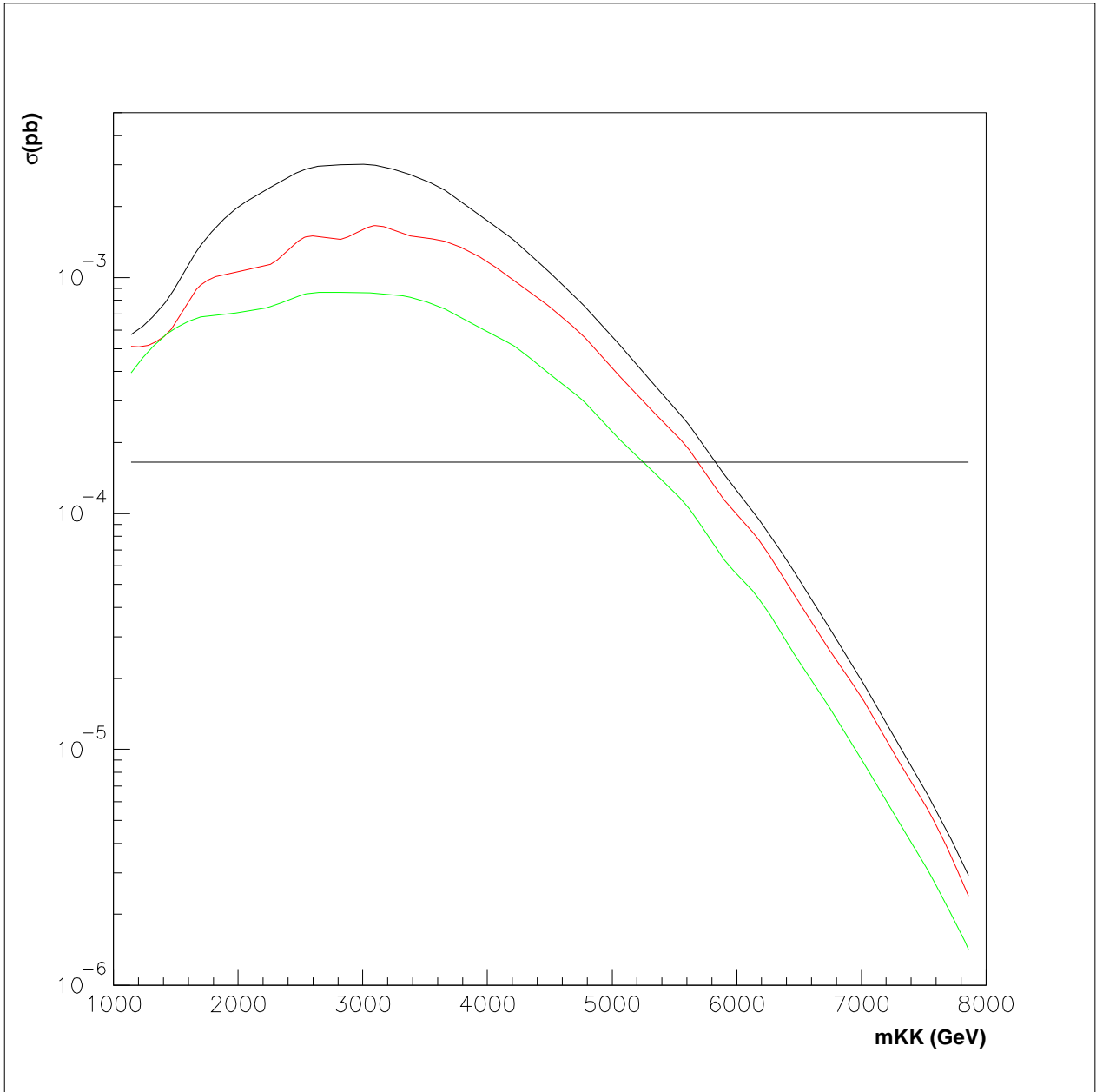


Figure 3.9. The production cross section for LHC using the following combined cuts: 1 *TeV* cut for the p_T of the two jets, 1 *TeV* for the \cancel{E}_T , 1 *TeV* for the invariant mass of the two jets and a 10 *TeV* fundamental scale for gravity.

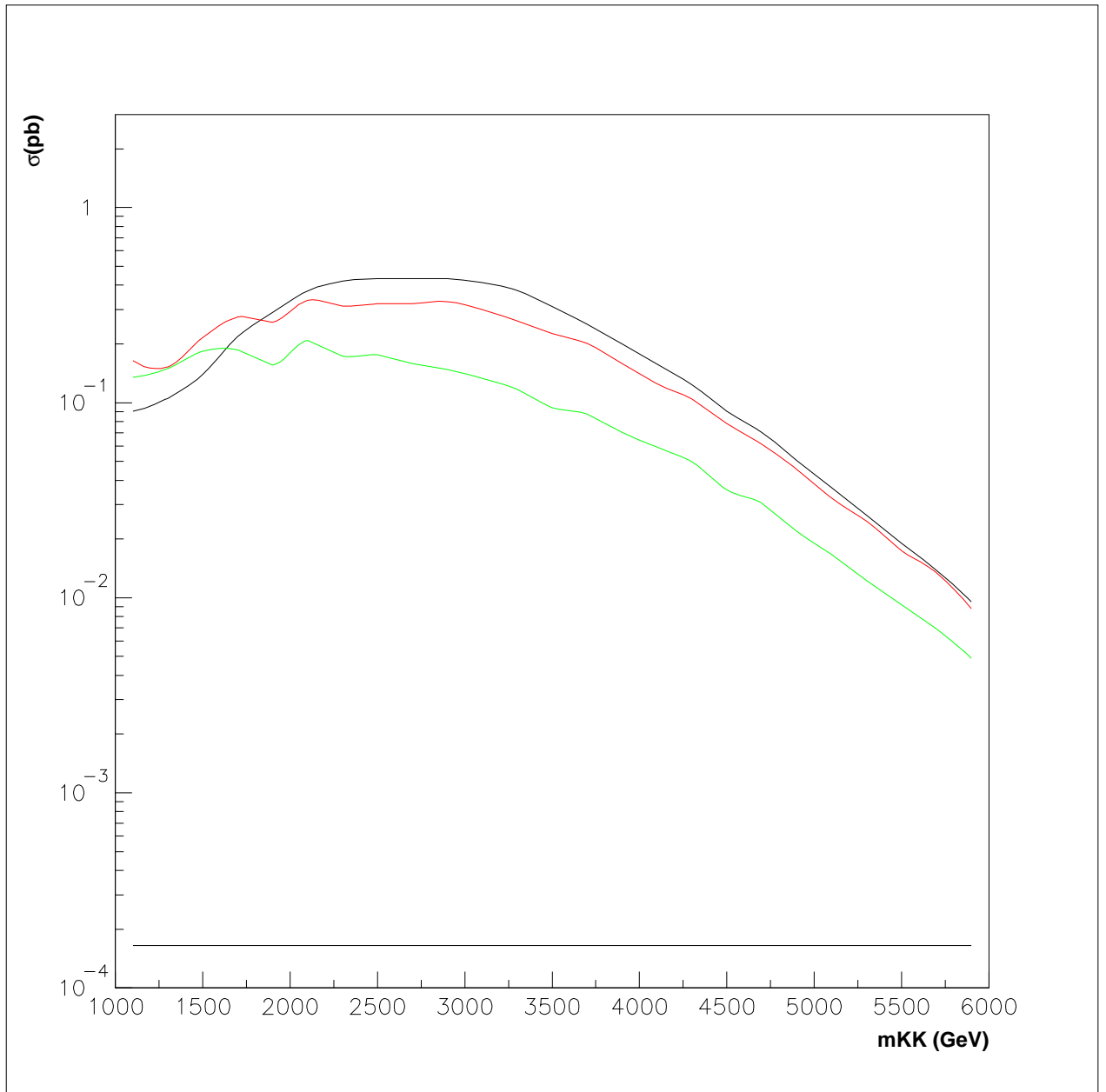


Figure 3.10. The production cross section for LHC using the following combined cuts: 1 TeV cut for the p_T of the two jets, 1 TeV for the \cancel{E}_T , 1 TeV for the invariant mass of the two jets and a 5 TeV fundamental scale for gravity.

3.2 Single KK plus graviton production

Due to the presence of KK number-breaking gravitational interactions, in our model it is possible to have again production of single KK excitations accompanied this time by the emission of a KK graviton. As opposed to the previous section, where virtual gravitons were mediating the interactions, this time the gravitons in the final state are real. There is also another important difference. While in the last section we had as internal propagators only spin 2 gravitons, for the production of KK gravitons accompanied by KK (or SM) particles, we need to take into account all the components of the decomposed 5D graviton, see (2.17). A typical process is depicted in Fig. 3.11 [13].

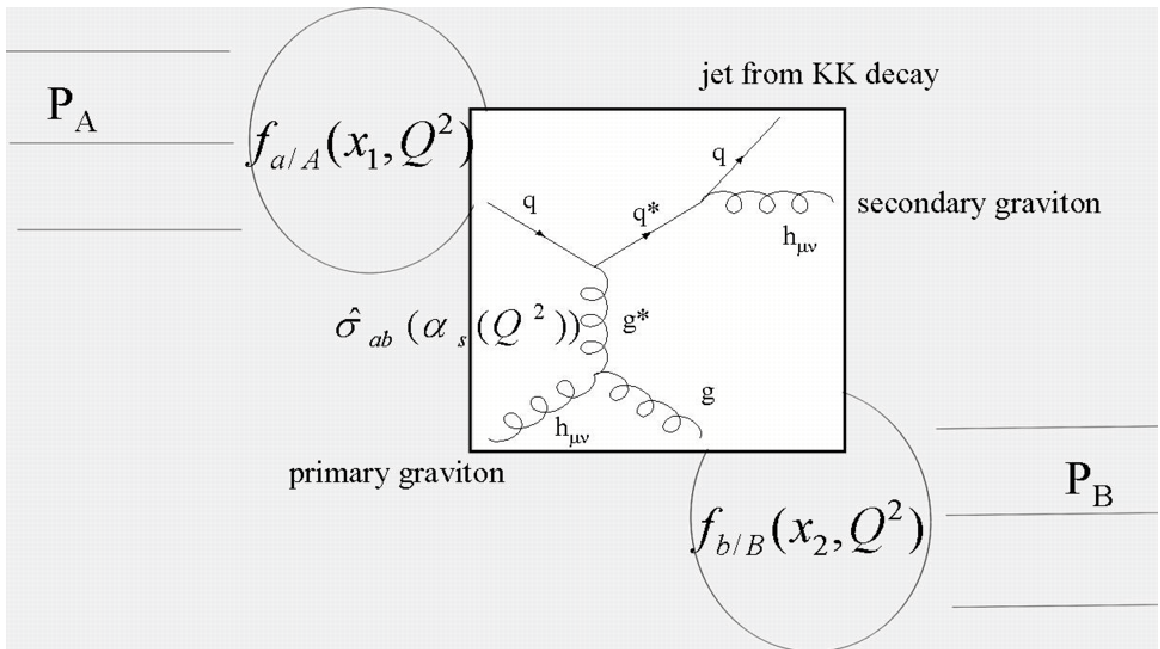


Figure 3.11. Proton-proton collisions creating KK plus graviton as primary particles which in turn create a jet plus a lot of missing energy.

As can be seen, the experimental signature for such a process would be a mono-jet coming from the decay of the KK excitation plus a lot of missing energy carried away by the primary graviton (the one produced in the primary interaction) and the secondary one (the one produced in the decay of the KK excited state). It worth emphasizing that the same signature can be obtained in the usual ADD-like scenarios

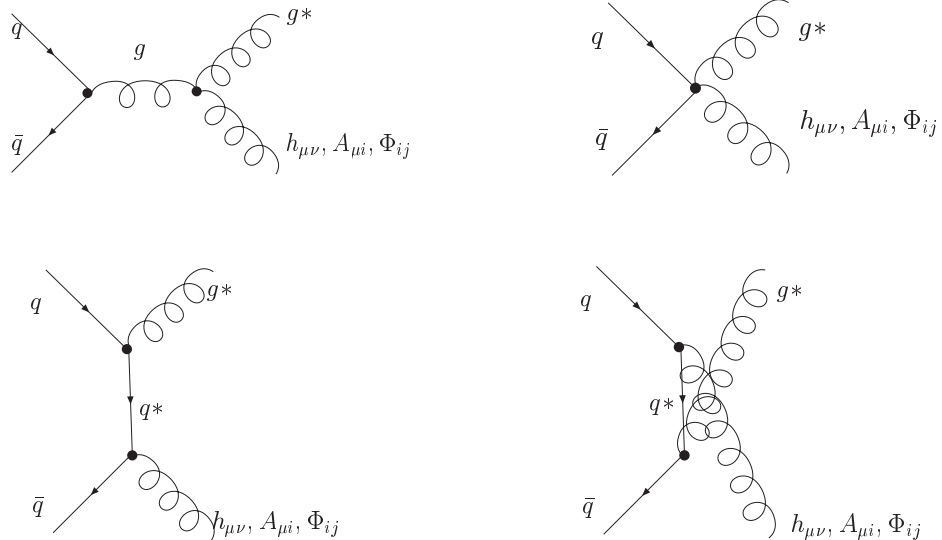


Figure 3.12. Feynman diagrams contributing to the production of a g^* and a graviton KK excitation (either $h_{\mu\nu}$, $A_{\mu i}$ or Φ_{ij}) at hadron colliders.

where the production of KK gravitons is accompanied by SM particles. The ADD-like signal will then act as an additional background for our model's signal. In the ADD case, on the external lines there are also only spin 2 gravitons, since SM particles do not couple with vector gravitons and the SM coupling to the scalar ones is proportional to their mass (thus, quite small).

3.2.1 Parton Processes and Amplitudes

For the monojet plus missing energy signal, there are 36 Feynman diagrams contributing. Some of them are reproduced in Fig. 3.12.

As can be expected, the expressions for the parton amplitudes are no longer simple expressions like in the case studied in the previous section. To give some idea of these dependencies, we will reproduce the dominant terms for some of the sub-processes:

1. for $q\bar{q} \rightarrow g^* h_{\mu\nu}$:

$$\sum_{\bar{q}} |M(q\bar{q} \rightarrow g^* h_{\mu\nu})|^2 \sim \frac{4}{3} * \left(\frac{M}{m_g}\right)^4 * \frac{t^4 u^2 + t^2 u^4}{s(t - M^2)^2 (u - M^2)^2}$$

2.for $qg \rightarrow q^* h_{\mu\nu}$:

$$\sum_{\bar{-}} |M(qg \rightarrow g^* h_{\mu\nu})|^2 \sim \frac{2}{3} * \left(\frac{M}{m_g}\right)^4 * \frac{t^4 u^2 + 3t^3 u^3 + 4t^2 u^4 + 2tu^5}{s(t - M^2)^2(u - M^2)^2}$$

3.for $gg \rightarrow g^* h_{\mu\nu}$:

$$\sum_{\bar{-}} |M(gg \rightarrow g^* h_{\mu\nu})|^2 \sim \frac{8}{3} * \left(\frac{M}{m_g}\right)^4 * \frac{t^6 u + 3t^5 * u^2 + 5t^4 u^3 + 5t^3 u^4 + 3t^2 u^5 + tu^6}{t^2 u^2 s^2}$$

In the above relations, we use the modified Mandelstam variables:

$$s = 2p_1 p_2, \quad t = -2p_1 p_3, \quad u = -2p_1 p_4$$

where p_1, p_2 are the momenta of the initial state partons, and p_3, p_4 the momenta of the final state ones. A full listing of the amplitudes squared and mediated, can be found in Appendix B.3.

In our model, in the case of the production of SM matter particles in the final state, the amplitudes are similar to those evaluated in the pure ADD case [28, 29] (when matter lives on the 4D brane); the only difference is the appearance of the thick brane form-factor (announced in chapter two)

$$\sigma = |\mathcal{F}_{00|n_5}^c|^2 \sigma_{ADD}, \quad (3.6)$$

with [21]:

$$\mathcal{F}_{00|n_5}^c = \frac{1}{\pi R} \int_0^{\pi R} dy \exp\left(\frac{2\pi i n_5 y}{r}\right) = i \frac{e^{ix} - 1}{x} .. \quad (3.7)$$

In the above expression, $x = \pi m_5 R$, where $m_5 = 2\pi n_5 / r$ is the graviton momentum along the fifth dimension. Since this form-factor is smaller than one, its contribution has the effect of multiplying the total cross-section (obtained after adding the contributions of all the gravitons in the KK tower) by a parameter $r < 1$. By numerical simulations, we find that the parameter r takes values roughly in the interval 1 (corresponding to the case $1/R \gg M_S$, where M_S is the upper limit on the graviton mass contributing to the process*) to around 0.7 (corresponding to the case when $1/R$ is of the same order of magnitude as M_S).

*The upper limit on the graviton mass is imposed by the collider energy and luminosity considerations.

For more than two extra dimensions, the heavy gravitons will bring the dominant contribution to the total cross-section

$$\sigma^T = \sum_{\vec{n}} \sigma^{\vec{n}} = \frac{M_{Pl}^2}{M_D^{N+2}} \int m_h^{N-1} dm_h d\Omega_N \sigma^{\vec{n}} \quad (3.8)$$

(where we have replaced the sum over graviton states by an integral [20]), due principally to the fact that the density of graviton states increases as m_h^{N-1} . At large masses, the form-factor (3.7) behaves like $1/m_5$, therefore one would expect a substantial reduction in the total cross-section. However, while it is true that most of the cross-section comes from large values for $m_h = 2\pi\sqrt{\vec{n}^2}/r$, that is for m_h of order M_s , this actually corresponds to significantly smaller values* of $m_5 = 2\pi n_5/r$ and thus, most of the gravitons contributing to the total cross section will have $x = \pi m_5 R \ll 1$ and therefore $|\mathcal{F}_{00|n_5}^c|^2 \sim 1$.

In the case of gravitons plus KK excitations † of a quark or gluon in the final state the situation is exactly the same like above. To first order, the signal is indistinguishable from that coming from the production of a SM quark or gluon and a graviton. One can even argue that, since in this case we produce also a massive particle in the final state (the KK excitation of matter), this type of process will not give a significant contribution. But this reasoning is not entirely correct.

To see that, let us consider again the cross-section for the production of a SM particle with a graviton of mass m_h . From dimensional analysis (see also [29]), one can estimate this cross-section to be of order

$$\sigma_{SM} \sim \frac{\alpha_s}{M_{Pl}^2} \left(1 + \mathcal{O}\left(\frac{m_h^2}{s}\right) \right). \quad (3.9)$$

(assuming here $m_h^2 \ll s$) Let us consider the case of a KK matter particle of mass M in the final state. A naive estimate will give an expression of the form (3.9), with terms of order M^2/s in the final state. However, if one evaluate the amplitude squared for the process with the spin 2 graviton in the final state, one obtains

$$\sigma_{KK} \sim \frac{\alpha_s}{M_{Pl}^2} \left(\frac{M}{m_h} \right)^4 \left(1 + \mathcal{O}\left(\frac{m_h^2}{s}\right) + \mathcal{O}\left(\frac{M^2}{s}\right) + \dots \right). \quad (3.10)$$

*For example, if we assume a flat distribution for the cross-section over a sphere of radius M_s in N dimensions, the average value for m_5 would be of order M_s/N^2 .

†Here we consider only q^* or g^* decaying to a SM quark or gluon by radiating a graviton since we are interested in collider phenomenology.

The term $(M/m_h)^4$ can lead to a great enhancement of the cross-section for producing light gravitons in the final state. To see how big this enhancement is, one just need remember that m_h can be as low as eV , while M is of order TeV ; this leads to a 10^{48} factor. The appearance of this enhancement factor is due to the breaking of translation invariance in the 5th dimension by the brane. This has as consequence the non conservation of 4D energy-momentum tensor of the matter $k^\mu T_{\mu\nu} \neq 0$, for interactions involving matter excitations with different KK numbers. Instead, one has $k^M T_{MN} = 0$ (with the indices M, N going from 0 to 5), or

$$k^\mu T_{\mu\nu} = -k^5 T_{5\nu} \sim \Delta m_{kk} ,$$

where we used the fact that the momentum in the fifth dimension is proportional to the KK mass. In our case, we have one SM particle becoming a first level excitation, therefore $\Delta m_{KK} = 1/R = M$. Then, if one considers the amplitude for the creation of a KK matter excitation by the radiation of a graviton with momentum k :

$$\sum_{\text{spin}} |\mathcal{M}(q \rightarrow q^* h^{\vec{n}})|^2 \sim \langle q^* | T_{\mu\nu} | q \rangle \langle q^* | T_{\rho\sigma} | q \rangle B^{\mu\nu, \rho\sigma}(k) ,$$

one sees that due to terms $\sim k^\mu k^\nu k^\rho k^\sigma / m_h^4$ in the graviton polarization sum $B^{\mu\nu, \rho\sigma}(k)$ (see, for example, [20] for the full expression), one will obtain $\sum_{\text{spin}} |\mathcal{M}(q \rightarrow q^* h^{\vec{n}})|^2 \sim (M/m_h)^4$ (see the examples given at the beginning of the subsection). Similar behavior holds for the production of a scalar graviton in the final state (although in this case terms $\sim k^\mu k^\nu / m_h^2$ are due to the $\partial^\mu \partial^\nu / m_{\vec{n}}^2$ factor in the interaction lagrangian rather than to the sum over polarizations), while for the case with a vector graviton field \tilde{A}^μ in the final state, one has $\sigma \sim \alpha_s / M_{Pl}^2 (M/m_h)^2$.

A behavior of the production cross-section $\sim (M/m_h)^4$ would mean that for the case of $N = 2, 3$ one would be able to probe very large values of M_D (by contrast, the total production cross section for large N values is not affected very much, since, as we have mentioned above, the contributions of heavy gravitons are enhanced by a density of states factor m_h^{N-1} , which will win over $(1/m_h)^4$ factor). However, we still have to take into account the form factors describing the overlap of graviton and matter wave functions on the brane. For the processes with the spin-2 graviton

or the scalar gravitons in the final state, the form factor multiplying the production cross-section will be $|\mathcal{F}_{01|n_5}^c|^2$, while for the vector graviton is $|\mathcal{F}_{01|n_5}^s|^2$. Here

$$\mathcal{F}_{01|n_5}^{(c,s)} = \frac{\sqrt{2}}{\pi R} \int_0^{\pi R} dy (\cos, \sin) \left(\frac{y}{R} \right) \exp \left(2\pi i \frac{n_5 y}{r} \right), \quad (3.11)$$

and therefore

$$|\mathcal{F}_{01|n_5}^c|^2 = \frac{4x^2}{(\pi^2 - x^2)^2} [1 + \cos(x)] , \quad |\mathcal{F}_{01|n_5}^s|^2 = \pi^2 \frac{|\mathcal{F}_{01|n_5}^c|^2}{x^2}, \quad (3.12)$$

with x as defined after (3.7). According to the discussion above, generally small values of x are relevant for the total cross-section; we then have

$$|\mathcal{F}_{01|n_5}^c|^2 \sim \frac{8x^2}{\pi^4} = \frac{8}{\pi^2} \frac{m_5^2}{M^2}, \quad |\mathcal{F}_{01|n_5}^s|^2 \sim \frac{8}{\pi^2}, \quad \text{for } x \ll 1. \quad (3.13)$$

We see then that the form-factors contribute additional terms of order $(m_h/M)^2$ to the cross-section for the production of spin-2 and scalar gravitons. For a small number of extra dimensions ($N = 2, 3$) this has an effect of making the enhancement factor in front of the cross-section the same for all final states, roughly $(M/m_h)^2$. This will enhance the cross-section somewhat, but not very much. (If one takes into account the density of graviton states $m_h dm_h$ for $N = 2$, one sees that this is a roughly logarithmic effect). In fact, we find that the cross-section for production of gravitons with a KK excitation is still smaller than the production of gravitons with SM particles (although typically lighter gravitons are predominant in the first case). For $N = 4$ to 6, the form factor has a net effect of reducing the contributions coming from spin 2 and scalar gravitons in the final state (unlike the enhancement due to breaking of 5D translational invariance, which is important mostly for light gravitons, the form-factor cancellation effect is valid for large graviton masses as well). As a consequence, we find that for such processes, the gravitons appearing in the final state for values of N larger than 4 are mostly vector gravitons. By contrast, for $N = 2, 3$ generally final states with spin-2 gravitons will dominate.

But this is not the whole story. As pointed out in [30], the orbifold compactification introduces two types of radiative corrections to the masses of the KK excitations.

The first type of correction is the bulk correction. It appears because the 5-dimensional Lorentz invariance is broken by the compactification itself. Since one

can not set the radius of the extra dimension(s) to zero, when one considers Feynman diagrams in extra dimensions, one will have non-local effects in a higher-dimensional, non-renormalizable theory. Fortunately, those loop diagrams give finite, well-behaved results (see (20)-(24) in the first reference from [30]).

The second type of correction are introduced by the orbifold. The orbifold itself is required as it is one way to obtain 4-D chiral fermions from the multi-component fermions of the higher dimensional theories. At the fixed points of the orbifold, the translational invariance is also broken. This means that additional terms (localized at the boundaries or, equivalently, on the two distinct 4-D branes situated at 0 and πR in the fifth dimension) in the Lagrangian will add additional radiative corrections to the bulk ones. We will refer again to [30] for the form of those corrections as well as for a detailed discussion about the radiative corrections the standard model in universal extra dimensions receives. As we will show in the next subsection, in the model we consider, the radiative corrections are of order 0.16 to the masses of the uncorrected KK levels.

3.2.2 Results

As explained in the previous subsection, the monojet plus missing energy signal in the UED plus fat branes scenario can be seen as having two components. The first one is given by the production of KK gravitons accompanied by zero mode KKs (which are the SM particles). This component of the signal can be also obtained in the ADD-like models. Again, as mentioned before, the experimental signature of the two cases is the same. The apparition of the form-factor multiplying the vertex) in the case of the UED plus fat branes proves to have only minor consequences. However, the second component of the signal, namely the production of KK excited states of quarks and gluons, can not appear in the ADD models. Let us analyze the two parts of the monojet signal into some more detail and let us look first at the graviton plus zero mode KK production.

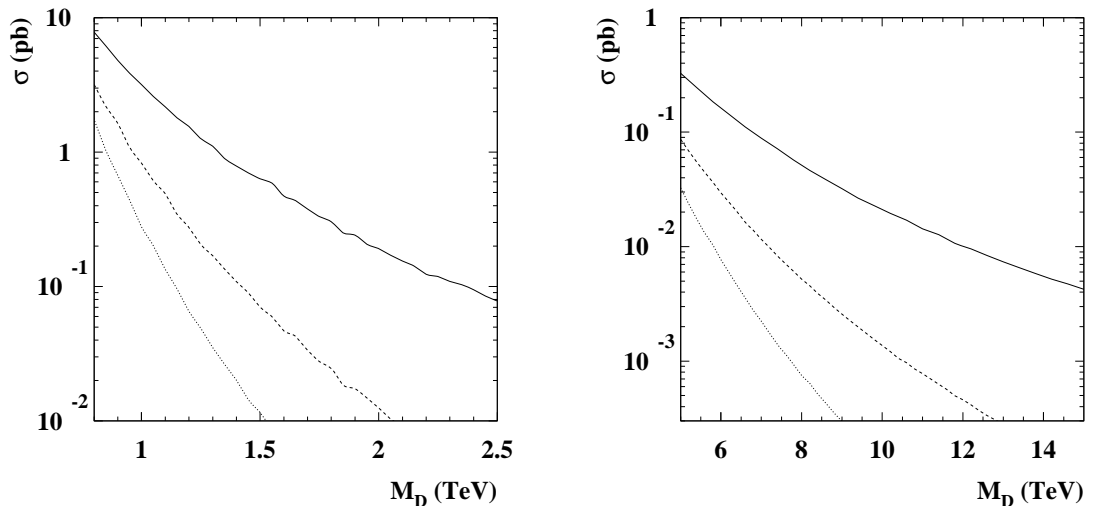


Figure 3.13. The jet+ missing energy cross section from graviton and SM quark or gluon production at Tevatron Run II (left panel) and LHC (right panel). The solid, dashed and dotted lines correspond to $N = 2, 4$ and 6 extra dimensions.

In Fig. 3.13 we plot the jet + \cancel{E}_T cross section* as a function of the fundamental gravity scale M_D for Tevatron Run II and LHC. Cuts on the jet transverse momentum ($p_T > 200 \text{ GeV}$ at Tevatron, $p_T > 1 \text{ TeV}$ at LHC) and rapidity ($|y| < 3.0$) have been used. The results are similar with the pure ADD cross-sections presented in [28, 29].

Let us move now to second component of the monojet plus missing energy signal and let us consider first the case when the KK particle decay directly into SM plus graviton.

Using the same cuts as for the case of SM particle production, we plot in Fig. 3.14 (left panel) the cross section for the production of one quark or gluon KK excitation and a graviton at the LHC as a function of the mass of the KK particle m_{KK} . We see that the production cross-section is generally smaller than the signal due to production of the SM particle together with graviton. The flatness of the cross-section for small values of m_{KK} is due to the large p_T cut imposed on the momentum

*The SM background (assumed to come only from jet + Z production, with Z decaying to neutrinos) at parton level, and with the cuts above is around 0.14 pb for Tevatron and 10 fb for LHC.

of the observable jet. Since in this case the jet comes from the decay of a massive particle (the KK excitation), its transverse momentum will tend to increase with the mass of the particle. This partially compensates for the decrease in cross-section due to the production of heavier particles.

In Fig. 3.14 (right panel) we present the cross section as a function of the cut p_T^{min} on the transverse momentum for the observable jet. The plot is made for $N = 2$ extra dimensions. Again as above, for small values of p_T^{min} , the cross-section for the production of the SM particles dominates (this is a consequence of the form-factor $\mathcal{F}_{01|n}^c$ multiplying the amplitude rather than the appearance of a massive KK particle in the final state). However, the transverse momentum of the jets due to production of a SM particle falls faster than the p_T of the jets coming from the decay of the heavy KK excitation, and as it can be seen in figure, at very large p_T the two signals are of comparable magnitude. This suggests that if one wants to look for the production of

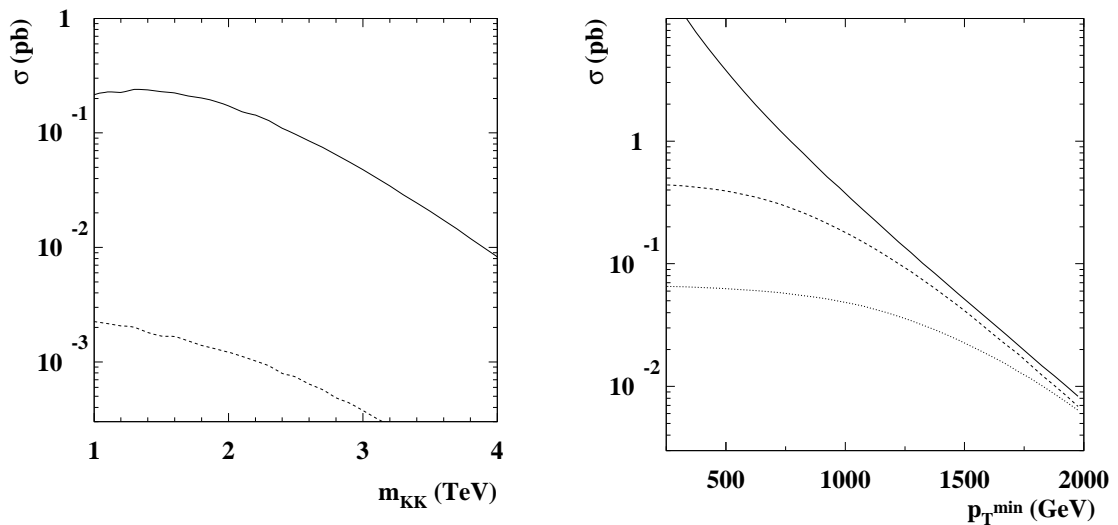


Figure 3.14. Left panel: the jet+ missing energy cross section from graviton and KK quark or gluon production at LHC. The solid line corresponds to $N = 2$, while the dashed line corresponds to $N = 4$. Right panel: the distribution of the cross-section as a function of the cut imposed on the jet transverse momentum, for production of SM particle (solid line), and production of KK excitations with $m_{KK} = 2$ TeV (dashed line) and $m_{KK} = 3$ TeV (dotted line). M_D is taken 5 TeV for both panels.

KK excitations of matter in this channel, one should look primarily at very high p_T events.

So far we saw that the direct decay of the KK excitation into SM plus graviton does not provide a very good signal for identifying KK particle production at hadron colliders. But not all hope is lost as we still have to investigate the possibility of KK excitations cascading to the LKP (which for the purpose of this thesis will be the γ^*), which in turn will decay gravitationally to a photon plus a graviton. The signal in this case will be a high p_T photon in the final state plus missing energy (there will also be some soft jets and leptons, but we will not consider those in our analysis). The SM background in this case is much smaller than for the case of a jet + \cancel{E}_T ; the signal due to the production of a SM photon with a graviton will also be smaller, since the production process for such a signal will be an electroweak process rather than a strong one. For example, at the LHC, for a p_T cut of 500 GeV , the SM background is ~ 1 fb. With a 100 fb^{-1} of integrated luminosity, a 5σ discovery would then require 50 signal events, of a cross-section of 0.5 fb. From direct production of a SM photon with a graviton, the values of M_D for which the cross-section will reach 0.5 fb will be 5.4 TeV for $N = 6$, 6 TeV for $N = 4$ and 8.3 TeV for $N = 2$.

In the case of production of a gluon/quark KK excitation which subsequently decays to a photon, the values of M_D corresponding to a 0.5 fb cross-section can be as high as ~ 7 TeV for $N = 6$, 10 TeV for $N = 4$ and 40 TeV for $N = 2$, depending on the value of $1/R$. We show in Figs. 3.15, 3.16(left panel) with the solid lines the discovery reach in the $(M_D, 1/R)$ plane (that is, for points below and to the left of the solid lines, the cross-section will be bigger than 0.5 fb). The dashed lines correspond to values of parameters for which the gravitational decay widths start becoming important; that is, for points below the dashed lines the quark and gluon KK excitations will decay predominantly to γ^* , while for points above they will decay directly to SM quarks and gluons through graviton radiation. Therefore, in the region below both the solid and dashed lines, the signal will be photon + \cancel{E}_T , and it will be large enough to ensure discovery. We see that in this channel we can probe values of M_D similar to those achievable in the jet + \cancel{E}_T channel for $N = 4$ and $N = 6$ (from

Fig. 3.13) and almost twice as large for $N = 2$ (the 5σ discovery reach from jet + missing energy being ~ 20 TeV in this case).

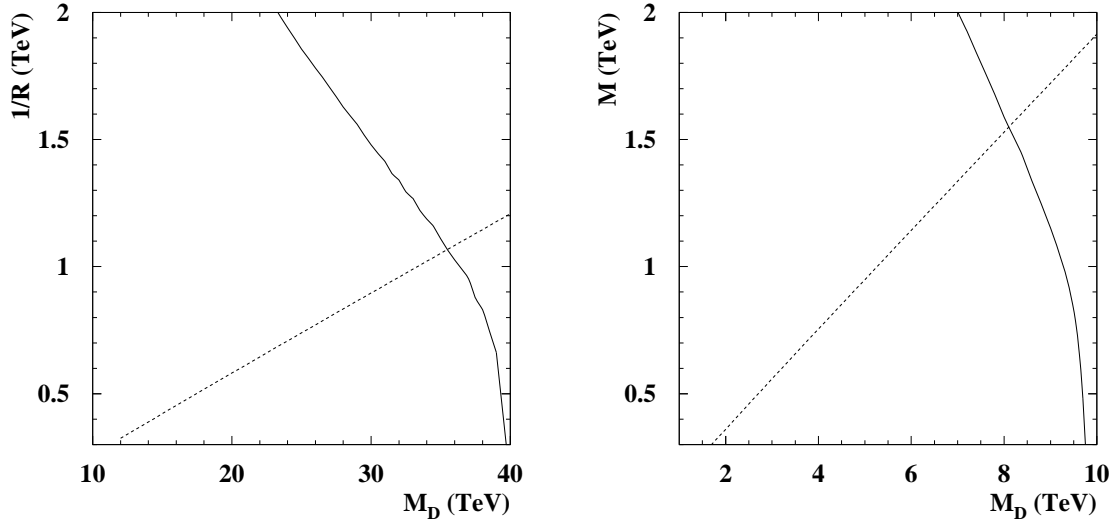


Figure 3.15. Solid lines: the 5σ discovery reach at the LHC in the photon + \cancel{E}_T channel for $N = 2$ (left panel) and $N = 4$ (right panel). For values of $M_D, 1/R$ below the dashed lines, the KK quarks and gluons decay first to the LKP.

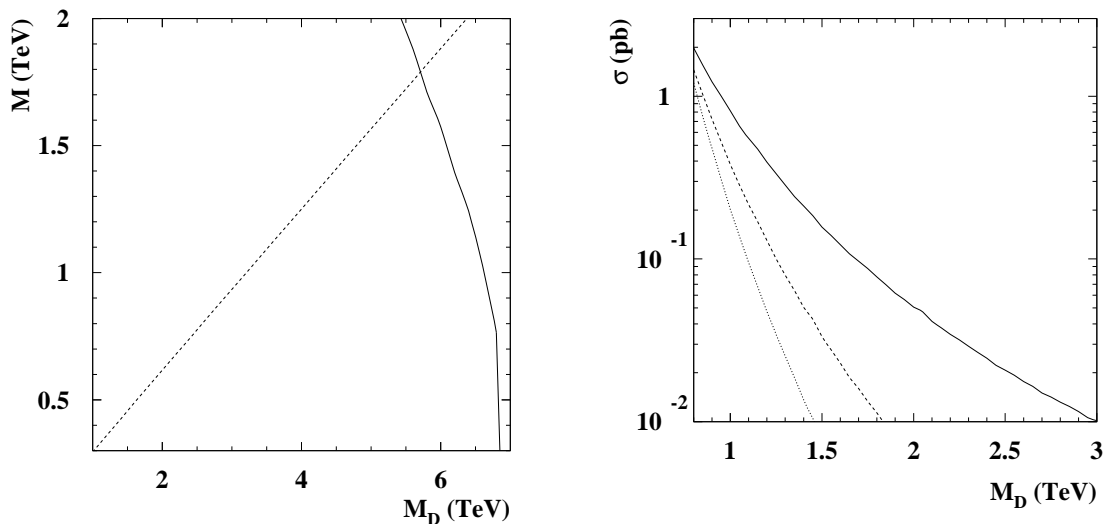


Figure 3.16. Left panel: the 5σ discovery reach at the LHC in the photon + \cancel{E}_T channel for $N = 6$. Right panel: the SM photon + \cancel{E}_T cross-section at the Tevatron Run II, with $p_T > 100$ GeV (solid, dashed and dotted lines correspond to $n = 2, 4$ and 6 extra dimensions respectively).

The case for the Tevatron is somewhat different. As it can be seen from Figs. 3.15, 3.16, the requirement that g^* and q^* decay first to the LKP implies rather large values of M_D ($> 10 \text{ TeV}$ for $N = 2$). This means that the production cross-section is highly suppressed. Typically, for $N = 4, 6$ there is just a small region of values for M_D where g^* and q^* both decay to γ^* and are produced in enough numbers to be observable. However, in that region the signal coming from production of SM photons plus KK gravitons is predominant. We show in Fig. 3.16(right panel) the cross-section for SM photon production plus \cancel{E}_T (from KK gravitons), with a cut on photon p_T of 100 GeV . The Standard Model background (from $Z\gamma$ production) is $\sim 80 \text{ fb}$. It is interesting to note that the the M_D discovery reach at the Tevatron is roughly similar in the jet + \cancel{E}_T channel versus photon + \cancel{E}_T channel. The reason is that while the production cross-section is suppressed by a factor $\alpha_{em}/\alpha_s \sim 1/10$, the background is similarly suppressed, and one can use softer cuts (using a p_T cut of 100 GeV as opposed to 200 GeV will increase the cross-section by a factor of 10). Moreover, the predominant initial state responsible for the production cross-section is $q\bar{q}$, which favors processes with photons in the final state (whereas for the LHC is qg and gg , resulting in additional suppression of final state photons).

CHAPTER 4

LEPTONS AND EXTRA DIMENSIONS

So far, the use of the UED with fat branes model gave reasonable results for the collider physics. But what are the implications of this model when used for the neutrino and charged lepton physics? In this chapter we present the new results obtained by applying the UED with fat branes scenario to the lepton sector [14].

But before going any further, let us review what is the current situation with the lepton part of the SM.

4.1 Current situation in lepton physics

Charged leptons (as opposed to hadrons) experience only electroweak and gravitational interactions; their SM lagrangian contains only (2.4) and the first term in (2.8). There is also another important difference between quarks and leptons. The mixing in the quark sector is minimal. But the leptons exhibit almost maximal mixing. While the properties of the charged leptons are well known (see Table A.1 and Table A.2) and their interactions relatively well understood, the neutrinos continue to rise many more questions. At the time of the writing of this thesis, two excellent sources of information dedicated to neutrino physics are the websites maintained by the American Physical Society (APS) [31] and by C. Giunti and M. Laveder [32].

In the last few years, atmospheric [33] and solar [34] experiments have well established the neutrino oscillations. This is usually interpreted as evidence for the existence of massive neutrinos. The argument goes as follows: the conventional SM does not allow for neutrino masses because it lacks the right-handed singlet neutrino fields thus, the easiest way to accommodate the experimental facts, is to minimally extend SM (still in four dimensions) with the required fields and to give masses to

the neutrinos via an elegant mechanism called the seesaw mechanism* [35]. The problem is that the neutrino oscillation experiments depend only on $\Delta m_{ij}^2 = m_j^2 - m_i^2$ and can not give the overall scale for the neutrino masses. This led to investigate possible scenarios for neutrino masses involving extra dimensions. An interesting idea to solve the puzzle of neutrino masses in the context of extra dimensions has been proposed in [36, 37] (the ADD model). Here, all the SM particles are confined to the four dimensional wall (three space and one time, the so called D_3 brane). There exists a SM singlet right-handed (RH) neutrino, which, like gravity, propagates into the sub-mm size extra dimension. The Yukawa couplings of the SM left-handed neutrino with this RH neutrino then gives a tiny Dirac mass for the LH neutrino. In this picture, the smallness of the neutrino mass arises from the smallness of the effective four dimensional Yukawa coupling due to large volume of the extra dimension in which the RH neutrino propagates. Several extensions of this idea to study the neutrino masses and mixings in detail have been pursued [38].

Now the important question is: *Can an UED model incorporating fat branes shade some light on the problem of neutrino masses?* As i will show in the following, applying the UED with fat branes to leptons provides some interesting answers.

4.2 Leptons in UED with fat branes

4.2.1 The Model

In this section, we present a model which can account for large hierarchy among the charged lepton masses, while giving practically no hierarchy among the light neutrino masses. The light neutrinos get a tiny mass as in the ADD mechanism; but

*It postulates the existence of a massive SM singlet right handed neutrino with Majorana masses of order of $M \sim 10^{14} GeV$. The Yukawa coupling of the left-handed neutrino to this heavy right-handed neutrino then gives a Dirac mass of the order of the charged lepton masses, m_l . As a result, the left-handed neutrino obtains a tiny mass of the order of m_l^2/M . See-saw model naturally does not lead to lack of hierarchy among the light neutrino masses. In addition, in this mechanism, the light neutrino masses are Majorana particles and will lead to neutrino-less double beta decay.

their masses are related to the corresponding charged lepton masses. The neutrinos are naturally Dirac particles. When extended to accommodate two or three families, the model naturally provides large mixings among neutrinos. Our model unifies the ADD scenario [5] with the scenario of the Universal Extra Dimensions (UED) [11]. The SM particles of one family live in a fat brane [19, 21, 22] of TeV^{-1} size or smaller which is a tiny part of the submm size extra dimensions. The graviton as well as the SM singlet neutrinos propagate in the submm size extra dimensions. The three SM fermion families live in fat branes of three different sizes (R_1, R_2, R_3) . Since all the charged leptons get their masses from the Yukawa couplings in five dimensions of sizes (R_1, R_2, R_3) , their mass hierarchies are naturally obtained from the hierarchy of the sizes of the fat branes. Note that our model is different from the split fermions in extra dimensions model [39] where the hierarchy of the charged fermion masses are obtained from the different overlaps of the SM Higgs field wave function to the split fermion locations. Light neutrinos, on the other hand, as in ADD, get their masses from their Yukawa couplings with the SM singlet bulk neutrino propagating in the submm size extra dimensions. So, their masses are of the same order, and hence there is no hierarchy among the light neutrino masses. The neutrino masses are much smaller compared to the charged lepton masses because their Yukawa interactions get diluted by the volume of the submm size dimensional space compared to these of the charged leptons. Since the light neutrino masses are all of same order including their off-diagonal Yukawa coupling, large mixing among the neutrinos naturally arise.

To begin, we consider one extra dimension of size r (which, as in ADD model, is of submm size). This extra dimension is taken to be S^1 and is denoted by y . The gravity propagates all the way in this extra dimension. The SM singlet neutrino can propagate in y only in the space given by S^1/Z_2 orbifold. All the SM particles of the first family can propagate only up to a distance R within the 5^{th} dimension of size r . Thus, these SM particles live in a fat brane of thickness R , and the space in which they propagate is S^1/Z_2 orbifold of size R . We denote the left-handed lepton doublet $(\nu_e, e)_L$ by $l(x, y)$, RH lepton singlet by $l_R(x, y)$, Higgs doublet by $H(x, y)$, and the SM singlet neutrino by $N(x, y)$. Note that l , l_R and H are confined to the

fat brane of size R (of TeV^{-1} size), while N and the gravity propagates in size r . We can expand the five dimensional fields in terms of their zero modes and the KK excitations as follows:

$$l(x, y) = \frac{1}{\sqrt{\pi R}} \left\{ l_L^0(x) + \sqrt{2} \sum_{n=1}^{\infty} \left[l_L^n(x) \cos\left(\frac{ny}{R}\right) + l_R^n(x) \sin\left(\frac{ny}{R}\right) \right] \right\}, \quad (4.1)$$

$$e_R(x, y) = \frac{1}{\sqrt{\pi R}} \left\{ e_R^0(x) + \sqrt{2} \sum_{n=1}^{\infty} \left[e_R^n(x) \cos\left(\frac{ny}{R}\right) + e_L^n(x) \sin\left(\frac{ny}{R}\right) \right] \right\}, \quad (4.2)$$

$$H(x, y) = \frac{1}{\sqrt{\pi R}} \left\{ H^0(x) + \sqrt{2} \sum_{n=1}^{\infty} H^n(x) \cos\left(\frac{ny}{R}\right) \right\}. \quad (4.3)$$

Note that the $l_L(x, y)$, $e_R(x, y)$ and $H(x, y)$ are even under $y \rightarrow -y$, while $l_R(x, y)$ and $e_L(x, y)$ are odd under $y \rightarrow -y$. The KK expansion for the SM singlet neutrino $N(x, y)$ is given by:

$$N(x, y) = \frac{1}{\sqrt{\pi r}} \left\{ N_R^0(x) + \sqrt{2} \sum_{n=1}^{\infty} \left[N_R^n(x) \cos\left(\frac{ny}{r}\right) + N_L^n(x) \sin\left(\frac{ny}{r}\right) \right] \right\}. \quad (4.4)$$

We have chosen only $N_R(x, y)$ to have zero mode, in analogy with that in the usual 4D where we have only SM singlet. The quarks in the first family are also assumed to be confined on the fat brane of size R , with $R^{-1} \sim TeV$. The SM gauge bosons are also confined to this fat brane as in the UED, and will have their KK excitations in the TeV scale satisfying the current experimental bounds.

Let us now discuss the charged lepton and neutrino masses in the effective four dimensional theory from our model. The charged lepton and Dirac neutrino mass terms arise from the Yukawa interactions:

$$S_1^{int} = \int d^4x \int_0^{\pi R} dy \left[y_5 \bar{l}(x, y) H(x, y) e(x, y) + \tilde{y}_5 \bar{l}(x, y) \tilde{H}(x, y) N(x, y) \right] + h.c. \quad (4.5)$$

where $\tilde{H}(x, y) = i\sigma_2 H^*(x, y)$, and y_5 and \tilde{y}_5 are five dimensional Yukawa couplings.

We assume that only the zero mode of the Higgs, $H^0(x)$ acquires vacuum expectation value which breaks the electroweak symmetry. This will then give rise to

Dirac masses to the charged lepton as well as the light neutrino. From (4.5), using the KK expansions of (4.1-4.3), we obtain:

$$S_1^{int} = \int d^4x \frac{1}{\sqrt{\pi R}} [y_5 \bar{e}_L e_R \frac{1}{\sqrt{2}}(v+h) + \tilde{y}_5 \bar{\nu}_L N_R \frac{1}{\sqrt{2}}(v+h)] + h.c. \quad (4.6)$$

where $\frac{v}{\sqrt{(2)}}$ is the vacuum expectation value of the Higgs field.

Defining the four dimensional Yukawa couplings y_4 and \tilde{y}_4 to be:

$$y_4 \equiv \frac{y_5}{\sqrt{\pi R}}, \quad \tilde{y}_4 \equiv \frac{\tilde{y}_5}{\sqrt{\pi r}} \quad (4.7)$$

we obtain:

$$m_e = y_4 \frac{v}{\sqrt{2}}, \quad m_{\nu_e} = \tilde{y}_4 \frac{v}{\sqrt{2}}. \quad (4.8)$$

Note that even though the five dimensional Yukawa couplings, y_5 and \tilde{y}_5 are of the same order, the effective four dimensional neutrino Yukawa coupling is hierarchically small compared to that of the charged leptons because of the large size of the extra dimension, r compared to the fat brane size, R . The SM singlet neutrino, N has a much larger space, r available compared to e_R , thus producing tiny effective four dimensional Yukawa coupling, \tilde{y}_4 compare to y_4 .

From (4.7) and (4.8), we note that:

$$\frac{m_{\nu_e}}{m_e} = \left(\frac{\tilde{y}_5}{y_5} \right) \sqrt{\frac{R}{r}}. \quad (4.9)$$

With $R^{-1} \sim 1 \text{ TeV}$, and $r \sim \text{submm} \sim 10^{-3} \text{ eV}$, we obtain from (4.9) (assuming \tilde{y}_5 and y_5 to be the same), $m_{\nu_e} \sim \sqrt{\frac{R}{r}} m_e \sim 1.5 \cdot 10^{-2} \text{ eV}$. This is in the right range as needed for the solar neutrino experiment.

In the above calculation, we have included only the zero mode of $N(x, y)$, namely N_R^0 . Since N propagates in the submm size dimension r , it will have KK excitations with mass of 10^{-3} eV and its integral multiples. These will then mix substantially with the left-handed neutrino, affecting its SM coupling and thus contradicting experiments. To solve this problem, we introduce a bulk SM singlet scalar field $\Phi(x, y)$ which is odd under $y \rightarrow -y$. Then, the KK expansion for $\Phi(x, y)$ takes the form:

$$\Phi(x, y) = \sum_{n=1}^{\infty} \Phi^n(x) \sin\left(\frac{ny}{r}\right). \quad (4.10)$$

This gives rise to additional bulk Yukawa interactions:

$$S_1^1 = \tilde{Y}_5 \int d^4x \int_0^{\pi r} dy \bar{N}(x, y) N(x, y) \Phi(x, y). \quad (4.11)$$

For simplicity, we assume that only $\Phi^{(1)}$ has vev in the 5D string scale. Note that all our interactions conserve lepton number. No Majorana mass is introduced, and all masses are Dirac masses.

From eq. (4.11), we obtain the effective four dimensional action:

$$S_1^1 = M \bar{N}_L^n N_R^m (\delta_{n-m-1,0} + \delta_{n-m+1,0}) \quad (4.12)$$

where $M \equiv \frac{\tilde{Y}_5 \langle \Phi \rangle}{\pi r}$ and $\langle \Phi \rangle$ is the vacuum expectation value of the singlet field $\Phi(x, y)$ in the TeV scale or higher.

We expect this mass, M , arising from the five dimensional SM singlet bulk fields N and Φ , M_0 to be in the string or five dimensional Plank scale. Including this SM singlet Dirac mass, given by eq.(4.12) into account, we get a mass matrix involving the zero modes $(\bar{\nu}_{eL}^0, \bar{N}_L^1, \bar{N}_L^2, \dots)$ and $(N_R^0, N_R^1, N_R^2, \dots)$. Taking only the first two KK excitations of N_L and N_R , the mass matrix is:

$$(\bar{\nu}_{eL}^0, \bar{N}_L^1, \bar{N}_L^2) \begin{pmatrix} m & \sqrt{2}m & \sqrt{2}m \\ 0 & m' & M \\ 0 & M & 2m' \end{pmatrix} \begin{pmatrix} N_R^0 \\ N_R^1 \\ N_R^2 \end{pmatrix} \quad (4.13)$$

where $m' \equiv \frac{1}{r}$.

The mass matrix in (4.13) is diagonalized by a bi-unitary transformation. The three mass eigenvalues are $\sim m, M, M$, and to order m/M , the corresponding eigenstates are :

$$\begin{pmatrix} 1 \\ O(m/M) \\ O(m/M) \end{pmatrix}, \begin{pmatrix} O(m/M) \\ 1 \\ 1 \end{pmatrix}, \begin{pmatrix} O(m/M) \\ -1 \\ 1 \end{pmatrix} \quad (4.14)$$

Two Weyl neutrinos, ν_L^0 and N_R^0 forms a 4-component massive Dirac neutrino of mass approximately m , where the (N_L^1, N_R^1) and (N_L^2, N_R^2) form two massive Dirac neutrinos N^1 and N^2 with very large mass $\sim M$. Note that while there is large mixing

between N_L^1 and N_R^1 , or N_L^2 and N_R^2 ; there is only a tiny mixing of order m/M of N_L^0 with N_L^1 or N_L^2 and N_R^0 with N_R^1 or N_R^2 . With $m \sim 10^{-2} eV$, and $M \sim \text{few } TeV$, this mixing is negligibly small to affect the ν_{eL} coupling in the SM model.

The same conclusion holds if we include the higher level KK excitations of N . If we include KK excitations of N up to the n^{th} level, then the mass matrix involving $(\bar{\nu}_{eL}^0, \bar{N}_L^1, \bar{N}_L^2, \dots, \bar{N}_L^n)$ and $(N_R^0, N_R^1, N_R^2, \dots, N_R^n)$ gives one light eigenvalue with mass $\sim m$ and $(n - 1)$ eigenvalues of mass $\sim M$ in the TeV scale or higher. Note that the Weyl neutrinos ν_{eL}^0 and N_R^0 form a light Dirac neutrino; ν_e of mass $\sim m$. The KK excitations N_L^i and N_R^i form a massive Dirac neutrino N^i of mass $\sim M$.

Thus our model produces the large hierarchy between the light neutrino and charged lepton masses as well as the right magnitude for the left-handed light neutrino mass. Also, in one family, we have only one light Dirac neutrino, and a large number of very heavy ($\sim TeV$) SM singlet Dirac neutrinos. The mixing between the light neutrino and the heavy singlet Dirac neutrino are highly suppressed (of order m_ν/M with $M \sim TeV$).

Let us now consider two families of fermions. As in the previous section, we restrict ourself in only one extra dimension. The left handed doublets are $l_e(x, y)$ and $l_\mu(x, y)$. In addition to $N(x, y)$, we introduce a second SM singlet neutrino in the bulk, $N'(x, y)$. Then, we will have bulk interactions for the 2^{nd} family similar to (4.5) and (4.11) with the replacements

$$l(x, y) \rightarrow l_\mu(x, y), e(x, y) \rightarrow \mu(x, y), N(x, y) \rightarrow N'(x, y).$$

We also have the additional bulk interactions:

$$S_{12} = \int d^4x \int_0^{\pi R} dy [y_{5(e\mu)} \bar{l}_e(x, y) H(x, y) \mu(x, y) + \tilde{y}_{5(e\mu)} \bar{l}_e(x, y) \tilde{H}(x, y) N'(x, y) + (e \leftrightarrow \mu)] + h.c. \quad (4.15)$$

and

$$S_{12} = \tilde{Y}'_5 \int d^4x \int_0^{\pi r} dy M'_0 \left[\bar{N}(x, y) N'(x, y) + \bar{N}'(x, y) N(x, y) \right] \Phi(x, y). \quad (4.16)$$

Using the KK decompositions for $l_e(x, y)$, $l_\mu(x, y)$, $H(x, y)$, $N(x, y)$ and $N'(x, y)$ and integrating over y in (4.5) and (4.11), and in similar equations for the 2-nd family,

as well as (4.6) and (4.15), we obtain the mass terms in the effective four dimensional theory involving $(\bar{\nu}_{eL}^0, \bar{N}_L^1, \bar{N}_L^2, \dots; \bar{\nu}_{\mu L}^0, \bar{N}_L^1, \bar{N}_L^2, \dots)$ and $(N_R^0, N_R^1, N_R^2, \dots; N_R^0, N_R^1, N_R^2, \dots)$.

Again, keeping the terms only up to N_L^2, N_L^2 and N_R^2, N_R^2 , we get a 6x6 mass matrix. Choosing the basis to be $\bar{L} = (\bar{\nu}_{eL}^0, \bar{\nu}_{\mu L}^0, \bar{N}_L^1, \bar{N}_L^1, \bar{N}_L^2, \bar{N}_L^2)$, $R = (N_R^0, N_R^0, N_R^1, N_R^1, N_R^2, N_R^2)$, we get

$$S_{mass} = \int d^4x \bar{L} \mathcal{M} R \quad (4.17)$$

where

$$\mathcal{M} = \begin{pmatrix} m & q & \sqrt{2}m & \sqrt{2}q & \sqrt{2}m & \sqrt{2}q \\ q & p & \sqrt{2}q & \sqrt{2}p & \sqrt{2}q & \sqrt{2}p \\ 0 & 0 & m' & 0 & M & M'' \\ 0 & 0 & 0 & p' & M'' & M' \\ 0 & 0 & M & M'' & 2m' & 0 \\ 0 & 0 & M'' & M' & 0 & 2p' \end{pmatrix} \quad (4.18)$$

In (4.17), M's are the string scale masses coming from (4.11) and (4.16), p is the analogue of m from (4.13) for the muon sector, q is the cross-term between the e and μ sector coming from (4.6).

The mass matrix \mathcal{M} can be diagonalized by a bi-unitary transformation. Two of the eigenvalues are small with mass of order m and p. These are the masses of the two light neutrinos, m_{ν_e} and m_{ν_μ} . The other four eigenvalues are of order M, giving very heavy neutrinos which are essentially SM singlets. As in the one family model, the mixing between these light and heavy neutrinos are extremely small, of order m/M . Thus, the coupling of these light neutrinos to the gauge bosons are essentially same as in the SM. Two very important features of (4.18) to note are the following. The off-diagonal element q in the first (2×2) sector of \mathcal{M} is of the same order as m and p. So, the light masses m_{ν_e} and m_{ν_μ} are of the same order and thus there is no hierarchy between these two masses, as is the case experimentally. Furthermore, since m, p, q are all of the same order, we naturally get large mixing between m_{ν_e} and m_{ν_μ} , in agreement with the experimental observation. Enlarging the mass matrix (4.18) to include up to n^{th} KK excitations, we get two light Dirac neutrinos of mass $\sim m$ and two very heavy Dirac neutrinos of masses $\sim M$.

Although we have included only the first two KK modes of N and N' , this pattern persists if we include the other higher modes. We can easily extend the model to include three families. The left handed doublets are $l_e(e, y)$, $l_\mu(x, y)$ and $l_\tau(x, y)$. The SM singlets are $N(x, y)$, $N'(x, y)$ and $N''(x, y)$. Then, writing the bulk interactions analogous to (4.15) and (4.16) to include all the above fields, we get the three family mass matrix. Again, keeping the terms only up to $N_L^2, N_R^2, N_L'^2, N_R'^2, N_L''^2, N_R''^2$, we get a 9x9 mass matrix. Choosing the basis as:

$$\begin{aligned} \bar{L} &= (\bar{\nu}_{eL}^0, \bar{\nu}_{\mu L}^0, \bar{\nu}_{\tau L}^0, \bar{N}_L^1, \bar{N}'_L^1, \bar{N}''_L^1, \bar{N}_L^2, \bar{N}'_L^2, \bar{N}''_L^2), \\ R &= (N_R^0, N_R'^0, N_R''^0, N_R^1, N_R'^1, N_R''^1, N_R^2, N_R'^2, N_R''^2). \end{aligned}$$

The 9x9 mass matrix then becomes:

$$\mathcal{M} = \begin{pmatrix} m_0 & m_{01} & m_{02} & \sqrt{2}m_0 & \sqrt{2}m_{01} & \sqrt{2}m_{02} & \sqrt{2}m_0 & \sqrt{2}m_{01} & \sqrt{2}m_{02} \\ m_{01} & m_1 & m_{12} & \sqrt{2}m_{01} & \sqrt{2}m_1 & \sqrt{2}m_{12} & \sqrt{2}m_{01} & \sqrt{2}m_1 & \sqrt{2}m_{12} \\ m_{02} & m_{12} & m_2 & \sqrt{2}m_{02} & \sqrt{2}m_{12} & \sqrt{2}m_2 & \sqrt{2}m_{02} & \sqrt{2}m_{12} & \sqrt{2}m_2 \\ 0 & 0 & 0 & m'_0 & 0 & 0 & M_0 & M_{01} & M_{02} \\ 0 & 0 & 0 & 0 & m'_1 & 0 & M_{01} & M_1 & M_{12} \\ 0 & 0 & 0 & 0 & 0 & m'_2 & M_{02} & M_{12} & M_2 \\ 0 & 0 & 0 & M_0 & M_{01} & M_{02} & 2m'_0 & 0 & 0 \\ 0 & 0 & 0 & M_{01} & M_1 & M_{12} & 0 & 2m'_1 & 0 \\ 0 & 0 & 0 & M_{02} & M_{12} & M_2 & 0 & 0 & 2m'_2 \end{pmatrix}$$

The mass matrix, \mathcal{M} can be diagonalized by a bi-unitary transformation. Three of the eigenvalues are small, of the order of $\sim m$, while the other six eigenvalues are of the order $M \sim TeV$ scale or higher. The parameters in the mass matrix can be suitable chosen to obtain values of the light neutrino masses and mixings in the observed range. For example, one such choice is $m_0 = 0.00157$, $m_1 = 0.025$, $m_2 = 0.029$, $m_{01} = 0.015$, $m_{02} = 0$, $m_{12} = 0.028$, $m'_0 = m'_1 = m'_2 = 0.001$, $M_0 = 10^{14}$, $M_1 = 2 * 10^{15}$, $M_2 = 8 * 10^{15}$, $M_{01} = 10^{15}$, $M_{02} = 0$, $M_{12} = 6 * 10^{15}$.

In the numerical evaluations above, we used the following constrains:

$$7.1 \times 10^{-5} eV \leq \Delta m_{12}^2 \leq 8.9 \times 10^{-5} eV$$

$$\begin{aligned}
0.70 &\leq \sin^2 2\theta_{12} \leq 0.94 \\
1.4 \times 10^{-3} eV &\leq |\Delta m_{23}^2| \leq 3.3 \times 10^{-3} eV \\
\sin^2 2\theta_{23} &\geq 0.87 \\
\sin^2 2\theta_{13} &\leq 0.051 \ .
\end{aligned}$$

Although we have included only the first two KK modes of N , N' and N'' , this pattern of three light neutrino masses, and the rest very heavy, persists if we include any number of KK modes.

The model produces the hierarchy of masses between m_e and m_ν naturally if we assume that the 2^{nd} family lives in a fat brane of much smaller size. For three families, charged lepton mass ratios are essentially given by (assuming the bulk Yukawa couplings are of the same order):

$$m_e : m_\mu : m_\tau = \sqrt{\frac{1}{R_1}} : \sqrt{\frac{1}{R_2}} : \sqrt{\frac{1}{R_3}} \quad (4.19)$$

where R_1, R_2 and R_3 are the sizes of the fat branes for the three families. Using the experimental values of the masses in (4.19), we get :

$$R_1^{-1} : R_2^{-1} : R_3^{-1} \sim 1 \text{ TeV} : 10^4 \text{ TeV} : 10^6 \text{ TeV} \ . \quad (4.20)$$

4.2.2 Results

There are several interesting phenomenological implications (of our model) which can be tested in the upcoming neutrino experiments and high energy colliders. The light neutrinos in our model are Dirac particles. So neutrinoless double beta decay is not allowed in our model. This is a very distinctive feature of our model compared to the traditional see-saw mechanism. In the see-saw model, light neutrinos are Majorana particles, and thus neutrinoless double beta decay is allowed. Current limit on the double beta decay is $m_{ee} \sim 0.3 \text{ eV}$. This limit is expected to go down to about $m_{ee} \sim 0.01 \text{ eV}$ in future experiments [40]. If no neutrinoless double beta decay is observed to that limit, that will cast serious doubts on the see-saw model. In our model, of course, it is not allowed at any level.

Another interesting feature of our model is for the observation of the Kaluza-Klein (KK) excitations of the SM particles at the high energy colliders, such as LHC. In the ADD scenario, the SM particles are confined to a four dimensional wall (D_3 brane). So, no KK excitations of the SM particles exist. In the universal extra dimensions scenario, all the SM particles propagate into the extra dimensions, and the current limit on the compactification scale from Tevatron collider is about 350 GeV [10,11]. So, if the compactification scale is few TeV or lower, we would observe the KK excitations of all the SM particles at the upcoming LHC. In contrast, in our model, the SM particles live in a fat branes. The sizes of the fat branes are of different values for the three families. If the large extra dimension, r is of submm size, then to obtain the right value of the electron neutrino mass, (4.9), we get the size of the fat brane for the first family, $R_1^{-1} \sim 1 \text{ TeV}$, while the other sizes for the 2^{nd} and 3^{rd} families are around 10^4 TeV and 10^6 TeV respectively. Thus, unlike in the UED model, only the KK excitations of the first family will be observed at the LHC, but not those of the 2^{nd} and 3^{rd} family. Thus is a very distinguishing feature of our model compared to UED [12] and ADD models, or even to the simpler model used in the previous chapter.

In models in which the SM particles propagate into the extra dimensions, the unification of the three gauge couplings are accelerated due to the contribution of the KK modes of the SM particles. Above the compactification scale, the evolution of the gauge couplings become power law, instead of logarithmic as in the 4D case. In our model, since KK excitation of the 1st family has much lower compactification scale (order TeV) compared to the second and third family, the unification will take place at a higher scale than in UED.

One interesting question to ask in our model is where do the SM gauge bosons live? Since the three SM families live in fat branes of three different sizes, are their gauge coupling universal (i.e. same for all three families). To be specific, let us assume that the SM gauge bosons live in a fat brane of size R' , where $R' \geq R_i$. Then, their

coupling to the SM fermions of the i^{th} family is given by:

$$\begin{aligned}
S_{gauge}^i &= \int d^4x \int_0^{\pi R_i} dy \frac{1}{(\sqrt{\pi R_i})^2 \sqrt{\pi R}} g_5 \bar{f}_i(x, y) \Gamma^\mu T^a f_i(x, y) A_\mu^a \\
&= \int d^4x \frac{g_5}{\sqrt{\pi R}} [\bar{f}_i^0 \gamma^\mu T^a f_i^0 A_\mu^{a0} + KK \text{ terms}]
\end{aligned} \tag{4.21}$$

Note that as long as R_i is smaller than R , the four dimensional gauge couplings are universal for all three families. One very interesting implication of this is that the compactification scale for the SM gauge bosons are smaller than the sizes of the fat branes for all three SM fermionic families. Thus, in our model, the KK excitations of the gauge bosons are lighter than the KK excitations of the fermions, and will be the first ones to be observed at the LHC.

There are several other features of our model that can be tested in the high energy colliders such as the Tevatron or LHC. As in the UED, KK particles can only be pair produced in our model because of the KK number conservation. However, only the KK excitations of the gluons and the first family of fermions are accessible. The KK excitations of the 2^{nd} and 3^{rd} families are not accessible even at LHC. Thus, the number of final states in the production processes is significantly reduced. This effect is even more because of the doubling of the KK states. Because of this reduction in the production cross section, current Tevatron bound of 350 GeV [11],[19] on the compactification scale will be reduced further. Also, in our scenario, KK excitations of the gluons are lighter than the KK excitations of the quarks. One loop correction to the KK masses will be somewhat larger for the KK gluons than those of the KK quarks. However, if the R'^{-1} is significantly smaller than R_1^{-1} , this correction may not be enough (this is in contrast to UED where g^* is always heavier than q^*). This will have interesting implications for their decays and the final state collider signals.

CHAPTER 5

CONCLUSIONS

In this thesis we investigated the phenomenological consequences of models embedding extra dimensions and fat branes. As opposed to the standard Universal Extra Dimensions (UED) models, where the first KK excited states are stable due to KK number conservation and thus produced only in pairs, our model, involving matter fields propagating on fat branes, escapes the previously mentioned constrain by allowing for gravity interactions not obeying the KK number-conservation. In this way, in our model we can produce single KK excitations which in turn can either decay directly gravitationally into SM particles plus an undetectable graviton, or can cascade to the lightest KK particle (LKP) which will decay again gravitationally . So the experimental signal will be jet (or jets) plus missing energy. We have shown that for certain range of the parameter space, the UED plus fat branes scenario gives observable signal above the backgrounds in the two jet plus missing energy channel available at Tevatron or LHC. The Tevatron can probe in this channel KK masses up to few hundred* GeV while LHC's reach is up to $7 TeV$ (again, see the footnote).

In the case of the monojet plus missing energy channel, the background coming from the usual ADD scenario is typically bigger than the signal from UED plus fat branes, even when one imposes quite hard cuts on the missing transverse momentum of the jet. But this is valid only at tree level. When one includes radiative corrections, the degeneracy of the KK excitations for a given level is lifted and that allows for different decay chains. As a function of the parameters involved, now a KK excitation can either decay directly gravitationally (like in the two jet channel) or can cascade to the lightest KK particle (usually γ^*) which in turn will produce a γ and missing

*Depending on the assumed value of the fundamental scale of gravity, M_D , and on the number of extra dimensions.

energy. While the direct gravitational decay is still unobservable due to the ADD background, the single photon plus missing energy channel has a smaller background (mostly due to electroweak processes) and thus allowing for discovery. The LHC will be able to probe M_D scales between 7 TeV (for six extra dimensions) and 40 TeV (for two extra dimensions).

In the lepton sector, using a slightly more sophisticated UED plus fat branes scenario, we found that we can account for the observed neutrino masses and mixing angles and we were able also to relate the lack of hierarchy in neutrino masses with the highly hierarchical charged lepton masses.

In summary, we can conclude that the models based on UED and incorporating fat branes provide a rich phenomenology and their full potential is yet to be explored, understood and achieved.

BIBLIOGRAPHY

1. G. Nordstrom, Phys. Zeitsch. **15**, 504 (1914).
2. T. Kaluza, Sitzungsber. Preuss. Akad. Wiss. Berlin (Math. Phys.)**1921**, 966 (1921).
3. O. Klein, Z. Phys. **37**, 895 (1926); Nature **118**, 516 (1926).
4. S.L. Glashow, Nucl. Phys. **22**, 579 (1961); A. Salam, Weak and Electromagnetic Interactions in Elementary Particle Theory, W. Svortholm ed, Almquist and Wiksell, Stockholm 1968; S. Weinberg, Phys. Rev. Lett. **19**, 1264 (1967).
5. N. Arkani-Hamed, S. Dimopoulos and G. Dvali, Phys. Lett. **B** 429, 263 (1998); N. Arkani-Hamed, S. Dimopoulos and G. Dvali, Phys. Rev. **D** 59, 086004 (1999); I. Antoniadis, N. Arkani-Hamed, S. Dimopoulos and G. Dvali, Phys. Lett. **B** 436, 257 (1998).
6. G.R. Dvali, G. Gabadadze and M. Porrati, Phys. Lett. **B** 484, 112 (2000); N. Arkani-Hamed, S. Dimopoulos, G. Dvali and N. Kaloper, Phys. Rev. Lett. **84**, 586 (2000).
7. J.D. Lykken and S. Nandi, Phys. Lett. **B** 485, 224 (2000).
8. L. Randall and R. Sundrum, Phys. Rev. Lett. **83**, 3370 (1999); L. Randall and R. Sundrum, Phys. Rev. Lett. **83**, 4690 (1999).
9. A. De Rujula, A. Donini, M.B. Gavela and S. Rigolin, Phys. Lett. **B** 482, 195 (2000).
10. E. Accomando, I. Antoniadis and K. Benakli, Nucl. Phys. **B** 579, 3 (2000); P. Nath, Y. Yamada and M. Yamaguchi, Phys. Lett. **B** 466, 100 (1999); D.A. Dicus, C.D. McMullen and S. Nandi, Phys. Rev. **D** 65, 076007 (2002); T.G. Rizzo, Phys. Rev. **D** 61, 055005 (2000); M. Masip and A. Pomarol, Phys. Rev. **D** 60, 096005 (1999); T.G. Rizzo and J.D. Wells, Phys. Rev. **D** 61, 016007 (2000).
11. T. Appelquist, H.C. Cheng and B.A. Dobrescu, Phys. Rev. **D** 64 035002 (2001).
12. C. Macesanu, S. Nandi and C.M. Rujoiu, Phys. Rev. **D** 71, 036003 (2005).

13. C. Macesanu, S. Nandi and C.M. Rujoiu, Phys. Rev. **D** 73, 076001 (2006).
14. S. Nandi and C.M. Rujoiu, hep-ph/0603243.
15. S. Weinberg, Phys. Rev. Lett. **19**, 1264 (1967) ; A. Salam, p. 367 of Elementary particle Theory, ed. N. Svartholm (Almquist and Wiksells, Stockholm, 1969); S.L. Glashow, J. Illiopoulos and L. Maiani, Phys. Rev. **D** 2 1285 (1970).
16. S. Eidelman et al., Particle Data Group, Phys. Lett. **B** 592, 1 (2004).
17. K.R. Dienes, E. Dudas and T. Gherghetta, Nucl. Phys. **B** 537, 47 (1999).
18. J. Papavassiliou and A. Santamaria, Phys. Rev. **D** 63, 125014 (2001).
19. C. Macesanu, C.D. McMullen and S. Nandi, Phys. Rev. **D** 66, 015009 (2002).
20. T. Han, J.D. Lykken and R.J. Zhang, Phys. Rev. **D** 59, 105006 (1999).
21. C. Macesanu, A. Mitov and S. Nandi, Phys. Rev. **D** 68, 084008 (2003).
22. A. DeRujula, A. Donini, M.B. Gavela and S. Rigolin, Phys. Lett. **B** 482, 195 (2000); T.G. Rizzo, Phys. Rev. **D** 64, 095010 (2001).
23. I. Gogoladze and C. Macesanu, hep-ph/0605207.
24. J.A.M. Vermaseren, "New features of FORM", math-ph/0010025.
25. H. Baer, C.H. Cheng, F. Paige and X. Tata, Phys. Rev. **D** 52, 2746 (1995).
26. I. Gaines et al., Fermilab Report No. FERMILAB-FN-0642 (unpublished).
27. F. Maltoni and T. Stelzer, J. High Energy Physics **02**, 027 (2003).
28. G.F. Giudice, R. Rattazzi and J.D. Wells, Nucl. Phys. **B** 544, 3 (1999).
29. E.A. Mirabelli, M. Perelstein and M.E. Peskin, Phys. Rev. Lett. **82**, 2236 (1999).
30. H.C. Cheng, K.T. Matchev and M. Schmaltz, Phys. Rev. **D**66, 036005, 2002; Phys. Rev. **D**66, 056006, (2002); A. Datta, K. Kong, K.T. Matchev, Phys. Rev. **D**72, 096006 (2005) and Erratum-ibid. **D**72, 119901 (2005).
31. American Physical Society Multidivisional Neutrino Study, <http://www.aps.org/neutrino/index.cfm>.
32. Neutrino Unbound, <http://www.nu.to.infn.it/> .
33. Super-Kamiokande Collaboration, Y. Ashie et al., Phys. Rev. **D** 71 11205 (2005); Super-Kamiokande Collaboration, Y. Ashie et al., Phys. Rev. Lett. **93** 101801 (2004).

34. SNO Collaboration, S.N. Ahmed et al., nucl-ex/0309004; SNO Collaboration, Q.R. Ahmad et al., Phys. Rev. Lett. **89** 011301 (2002); Super-Kamiokande Collaboration, S. Fukuda et al., Phys. Lett. **B** 539 179 (2002); Super-Kamiokande Collaboration, M.B. Smy et al., Phys. Rev. **D** 69 011104 (2004).
35. P. Minkowski, Phys. Lett. **B** 67 421 (1977), M. Gell-Mann, P. Ramond, and R. Slansky, Supergravity (P. van Nieuwenhuizen et al. eds.), North Holland, Amsterdam, 1980, p. 315; T. Yanagida, in Proceedings of the Workshop on the Unified Theory and the Baryon Number in the Universe (O. Sawada and A. Sugamoto, eds.), KEK, Tsukuba, Japan, 1979, p. 95; S. L. Glashow, The future of elementary particle physics, in Proceedings of the 1979 Carg'ese Summer Institute on Quarks and Leptons (M. Levy et al. eds.), Plenum Press, New York, 1980, pp. 68771 R. N. Mohapatra and G. Senjanovic, Phys. Rev. Lett. **44** 912 (1980).
36. K.R. Dienes, E. Dudas and T. Gherghetta, Nucl. Phys. **B** 557 25 (1999).
37. N. Arkani-Hamed, S. Dimopoulos, G. Dvali and J. March-Russell, Phys. Rev. **D** 65 024032 (2002).
38. G. Dvali and A.Y. Smirnov, Nucl. Phys. **B** 563 466 (2000); R.N. Mohapatra, S. Nandi and A. Perez-Lorenzana, Phys. Lett. **B** 466 115 (1999); R.N. Mohapatra and A. Perez-Lorenzana, Nucl. Phys. **B** 576 466 (2000); *ibid.*, Nucl. Phys. **B** 593 451 (2001); H. Davoudias, P. Langacker and M. Perelestein, Phys. Rev. **D** 65 105015 (2002); R. Barbieri, P. Creminelli and A. Strumia, Nucl. Phys. **B** 585 28 (2000); A. Ioannisian and A. Pilaftsis, Phys. Rev. **D** 62 066001 (2000).
39. N. Arkani-Hamed and M. Schmaltz, Phys. Rev. **D** 61 115004 (2000); N. Arkani-Hamed, Y. Grossman and M. Schmaltz, Phys. Rev. **D** 61 033005 (2000).
40. L. Baudis et al. Phys. Rev. Lett. **83** 41 (1999); IGEX Collaboration, C.E. Aalseth et al., Phys. Rev. **D** 65 092007 (2002); I. Abd et al., hep-ex/0404039.

APPENDICES

APPENDIX A

Standard Model and Extra Dimensions

In this Appendix we give the SM particle content, the Feynman rules for matter-gravity interactions.

A.1 Standard Model particle content

Fields	Notation	$SU(3)_C$	$SU(2)_W$	$U(1)_Y$
Quarks	$Q_\alpha^i = \begin{pmatrix} u_\alpha^i \\ d_\alpha^i \end{pmatrix}$	3	2	$\frac{1}{3}$
	u_α^{ci}	$\bar{3}$	1	$-\frac{2}{3}$
	d_α^{ci}	$\bar{3}$	1	$\frac{1}{3}$
Leptons	$\ell_\alpha = \begin{pmatrix} \nu_\alpha \\ e_\alpha \end{pmatrix}$	1	2	-1
	e_α^c	1	1	2
Gluon	G_μ^a	8	1	0
Intermediate weak bosons	W_μ^r	1	3	0
Hypercharge gauge boson	B_μ	1	1	0
Higgs boson	$\phi = \begin{pmatrix} \phi^+ \\ \phi^0 \end{pmatrix}$	1	2	$\frac{1}{2}$

TABLE A.1. Particle content of the SM. Here $\alpha = 1, 2, 3$ is the generation index, $i = 1 - 3$ (color), $a = 1 - 8$ ($SU(3)_C$ generators) and $r = 1 - 3$ ($SU(2)_L$ generators).

Fields	Notation	Mass	Electric Charge
Quarks	u	$1.5 - 4MeV$	$+2/3$
	d	$4 - 8MeV$	$-1/3$
	s	$80 - 130MeV$	$-1/3$
	c	$1.15 - 1.35GeV$	$+2/3$
	b	$4.1 - 4.9GeV$	$-1/3$
	t	$178GeV$	$+2/3$
Leptons	ν_e	$< 3eV$	0
	ν_μ	$< 0.19MeV$	0
	ν_τ	$< 18.2MeV$	0
	e	$0.51MeV$	-1
	μ	$105.65MeV$	-1
	τ	$1776.99GeV$	-1
Gluon	g	0	0
Intermediate weak bosons	W^\pm	$80.42GeV$	± 1
	Z	$91.18GeV$	0
Hypercharge gauge boson	γ	0	0
Higgs boson	H	$> 114.4GeV$	0

TABLE A.2. Particle masses and electric charges according to [16]. Only the central values are quoted.

A.2 Feynman rules for matter-gravity interactions

The notations used in table A.3 are the following

	$T_{\mu\nu}$	$T_{5\mu}$	T_{55}
S	$(C_{\mu\nu,\rho\sigma}k_1^\rho k_2^\sigma + m_\Phi^2 \eta_{\mu\nu}) \mathcal{F}_{lm n}^{(cc)} + \frac{ml}{R^2} \eta_{\mu\nu} \mathcal{F}_{lm n}^{(ss)}$	$i \left(k_{2\mu} \frac{l}{R} \mathcal{F}_{lm n}^{(sc)} - k_{1\mu} \frac{m}{R} \mathcal{F}_{lm n}^{(cs)} \right)$	$(k_1 k_2 - m_\Phi^2) \mathcal{F}_{lm n}^{(cc)} + \frac{ml}{R^2} \mathcal{F}_{lm n}^{(ss)}$
V	$[(m_B^2 - k_1 k_2) C_{\mu\nu,\alpha\beta} - D_{\mu\nu,\alpha\beta}(k_1, k_2)] \mathcal{F}_{lm n}^{(cc)}$ $+ \frac{ml}{R^2} C_{\mu\nu,\alpha\beta} \mathcal{F}_{lm n}^{(ss)}$	$i \left[-\frac{m}{R} D'_{\rho\mu,\alpha\beta} k_1^\rho \mathcal{F}_{lm n}^{(cs)} \right.$ $\left. + \frac{l}{R} D'_{\mu\rho,\alpha\beta} k_2^\rho \mathcal{F}_{lm n}^{(sc)} \right]$	$-(D'_{\rho\sigma,\alpha\beta} k_1^\rho k_2^\sigma - m_B^2 \eta_{\alpha\beta}) \mathcal{F}_{lm n}^{(cc)}$ $-\frac{ml}{R^2} \eta_{\alpha\beta} \mathcal{F}_{lm n}^{(ss)}$
F	$\frac{1}{4} C'_{\mu\nu,\rho\sigma} \gamma^\rho (k_1 + k_2)^\sigma \mathcal{G}_{lm n}^{(c)\mp} + \eta_{\mu\nu} \mathcal{A}_{lmn}^\pm$	$\frac{i}{4} \left[(k_1 + k_2)_\mu \mathcal{G}_{l,-m n}^{(s)\pm} + \gamma_\mu \mathcal{B}_{lmn}^\pm \right]$	$\frac{1}{2} (k_1 + k_2) \mathcal{G}_{lm n}^{(c)\mp} \mp \frac{m_Q}{2} \mathcal{G}_{lm n}^{(s)\pm}$

TABLE A.3. The bilinear terms of the matter energy-momentum tensor in momentum representation.

$$\begin{aligned}
C_{\mu\nu,\rho\sigma} &= -\eta_{\mu\nu}\eta_{\rho\sigma} + \eta_{\mu\rho}\eta_{\nu\sigma} + \eta_{\mu\sigma}\eta_{\nu\rho} \\
C'_{\mu\nu,\rho\sigma} &= -2\eta_{\mu\nu}\eta_{\rho\sigma} + \eta_{\mu\rho}\eta_{\nu\sigma} + \eta_{\mu\sigma}\eta_{\nu\rho} \\
D_{\mu\nu,\rho\sigma}(k_1, k_2) &= \eta_{\mu\nu}k_{1\sigma}k_{2\rho} - [\eta_{\mu\sigma}k_{1\nu}k_{2\rho} + \eta_{\mu\rho}k_{1\sigma}k_{2\nu} - \eta_{\rho\sigma}k_{1\mu}k_{2\nu} + (\mu \leftrightarrow \nu)] \\
D'_{\rho\sigma,\alpha\beta} &= \eta_{\rho\sigma}\eta_{\alpha\beta} - \eta_{\rho\beta}\eta_{\alpha\sigma} \\
\mathcal{A}_{lmn}^{\pm} &= \frac{1}{2R} \left(l\mathcal{G}_{lm|n}^{(c)\pm} + m\mathcal{G}_{lm|n}^{(c)\mp} \right) \pm m_Q \mathcal{G}_{lm|n}^{(s)\pm} \\
\mathcal{B}_{lmn}^{\pm} &= \frac{1}{R} \left(l\mathcal{G}_{l,-m|n}^{(s)\pm} + m\mathcal{G}_{l,-m|n}^{(s)\mp} \right) \\
\mathcal{G}_{lm|n}^{(c)\pm} &= \left(\mathcal{F}_{l-m|n}^{(c)\pm} \pm \mathcal{F}_{l+m|n}^{(c)\pm} \gamma_5 \right) / 2 \\
\mathcal{G}_{lm|n}^{(s)\pm} &= \left(\mathcal{F}_{l+m|n}^{(s)\pm} \pm \mathcal{F}_{l-m|n}^{(s)\pm} \gamma_5 \right) / 2 \\
\mathcal{F}_{\dots l_i \dots |n}^{(\dots f_i \dots)} &= \int_0^{\pi R} dy \prod_i c_i f_i \left(\frac{l_i y}{R} \right) \exp(2\pi i \frac{ny}{r}) \tag{A.1}
\end{aligned}$$

with $f_i(\dots)$ either $\sin(\dots)$ or $\cos(\dots)$ and

$$c_i = \begin{cases} \sqrt{\frac{2}{\pi R}}, & l_i \neq 0 \\ \sqrt{\frac{1}{\pi R}}, & l_i = 0 \end{cases}$$

The upper/lower sign in the above relations corresponds to the case of the doublet/singlet interacting fermions.

APPENDIX B

Single KK production

In this Appendix we give the listing of an example FORM program for a gravity mediated process, the ISAJET input listing for two jet plus Z production and the amplitudes squared and mediated for KK graviton plus a KK excitation production.

B.1 FORM program listing

The following example program is giving the matrix element squared for the s-channel of the process $q\bar{q} \rightarrow q^*\bar{q}$. Of course, one still needs to compute the t and u channel diagrams from Fig. 3.2 as well as the interference terms in order to obtain the full result given in (5). Lines beginning with "*" are comment lines.

```
*-
*- production of SM fermions mediated by gravitons
*- vertices from MMN Phys. Rev.D71,036003(2005)
*- definitions of the "variables"
*-
Vectors k1,k2,k,q1,q2,q,kd,kt;
Indices mu,nu,si,ro, mu1,nu1,si1,ro1,phi,the,
    al,be,mup,nup,rop,sip;
* masses graviton,initial KK particle
Symbols mg,mKK,t,m,s,u,a,tp,up;
.global
```

```

*-
*- various functions for vertices from Phys.Rev.D59,105006(1999)
*- (Eqs. A10, A11, A12)
*- or ec. (24) from Phys. Rev.D71,036003(2005)
*-

G Cf(mu,nu,ro,si) = d_(mu,ro)*d_(nu,si) + d_(mu,si)*d_(nu,ro) -
                    d_(mu,nu)*d_(ro,si);

G Cfp(mu,nu,ro,si) = d_(mu,ro)*d_(nu,si) + d_(mu,si)*d_(nu,ro) -
                    2*d_(mu,nu)*d_(ro,si);

G ds(mu,nu,k) = d_(mu,nu) - k(mu)*k(nu)/mg^2;

.store

*-
*- projection operators for the two fermionic lines
*-

G PL1 = (1-g5_(1))/2;
G PR1 = (1+g5_(1))/2;
G PL2 = (1-g5_(2))/2;
G PR2 = (1+g5_(2))/2;

.store

*-
*- sum over polarizations of spin 2 graviton<=>the propagator

```


*- w/o $1/(s-m)$

*-

*G Bf(mu,nu,ro,si,k) = ds(mu,ro,k)*ds(nu,si,k) +

* ds(mu,si,k)*ds(nu,ro,k) -

* 2/3 * ds(mu,nu,k)*ds(ro,si,k) ;

*G Bfs(mu,nu,ro,si) = d_(mu,ro)*d_(nu,si) + d_(mu,si)*d_(nu,ro) -

* 2/3 * d_(mu,nu)*d_(ro,si) ;

*G Bfss(mu,nu,ro,si) = 2/3 * d_(mu,nu)*d_(ro,si) ;

G Bfeff(mu,nu,ro,si) = d_(mu,ro)*d_(nu,si) + d_(mu,si)*d_(nu,ro);

*- Note : you can use Bfeff for the spin 2 graviton propagator;

*- terms with k (also, the Bfss term) will be zero

.store

*-

*- interactions with the spin 2 graviton:

*- dirac spinor vertex with $h_{\mu\nu}$, both moments go in

*-

G Vspin1(mu,nu,k1,k2) = 1/8 * Cfp(mu,nu,ro,si)*g_(1,ro)*
(k1(si)-k2(si));

G Vspin2(mu,nu,k1,k2) = 1/8 * Cfp(mu,nu,ro,si)*g_(2,ro)*
(k1(si)-k2(si))*PL2 +

```

1/4 *d_(mu,nu) * mKK *PL2*a;

.store
*G Vspin2mix(mu,nu,k1,k2) = 1/8 * Cfp(mu,nu,ro,si)*g_(1,ro)*
*
*           (k1(si)+k2(si))*PL2 +
*
*           1/4 *d_(mu,nu) * mKK *PL2*a;
*.sort
*-
*- next functions defined for passing negative
*- arguments to functions in form....
*-
G Vspin1t(mu,nu,k1,k2) = 1/8 * Cfp(mu,nu,ro,si)*g_(1,ro)*
*           (k1(si)+k2(si));
G Vspin2t(mu,nu,k1,k2) = 1/8 * Cfp(mu,nu,ro,si)*g_(2,ro)*
*           (k1(si)+k2(si))*PL2 +
*           1/4 *d_(mu,nu) * mKK *PL2*a;
* Note that this last term does not matter, either; actually every term
* proportional to d_(mu,nu) in the second vertex will be 0
* note added:1/R is replaced by a*mKK....

*-
*- amplitude for qq->Q'qb'
*- k1 + k2 -> q1 + q2
*- (s-channel)
*- (will be the same for Q=Q')
*-

```

```

G MKK = Vspin1(mu,nu,k1,k2) * Bfeff(mu,nu,ro,si) *
    Vspin2(ro,si,q1,q2);
G MKKst = Vspin1(mu1,nu1,k1,k2) * Bfeff(mu1,nu1,ro1,si1) *
    Vspin2(ro1,si1,q1,q2);
contract;
.store

*- from s-channel
G MKKsq = g_(1,k2)*MKK*g_(1,k1)*g_(2,q2)*MKKst*(g_(2,q1)-mKK);
.sort
contract;
trace4 1;
trace4,2;

*- Kinematics s-ch
* k1 + k2 - q2 = q1 => s + u + t = mKK^2
* use up = -2 q1.k2, tp = -2 q1.k1
id q1= k1 + k2 - q2;
id k = k1 + k2;
id kt= k1 - q1;
*id q1.q1 = mKK^2;
id q2.q2 = 0;
id k1.k1 = 0;
id k2.k2 = 0;
id q1.q2 = (s-mKK^2)/2;
id k1.k2 = s/2;

```

```

id      q1.k1 = (mKK^2-t)/2;
id      q1.k2 = (mKK^2-u)/2;
id      q2.k1 = -u/2;
id      q2.k2 = -t/2;
*id     u = mKK^2-s-t;
.sort

*- RESULTS
b mKK,mg;
print MKKsq;
.end

```

B.2 Isajet code listing

```

TEST JJZ EXTRADIM QCD BACKGROUND
14000.,1000,1,1000/
ZJJ
P
1000,6000,20,7000,20,7000/
PT
20,6000,500,6000,500,6000/
MIJLIM
2,3,50,7000/
MTOT
20,7000/
NSIGMA
200/

```

```

NTRIES
1000000/
PDFLIB
'CTEQ',48D0/
END
STOP

```

B.3 Amplitudes squared and mediated for KK graviton plus a KK excitation production

Here we list all nine classes of Feynman diagrams contributing to the production of a KK graviton together with a KK excitation of a SM particle. The classification is based on the possible incoming states. Trying to keep the listing at a reasonable length, we use the following short-hand notations for the terms in the amplitudes:

$$\begin{aligned}
m_{KKsq} &= m_{KK} **2 \\
m_{KKfo} &= m_{KKsq} * m_{KKsq} \\
m_{KKsi} &= m_{KKsq} * m_{KKfo} \\
m_{KKei} &= m_{KKfo} * m_{KKfo} \\
m_{KKte} &= m_{KKsq} * m_{KKei} \\
m_{KKtw} &= m_{KKsi} * m_{KKsi} \\
m_{KKft} &= m_{KKfo} * m_{KKei} \\
m_{sq} &= m_{prodb} **2 \\
mg &= m_{prodb} \\
mgsq &= m_{sq} \\
mgfo &= mgsq * mgsq
\end{aligned}$$

$$\begin{aligned}
mgsi &= mgsq * mgfo \\
mgei &= mgfo * mgfo \\
mgte &= mgsq * mgei \\
(s, t, u)(i) &= (s, t, u)^{i-1} * s, i = 1 - n \\
s &= s1 \\
c11 &= 2./3. * (de_space - 1)/(de_space + 2) \\
c12 &= -2./(de_space + 2) \\
c22 &= 2. * (de_space + 1)/(de_space + 2) \tag{B.1}
\end{aligned}$$

1)

$$\begin{aligned}
t &= u1 + mgsq \\
u &= t1 + mKKsq
\end{aligned}$$

c -- for spin 2 graviton: q qb -> g* h_{mu,nu}

$$\begin{aligned}
Msq_qqb &= -(\\
&\cdot (-20*mgsq*mKKte)/3. - (14*mKKtw)/3. - (74*mgfo*mKKei)/3.- \\
&\cdot 4*mgei*mKKfo - 16*mgsi*mKKsi - 4*mgei*t*u + \\
&\cdot mgei*mKKsq*(4*t + 4*u) + mKK**10*(18*t + 18*u) + \\
&\cdot mgsi*mKKfo*(24*t + 24*u) + \\
&\cdot mgsq*mKKei*((116*t)/3. + (116*u)/3.) + \\
&\cdot mgfo*mKKsi*((194*t)/3. + (194*u)/3.) + \\
&\cdot mgsq*mKKsi*((-170*t^2)/3. - 134*t*u - (170*u^2)/3.) + \\
&\cdot mgfo*mKKfo*((-140*t^2)/3. - (382*t*u)/3. - (140*u^2)/3.) + \\
&\cdot mKKei*((-82*t^2)/3. - (218*t*u)/3. - (82*u^2)/3.) + \\
&\cdot mgsi*mKKsq*(-7*t^2 - 34*t*u - 7*u^2) + \\
&\cdot (mKK**10*(-t^2/3. - (16*t*u)/3. - u^2/3.))/mg**2 - 8*t^4*u^2 +
\end{aligned}$$

$$\begin{aligned}
& \cdot \text{mgsi}(8*t^2*u + 8*t*u^2) + \\
& \cdot (\text{mKKei}((4*t^3)/3. + 14*t^2*u + 14*t*u^2 + (4*u^3)/3.))/\text{mg}^{**2} + \\
& \cdot \text{mgfo}*\text{mKKsq}(4*t^3 + 72*t^2*u + 72*t*u^2 + 4*u^3) + \\
& \cdot \text{mKKsi}(((62*t^3)/3. + (266*t^2*u)/3. + (266*t*u^2)/3. + \\
& \cdot (62*u^3)/3.)) + \text{mgsq}*\text{mKKfo}* \\
& \cdot (28*t^3 + (410*t^2*u)/3. + (410*t*u^2)/3. + 28*u^3) + \\
& \cdot \text{mgfo}*(-6*t^3*u - 24*t^2*u^2 - 6*t*u^3) + \\
& \cdot (\text{mKKei}((-2*t^3*u)/3. - (4*t^2*u^2)/3. - (2*t*u^3)/3.))/\text{mg}^{**4} + \\
& \cdot \text{mKKfo}((-22*t^4)/3. - 50*t^3*u - (232*t^2*u^2)/3. - 50*t*u^3 - \\
& \cdot (22*u^4)/3.)) + \text{mgsq}*\text{mKKsq}* \\
& \cdot (-t^4 - (128*t^3*u)/3. - (316*t^2*u^2)/3. - (128*t*u^3)/3. - u^4) + \\
& \cdot (\text{mKKsi}(-t^4 - (38*t^3*u)/3. - 16*t^2*u^2 - (38*t*u^3)/3. - u^4))/ \\
& \cdot \text{mg}^{**2} - 8*t^2*u^4 + (\text{mKKsi}* \\
& \cdot ((2*t^4*u)/3. + 2*t^3*u^2 + 2*t^2*u^3 + (2*t*u^4)/3.))/\text{mg}^{**4} + \\
& \cdot \text{mgsq}(2*t^4*u + 18*t^3*u^2 + 18*t^2*u^3 + 2*t*u^4) + \\
& \cdot (\text{mKKfo}((16*t^4*u)/3. + 4*t^3*u^2 + 4*t^2*u^3 + (16*t*u^4)/3.))/ \\
& \cdot \text{mg}^{**2} + \text{mKKsq}((38*t^4*u)/3. + 30*t^3*u^2 + 30*t^2*u^3 + \\
& \cdot (38*t*u^4)/3.)) + (\text{mKKsq}*(-2*t^4*u^2 + 4*t^3*u^3 - 2*t^2*u^4))/ \\
& \cdot \text{mg}^{**2} \\
& \cdot + (\text{mKKfo}((-4*t^4*u^2)/3. - (4*t^2*u^4)/3.))/\text{mg}^{**4})
\end{aligned}$$

$$\text{Msq_qqb} = \text{Msq_qqb}/(t-\text{mKKsq})^{**2}/(u-\text{mKKsq})^{**2}/s *2./9. /2.$$

2)

$$t = t1$$

$$u = u1 - \text{mKKsq} + m_sq$$

c -- for spin 2 graviton: $g g \rightarrow g^* h_{\{\mu,\nu\}}$

$$\begin{aligned}
\text{Msq_gg} = & -16*mgte*t*u + 16*t^6*u + 48*t^5*u^2 \\
& . + 80*t^4*u^3 + 80*t^3*u^4 + \\
& . 48*t^2*u^5 + 16*t*u^6 + mgsq*mKKei* \\
& . ((-592*t^2)/3. + (80*t*u)/3. - (592*u^2)/3.) + \\
& . mg*si*mKKfo*(-136*t^2 + (160*t*u)/3. - 136*u^2) + \\
& . (mKKtw*((-88*t^2)/3. - (128*t*u)/3. - \\
& . (88*u^2)/3.))/mgsq + \\
& . (mKKft*((16*t^2)/3. + (40*t*u)/3. + \\
& . (16*u^2)/3.))/mgfo + \\
& . mg**8*mKKsq*(32*t^2 + 16*t*u + 32*u^2) + \\
& . mKKte*(96*t^2 + (128*t*u)/3. + 96*u^2) + \\
& . mg**4*mKKsi*((688*t^2)/3. - (280*t*u)/3. + \\
& . (688*u^2)/3.) + \\
& . mgei*(48*t^2*u + 48*t*u^2) + \\
& . mgsq*mKKsi*(-448*t^3 - 136*t^2*u - 136*t*u^2 \\
& . - 448*u^3) + \\
& . (mKKte*(-96*t^3 - 152*t^2*u - 152*t*u^2 - \\
& . 96*u^3))/mgsq + \\
& . mg*si*mKKsq*(-96*t^3 - 64*t^2*u - 64*t*u^2 \\
& . - 96*u^3) + \\
& . (mKKtw*(16*t^3 + 56*t^2*u + 56*t*u^2 + \\
& . 16*u^3))/mgfo + \\
& . mKKei*(288*t^3 + 200*t^2*u + 200*t*u^2 + 288*u^3) + \\
& . mgfo*mKKfo*(336*t^3 + 48*t^2*u + 48*t*u^2 + 336*u^3) +
\end{aligned}$$

$$\begin{aligned}
& \cdot \text{mgSi}*(-80*t^3*u - 64*t^2*u^2 - 80*t*u^3) + \\
& \cdot \text{mgSq}*\text{mKKfo}*(-312*t^4 - (904*t^3*u)/3. + \\
& \cdot (352*t^2*u^2)/3. - \\
& \cdot (904*t*u^3)/3. - 312*u^4) + \\
& \cdot (\text{mKKei}*((-376*t^4)/3. - (632*t^3*u)/3. - \\
& \cdot (640*t^2*u^2)/3. - \\
& \cdot (632*t*u^3)/3. - (376*u^4)/3.))/\text{mg}^{**2} + \\
& \cdot (\text{mKKte}*((56*t^4)/3. + (248*t^3*u)/3. + \\
& \cdot (400*t^2*u^2)/3. + \\
& \cdot (248*t*u^3)/3. + (56*u^4)/3.))/\text{mg}^{**4} + \\
& \cdot \text{mgfo}*\text{mKKsq}*(112*t^4 + 168*t^3*u - 96*t^2*u^2 \\
& \cdot + 168*t*u^3 + \\
& \cdot 112*u^4) + \text{mKKsi}*((920*t^4)/3. + \\
& \cdot (1024*t^3*u)/3. + \\
& \cdot (368*t^2*u^2)/3. + (1024*t*u^3)/3. + \\
& \cdot (920*u^4)/3.) + \\
& \cdot \text{mgfo}*(80*t^4*u + 48*t^3*u^2 + 48*t^2*u^3 + \\
& \cdot 80*t*u^4) + \\
& \cdot (\text{mKKsq}*(8*t^4*u^3 + 8*t^3*u^4))/\text{mgSq} + \\
& \cdot (\text{mKKsi}*((-224*t^5)/3. - 144*t^4*u - (352*t^3*u^2)/3. - \\
& \cdot (352*t^2*u^3)/3. - 144*t*u^4 - \\
& \cdot (224*u^5)/3.))/\text{mgSq} + \\
& \cdot \text{mgSq}*\text{mKKsq}*(-64*t^5 - 184*t^4*u + 8*t^3*u^2 + \\
& \cdot 8*t^2*u^3 - \\
& \cdot 184*t*u^4 - 64*u^5) + (\text{mKKei}* \\
& \cdot ((32*t^5)/3. + 56*t^4*u + (376*t^3*u^2)/3. +
\end{aligned}$$

$$\begin{aligned}
& \cdot (376*t^2*u^3)/3. + \\
& \cdot (56*t*u^4 + (32*u^5)/3.))/mgfo + \\
& \cdot mKKfo*(128*t^5 + (736*t^4*u)/3. + 96*t^3*u^2 + \\
& \cdot 96*t^2*u^3 + \\
& \cdot (736*t*u^4)/3. + 128*u^5) + \\
& \cdot mgsq*(-48*t^5*u - 64*t^4*u^2 - 48*t^3*u^3 \\
& \cdot - 64*t^2*u^4 - \\
& \cdot 48*t*u^5) + (mKKfo*(-16*t^6 - 40*t^5*u - \\
& \cdot (80*t^4*u^2)/3. - \\
& \cdot (80*t^2*u^4)/3. - 40*t*u^5 - 16*u^6))/mgsq + \\
& \cdot (mKKsi*((8*t^6)/3. + (56*t^5*u)/3. + \\
& \cdot (152*t^4*u^2)/3. + \\
& \cdot 72*t^3*u^3 + (152*t^2*u^4)/3. + (56*t*u^5)/3. \\
& \cdot + (8*u^6)/3.))/ \\
& \cdot mgfo + mKKsq*(16*t^6 + 80*t^5*u + 112*t^4*u^2 + \\
& \cdot 104*t^3*u^3 + \\
& \cdot 112*t^2*u^4 + 80*t*u^5 + 16*u^6) + \\
& \cdot (mKKfo*((8*t^6*u)/3. + 8*t^5*u^2 + (40*t^4*u^3)/3. + \\
& \cdot (40*t^3*u^4)/3. + 8*t^2*u^5 + (8*t*u^6)/3.))/mgfo
\end{aligned}$$

$$Msq_gg = -Msq_gg/t^2/u^2/s^2 *3./16.$$

3)

$$t = t1 + mKKsq$$

$$u = u1 + m_sq$$

c -- for spin 2 graviton: q g -> q* h_{mu,nu}

Msq_qg =

$$\begin{aligned}
& \cdot \left((55 \cdot \text{mgsq} \cdot \text{mKKte}) / 3. + (22 \cdot \text{mKKtw}) / 3. + (28 \cdot \text{mgfo} \cdot \text{mKKei}) / 3. + \right. \\
& \cdot 5 \cdot \text{mgsi} \cdot \text{mKKsi} + \text{mgsq} \cdot \text{mKKei} \cdot ((-140 \cdot t) / 3. - 79 \cdot u) + \\
& \cdot \text{mKK} \cdot 10 \cdot ((-76 \cdot t) / 3. - (142 \cdot u) / 3.) + \\
& \cdot \text{mgfo} \cdot \text{mKKsi} \cdot ((-52 \cdot t) / 3. - 20 \cdot u) + 8 \cdot t \cdot u \cdot u^5 + \\
& \cdot \text{mgsi} \cdot \text{mKKfo} \cdot (-16 \cdot t + u) + \\
& \cdot \text{mgfo} \cdot \text{mKKfo} \cdot (18 \cdot t^2 + (158 \cdot t \cdot u) / 3. - 6 \cdot u^2) + \\
& \cdot \text{mgsi} \cdot \text{mKKsq} \cdot (3 \cdot t^2 + 16 \cdot t \cdot u - 4 \cdot u^2) + 4 \cdot t^4 \cdot u^2 + \\
& \cdot (\text{mKK} \cdot 10 \cdot (t^2 / 3. + (8 \cdot t \cdot u) / 3. + (8 \cdot u^2) / 3.)) / \text{mgsq} + \\
& \cdot \text{mgsq} \cdot \text{mKKsi} \cdot ((124 \cdot t^2) / 3. + (418 \cdot t \cdot u) / 3. + (284 \cdot u^2) / 3.) + \\
& \cdot \text{mKKei} \cdot (36 \cdot t^2 + (404 \cdot t \cdot u) / 3. + 122 \cdot u^2) + \\
& \cdot \text{mgsi} \cdot (-(t^2 \cdot u) - 4 \cdot t \cdot u^2) + \\
& \cdot \text{mKKsi} \cdot ((-68 \cdot t^3) / 3. - (406 \cdot t^2 \cdot u) / 3. - (694 \cdot t \cdot u^2) / 3. - 120 \cdot u^3) + \\
& \cdot \text{mgsq} \cdot \text{mKKfo} \cdot ((-46 \cdot t^3) / 3. - (320 \cdot t^2 \cdot u) / 3. - 142 \cdot t \cdot u^2 - 24 \cdot u^3) + \\
& \cdot (\text{mKKei} \cdot ((-4 \cdot t^3) / 3. - 11 \cdot t^2 \cdot u - (56 \cdot t \cdot u^2) / 3. - (56 \cdot u^3) / 3.)) / \\
& \cdot \text{mgsq} + 12 \cdot t^3 \cdot u^3 + \text{mgfo} \cdot \text{mKKsq} \cdot \\
& \cdot (-2 \cdot t^3 - (74 \cdot t^2 \cdot u) / 3. - 40 \cdot t \cdot u^2 + 12 \cdot u^3) + \\
& \cdot (\text{mKKei} \cdot ((2 \cdot t^3 \cdot u) / 3. + (2 \cdot t^2 \cdot u^2) / 3. + (16 \cdot t \cdot u^3) / 3.)) / \text{mgfo} + \\
& \cdot \text{mgfo} \cdot (6 \cdot t^2 \cdot u^2 + 12 \cdot t \cdot u^3) + (\text{mKKsq} \cdot (2 \cdot t^4 \cdot u^2 + 2 \cdot t^3 \cdot u^3)) / \text{mgsq} + \\
& \cdot \text{mgsq} \cdot \text{mKKsq} \cdot (t^4 + 26 \cdot t^3 \cdot u + 76 \cdot t^2 \cdot u^2 + 66 \cdot t \cdot u^3 - 8 \cdot u^4) + \\
& \cdot 16 \cdot t^2 \cdot u^4 + (\text{mKKsi} \cdot (t^4 + (34 \cdot t^3 \cdot u) / 3. + 24 \cdot t^2 \cdot u^2 + \\
& \cdot (82 \cdot t \cdot u^3) / 3. + (68 \cdot u^4) / 3.)) / \text{mgsq} + \\
& \cdot \text{mKKfo} \cdot ((14 \cdot t^4) / 3. + (182 \cdot t^3 \cdot u) / 3. + (520 \cdot t^2 \cdot u^2) / 3. + \\
& \cdot 156 \cdot t \cdot u^3 + 40 \cdot u^4) + \text{mKKsq} \cdot \\
& \cdot ((-26 \cdot t^4 \cdot u) / 3. - 52 \cdot t^3 \cdot u^2 - 84 \cdot t^2 \cdot u^3 - 48 \cdot t \cdot u^4) +
\end{aligned}$$

$$\begin{aligned}
& \cdot \text{mgsq} * (-t^4 * u - 6 * t^3 * u^2 - 18 * t^2 * u^3 - 16 * t * u^4) + \\
& \cdot (\text{mKKfo} * (-3 * t^4 * u - 8 * u^5 - 14 * t^3 * u^2 - (32 * t^2 * u^3) / 3. - \\
& \cdot (32 * t * u^4) / 3.)) / \text{mgsq} + \\
& \cdot (\text{mKKsi} * ((-2 * t^4 * u) / 3. - (4 * t^3 * u^2) / 3. - 6 * t^2 * u^3 - \\
& \cdot (16 * t * u^4) / 3.)) / \text{mgfo} + \\
& \cdot (\text{mKKfo} * ((4 * t * u^5) / 3. + (2 * t^4 * u^2) / 3. + 2 * t^3 * u^3 + \\
& \cdot (8 * t^2 * u^4) / 3.)) / \text{mgfo})
\end{aligned}$$

$$\text{Msq_qg} = \text{Msq_qg} / (t - \text{mKKsq})^{**2} / (u - \text{mKKsq})^{**2} / s * 1. / 12. * 2.$$

4)

$$t = t1 + \text{mKKsq}$$

$$u = u1 + \text{m_sq}$$

c -- for spin 1 gravitons: q qb -> g* A_{\mu}

$$\begin{aligned}
\text{Msq_qqba} &= \text{mgsi} * \text{mKKsi} * (- 1) + \\
& \cdot \text{mgsi} * \text{mKKfo} * (t + u) + \\
& \cdot \text{mgsi} * \text{mKKsq} * (1./8.*t^2 - 5./4.*t*u + 1./8.*u^2) + \\
& \cdot \text{mgfo} * \text{mKKei} * (- 5./2.) + \\
& \cdot \text{mgfo} * \text{mKKsi} * (3*t + 3*u) + \\
& \cdot \text{mgfo} * \text{mKKfo} * (- 7./8.*t^2 - 7./4.*t*u - 7./8.*u^2) + \\
& \cdot \text{mgfo} * \text{mKKsq} * (- 3./8.*t^3 - 1./8.*t^2*u - 1./8.*t*u^2 - \\
& \cdot 3./8.*u^3) + \\
& \cdot \text{mgfo} * (1./8.*t^3*u + 3./4.*t^2*u^2 + 1./8.*t*u^3) + \\
& \cdot \text{mgsq} * \text{mKKte} * (- 3./2.) + \\
& \cdot \text{mgsq} * \text{mKKei} * (9./2.*t + 9./2.*u) +
\end{aligned}$$

```

. mgsq*mKKsi * ( - 13./4.*t2 - 9./2.*t*u - 13./4.*u2 )+
. mgsq*mKKfo * ( 1./2.*t3 - 1./2.*t2*u - 1./2.*t*u2 +
. 1./2.*u3 )+
. mgsq*mKKsq * ( 1./4.*t4 + 9./8.*t3*u + 7./4.*t2*u2 +
. 9./8.*t*u3 + 1./4.*u4 )+
. mgsq * ( - 1./8.*t4*u - 3./8.*t3*u2 - 3./8.*t2*u3 -
. 1./8.*t*u4 )+
. mKKsi/mgsq * ( 1./2.*t3*u + t2*u2 + 1./2.*t*u3 )+
. mKKfo/mgsq * ( - 1./2.*t4*u - 3./2.*t3*u2 - 3./2.*t2*u3 -
. 1./2.*t*u4)+ mKKsq/mgsq * ( t4*u2 + t2*u4 )+
. mKKei * ( - 1./4.*t2 - 1./4.*u2 )+
. mKKsi * ( - 5./2.*t2*u - 5./2.*t*u2 )+
. mKKfo * ( 1./4.*t4 + 3*t3*u + 5*t2*u2 + 3*t*u3 + 1./4.*u4 )+
. mKKsq * ( - 3./2.*t4*u - 3./2.*t3*u2 - 3./2.*t2*u3 -
. 3./2.*t*u4 )+1./2.*t4*u2 - t3*u3 + 1./2.*t2*u4

```

$$\text{Msq_qqba} = \text{Msq_qqba}/(t-m\text{KKsq})^{**2}/(u-m\text{KKsq})^{**2}/s^{*2./9. /2.}$$

5)

$$t = t1 + m\text{KKsq}$$

$$u = u1 + m_sq$$

c -- for spin 1 gravitons: g g -> g* A_{\mu}

```

Msq_gg = mgei*mKKsq * ( 2*t2 - 4*t*u + 2*u2 )+
. mgsi*mKKfo * ( - 12*t2 + 6*t*u - 12*u2 )+
. mgsi*mKKsq * ( - 12*t3 + 8*t2*u + 8*t*u2 - 12*u3 )+
. mgsi * ( 2*t3*u + 2*t*u3 )+

```

$$\begin{aligned}
& \cdot \text{mgfo} * \text{mKKsi} * (28*t^2 + 16*t*u + 28*u^2) + \\
& \cdot \text{mgfo} * \text{mKKfo} * (48*t^3 + 18*t^2*u + 18*t*u^2 + 48*u^3) + \\
& \cdot \text{mgfo} * \text{mKKsq} * (22*t^4 + 6*t^3*u - 16*t^2*u^2 + 6*t*u^3 + 22*u^4) + \\
& \cdot \text{mgfo} * (- 2*t^4*u - 2*t^3*u^2 - 2*t^2*u^3 - 2*t*u^4) + \\
& \cdot \text{mgsq} * \text{mKKei} * (- 32*t^2 - 44*t*u - 32*u^2) + \\
& \cdot \text{mgsq} * \text{mKKsi} * (- 72*t^3 - 102*t^2*u - 102*t*u^2 - 72*u^3) + \\
& \cdot \text{mgsq} * \text{mKKfo} * (- 58*t^4 - 80*t^3*u - 68*t^2*u^2 - 80*t*u^3 - 58*u^4) + \\
& \cdot \text{mgsq} * \text{mKKsq} * (- 16*t^5 - 24*t^4*u - 8*t^3*u^2 - 8*t^2*u^3 - \\
& \cdot 24*t*u^4 - 16*u^5) + \\
& \cdot \text{mgsq} * (2*t^3*u^3) + \\
& \cdot \text{mKKtw} / \text{mgsq} * (- 4*t^2 - 10*t*u - 4*u^2) + \\
& \cdot \text{mKKte} / \text{mgsq} * (- 12*t^3 - 42*t^2*u - 42*t*u^2 - 12*u^3) + \\
& \cdot \text{mKKei} / \text{mgsq} * (- 14*t^4 - 62*t^3*u - 100*t^2*u^2 - 62*t*u^3 - 14* \\
& \cdot u^4) + \\
& \cdot \text{mKKsi} / \text{mgsq} * (- 8*t^5 - 42*t^4*u - 94*t^3*u^2 - 94*t^2*u^3 - 42*t* \\
& \cdot u^4 - 8*u^5) + \\
& \cdot \text{mKKfo} / \text{mgsq} * (- 2*t^6 - 14*t^5*u - 38*t^4*u^2 - 54*t^3*u^3 - 38* \\
& \cdot t^2*u^4 - 14*t*u^5 - 2*u^6) + \\
& \cdot \text{mKKsq} / \text{mgsq} * (- 2*t^6*u - 6*t^5*u^2 - 10*t^4*u^3 - 10*t^3*u^4 - 6* \\
& \cdot t^2*u^5 - 2*t*u^6) + \\
& \cdot \text{mKKte} * (18*t^2 + 36*t*u + 18*u^2) + \\
& \cdot \text{mKKei} * (48*t^3 + 118*t^2*u + 118*t*u^2 + 48*u^3) + \\
& \cdot \text{mKKsi} * (50*t^4 + 134*t^3*u + 184*t^2*u^2 + 134*t*u^3 + 50*u^4) + \\
& \cdot \text{mKKfo} * (24*t^5 + 68*t^4*u + 104*t^3*u^2 + 104*t^2*u^3 + 68*t*u^4 + \\
& \cdot 24*u^5) + \\
& \cdot \text{mKKsq} * (4*t^6 + 14*t^5*u + 20*t^4*u^2 + 20*t^3*u^3 + 20*t^2*u^4 +
\end{aligned}$$

$$\begin{aligned} & \cdot 14*t*u^5 + 4*u^6)- \\ & \cdot 2*t^4*u^3 - 2*t^3*u^4 \end{aligned}$$

$$\text{Msq_gg} = -\text{Msq_gg}/t^2/u^2/s^2 *3./16.$$

6)

$$t = t1 + mKKsq$$

$$u = u1 + m_sq$$

c -- for spin 1 gravitons: q g -> q* A_{\mu}

$$\begin{aligned} \text{Msq_qg} = & \text{mgsi}*mKKsi * (- 27./4.)+ \\ & \cdot \text{mgsi}*mKKfo * (7./2.*t + 45./4.*u)+ \\ & \cdot \text{mgsi}*mKKsq * (- 3./4.*t^2 - 7./2.*t*u - 5*u^2)+ \\ & \cdot \text{mgsi} * (1./4.*t^2*u + t*u^2)+ \\ & \cdot \text{mgfo}*mKKei * (- 35)+ \\ & \cdot \text{mgfo}*mKKsi * (101./2.*t + 151./2.*u)+ \\ & \cdot \text{mgfo}*mKKfo * (- 14*t^2 - 89*t*u - 52*u^2)+ \\ & \cdot \text{mgfo}*mKKsq * (1./2.*t^3 + 43./2.*t^2*u + 37*t*u^2 + 13*u^3)+ \\ & \cdot \text{mgfo} * (- 7*t^2*u^2 - t*u^3)+ \\ & \cdot \text{mgsq}*mKKte * (- 45)+ \\ & \cdot \text{mgsq}*mKKei * (124*t + 129*u)+ \\ & \cdot \text{mgsq}*mKKsi * (- 401./4.*t^2 - 541./2.*t*u - 141*u^2)+ \\ & \cdot \text{mgsq}*mKKfo * (43./2.*t^3 + 669./4.*t^2*u + 205*t*u^2 + 66*u^3)+ \\ & \cdot \text{mgsq}*mKKsq * (- 1./4.*t^4 - 32*t^3*u - 73*t^2*u^2 - \\ & \cdot 54*t*u^3 - 12*u^4)+ \\ & \cdot \text{mgsq} * (1./4.*t^4*u + 9*t^3*u^2 + 6*t^2*u^3)+ \end{aligned}$$

```

. mKKte/mgsq * ( - 4*t2 - 8*t*u )+
. mKKei/mgsq * ( 8*t3 + 24*t2*u + 16*t*u2 )+
. mKKsi/mgsq * ( - 4*t4 - 21*t3*u - 29*t2*u2 - 16*t*u3 )+
. mKKfo/mgsq * ( 5*t4*u + 14*t3*u2 + 17*t2*u3 + 8*t*u4 )+
. mKKsq/mgsq * ( - t4*u2 - 3*t3*u3 - 4*t2*u4 -2*t*u5)+
. mKKtw * ( - 8 )+
. mKKte * ( 48*t + 48*u )+
. mKKei * ( - 167./2.*t2 - 172*t*u - 84*u2 )+
. mKKsi * ( 52*t3 + 389./2.*t2*u + 212*t*u2 + 68*u3 )+
. mKKfo * ( - 17./2.*t4 - 82*t3*u - 155*t2*u2 - 113*t*u3 -
. 26*u4 )+
. mKKsq * ( 23./2.*t4*u + 36*t3*u2 + 40*t2*u3 + 24*t*u4 + 4*u5 )-
. 3*t4*u2 - 3*t3*u3

```

$$\text{Msq_qg} = \text{Msq_qg}/(\text{t}-\text{mKKsq})^{**2}/(\text{u}-\text{mKKsq})^{**2} /\text{s} *1./12. *2.$$

7)

$$t = t1 + \text{mKKsq}$$

$$u = u1 + \text{m_sq}$$

c -- for spin 0 gravitons: q qb -> g* Phi

```

Msq_qqb = mgfo*mKKei * ( - 8*c11 + 8*c12 - 2*c22 )+
. mgfo*mKKsi * ( 8*t*c11 - 8*t*c12 + 2*t*c22 + 8*u*c11
. - 8*u*c12 + 2*u*c22 )+
. mgfo*mKKfo * ( - 2*t2*c11 + 2*t2*c12 - 1./2.*t2*c22 -
. 4*t*u*c11 +

```


$$\begin{aligned}
& . 4*t*u*c12 - t*u*c22 - 2*u^2*c11 + 2*u^2*c12 - 1./2.*u^2*c22)+ \\
& . mgsq*mKKte * (- 32*c11 + 12*c12)+ \\
& . mgsq*mKKei * (56*t*c11 - 20*t*c12 + 56*u*c11 - 20*u*c12)+ \\
& . mgsq*mKKsi * (- 32*t^2*c11 + 11*t^2*c12 + 1./2.*t^2*c22 - \\
& . 72*t*u*c11 + \\
& . 14*t*u*c12 + 3*t*u*c22 - 32*u^2*c11 + 11*u^2*c12 + 1./2.*u^2*c22)+ \\
& . mgsq*mKKfo *(6*t^3*c11 - 2*t^3*c12 - 1./2.*t^3*c22 + 26*t^2*u*c11+ \\
& . 2*t^2*u*c12 - 7./2.*t^2*u*c22 + 26*t*u^2*c11 + 2*t*u^2*c12 - \\
& . 7./2.*t*u^2*c22 + 6*u^3*c11 - 2*u^3*c12 - 1./2.*u^3*c22)+ \\
& . mgsq*mKKsq * (- 2*t^3*u*c11 - 2*t^3*u*c12 + 3./2.*t^3*u*c22 - \\
& . 4*t^2*u^2*c11 - 4*t^2*u^2*c12 + t^2*u^2*c22 - 2*t*u^3*c11 - \\
& . 2*t*u^3*c12 + 3./2.*t*u^3*c22)+ \\
& . mKKte/mgsq * (1./2.*t^2*c11 + 11*t*u*c11 + 1./2.*u^2*c11)+ \\
& . mKKei/mgsq * (- 1./2.*t^3*c11 - 39./2.*t^2*u*c11 - \\
& . 39./2.*t*u^2*c11 - 1./2.*u^3*c11)+ \\
& . mKKsi/mgsq * (23./2.*t^3*u*c11 + t^3*u*c12 + 21*t^2*u^2*c11 + \\
& . 2*t^2*u^2*c12 + 23./2.*t*u^3*c11 + t*u^3*c12)+ \\
& . mKKfo/mgsq * (- 2*t^4*u*c11 - t^4*u*c12 - 6*t^3*u^2*c11 - 3*t^3* \\
& . u^2*c12 - 6*t^2*u^3*c11 - 3*t^2*u^3*c12 - 2*t*u^4*c11 - t*u^4*c12)+ \\
& . mKKsq/mgsq * (2*t^4*u^2*c12 + 2*t^2*u^4*c12)+ \\
& . mKKei/mgfo * (- 1./2.*t^3*u*c11 - t^2*u^2*c11 - 1./2.*t*u^3*c11)+ \\
& . mKKsi/mgfo * (1./2.*t^4*u*c11 + 3./2.*t^3*u^2*c11 + \\
& . 3./2.*t^2*u^3*c11 + 1./2.*t*u^4*c11)+ \\
& . mKKfo/mgfo * (- t^4*u^2*c11 - t^2*u^4*c11)+ \\
& . mKKtw * (- 26*c11)+ \\
& . mKKte * (66*t*c11 + 66*u*c11)+
\end{aligned}$$

$$\begin{aligned}
& . \text{mKKei} * (- 125./2.*t^2*c_{11} - t^2*c_{12} - 125*t*u*c_{11} - \\
& . 14*t*u*c_{12} - 125./2.*u^2*c_{11} - u^2*c_{12})+ \\
& . \text{mKKsi} * (26*t^3*c_{11} + t^3*c_{12} + 86*t^2*u*c_{11} + 23*t^2*u*c_{12} + \\
& . 86*t*u^2*c_{11} + 23*t*u^2*c_{12} + 26*u^3*c_{11} + u^3*c_{12})+ \\
& . \text{mKKfo} * (- 4*t^4*c_{11} - 24*t^3*u*c_{11} - 13*t^3*u*c_{12} - \\
& . 1./2.*t^3*u*c_{22} - 40*t^2*u^2*c_{11} - 22*t^2*u^2*c_{12} - t^2*u^2*c_{22} - \\
& . 24*t*u^3*c_{11} - 13*t*u^3*c_{12} - 1./2.*t*u^3*c_{22} - 4*u^4*c_{11})+ \\
& . \text{mKKsq} * (2*t^4*u*c_{11} + 2*t^4*u*c_{12} + 1./2.*t^4*u*c_{22} + \\
& . 6*t^3*u^2*c_{11} \\
& . + 6*t^3*u^2*c_{12} + 3./2.*t^3*u^2*c_{22} + 6*t^2*u^3*c_{11} + 6*t^2*u^3*c_{12} + \\
& . 3./2.*t^2*u^3*c_{22} + 2*t*u^4*c_{11} + 2*t*u^4*c_{12} + 1./2.*t*u^4*c_{22})- \\
& . t^4*u^2*c_{22} - t^2*u^4*c_{22}
\end{aligned}$$

$$\text{Msq_qqb} = \text{msq_qqb}/(t-\text{mKKsq})^{**2}/(u-\text{mKKsq})^{**2}/s \quad *2./9. /2.$$

8)

$$t = t_1 + \text{mKKsq}$$

$$u = u_1 + \text{m_sq}$$

c -- for spin 0 gravitons: q g -> q* Phi

$$\begin{aligned}
\text{Msq_qg} &= \text{mgsi}*\text{mKKsi} * (4*c_{12} - 3*c_{22})+ \\
& . \text{mgsi}*\text{mKKfo} * (- 4*t*c_{12} + t*c_{22} - 4*u*c_{12} + 4*u*c_{22})+ \\
& . \text{mgsi}*\text{mKKsq} * (4*t*u*c_{12} - u^2*c_{22})+ \\
& . \text{mgsi} * (- t*u^2*c_{22})+ \\
& . \text{mgfo}*\text{mKKei} * (8*c_{11} - 10*c_{12} + 2*c_{22})+ \\
& . \text{mgfo}*\text{mKKsi} * (- 20*t*c_{11} + 14*t*c_{12} - 2*t*c_{22} - 4*u*c_{12} +
\end{aligned}$$

$$\begin{aligned}
& . 8*u*c22)+ \\
& . mgfo*mKKfo * (12*t2*c11 + 4*t*u*c11 + 4*t*u*c12 - t*u*c22 + \\
& . 6*u2*c12 - 11*u2*c22)+ \\
& . mgfo*mKKsq * (- 4*t2*u*c11 - 8*t2*u*c12 - t2*u*c22 - \\
& . 2*t*u2*c12 - 4*t*u2*c22 + 3*u3*c22)+ \\
& . mgfo * (3*t2*u2*c22 + 3*t*u3*c22)+ \\
& . mgsq*mKKte * (5*c11 - 4*c12)+ \\
& . mgsq*mKKei * (- 7*t*c11 + 4*t*c12)+ \\
& . mgsq*mKKsi * (8*t2*c11 + 4*t2*c12 - t2*c22 - 4*t*u*c11 +2*t*u* \\
& . c12 - 2*t*u*c22 - 5*u2*c11 + 14*u2*c12 - 8*u2*c22)+ \\
& . mgsq*mKKfo * (- 8*t3*c11 - 4*t3*c12 + t3*c22 + 8*t2*u*c11 -26* \\
& . t2*u*c12 + 2*t2*u*c22 + 3*t*u2*c11 - 2*t*u2*c22 - 6*u3*c12 + 8* \\
& . u3*c22)+ \\
& . mgsq*mKKsq * (12*t3*u*c12 + 10*t2*u2*c12 + 7*t2*u2*c22 - 6*t* \\
& . u3*c12 + 10*t*u3*c22 - 2*u4*c22)+ \\
& . mgsq * (- 3*t3*u2*c22 - 6*t2*u3*c22 - 4*t*u4*c22)+ \\
& . mKKte/mgsq * (- t2*c11 - 2*t*u*c11 - 8*u2*c11)+ \\
& . mKKei/mgsq * (t3*c11 + 6*t2*u*c11 + 14*t*u2*c11 + 8*u3*c11)+ \\
& . mKKsi/mgsq * (- 4*t3*u*c11 - 2*t3*u*c12 - 21*t2*u2*c11 -2*t2 \\
& . *u2*c12 + 2*t*u3*c11 - 16*t*u3*c12 - 2*u4*c11)+ \\
& . mKKfo/mgsq * (2*t4*u*c12 + 9*t3*u2*c11 + 4*t3*u2*c12 + 2*t2* \\
& . u3*c11 + 18*t2*u3*c12 - 4*t*u4*c11 + 16*t*u4*c12)+ \\
& . mKKsq/mgsq * (- 2*t4*u2*c12 - 6*t3*u3*c12 - 8*t2*u4*c12 - 4* \\
& . t*u5*c12)+ \\
& . mKKei/mgfo * (t3*u*c11 + t2*u2*c11 + 8*t*u3*c11)+ \\
& . mKKsi/mgfo * (- t4*u*c11 - 2*t3*u2*c11 - 9*t2*u3*c11 - 8*t*
\end{aligned}$$

```

. u4*c11 )+
. mKKfo/mgfo * ( t4*u2*c11 + 3*t3*u3*c11 + 4*t2*u4*c11 + 2*t*u5
. *c11 )+
. mKKtw * ( 2*c11 )+
. mKKte * ( - 2*t*c11 - 8*u*c11 )+
. mKKei * ( 2*t2*c12 + 7*t*u*c11 + 4*t*u*c12 - 3*u2*c11 +
. 16*u2*c12)+
. mKKsi * (-4*t3*c11 - 2*t3*c12 + 7*t2*u*c11 - 8*t2*u*c12 + 4*t*
. u2*c11 - 12*t*u2*c12 + 3*u3*c11 - 16*u3*c12 )+
. mKKfo * ( 4*t4*c11 + 4*t3*u*c11 + 4*t3*u*c12 + t3*u*c22 -13*t2*
. u2*c11 + 14*t2*u2*c12 + t2*u2*c22 + 3*t*u3*c11 - 12*t*u3*c12
. + 8*t*u3*c22 + 4*u4*c12 )+
. mKKsq * ( - 4*t4*u*c11 - t4*u*c22 - 6*t3*u2*c12 - 2*t3*u2*c22
. + 4*t2*u3*c12 - 9*t2*u3*c22 + 8*t*u4*c12 - 8*t*u4*c22 )+
. t4*u2*c22 + 3*t3*u3*c22 + 4*t2*u4*c22 + 2*t*u5*c22

```

$$\text{Msq_qg} = \text{Msq_qg}/(\text{t}-\text{mKKsq})^{**2}/(\text{u}-\text{mKKsq})^{**2} /\text{s} *1./12. *2.$$

9)

$$t = t1 + \text{mKKsq}$$

$$u = u1 + \text{m_sq}$$

c -- for spin 0 gravitons: g g -> g* Phi

```

Msq_gg = mgte * ( - 2*t*u*c22 )+
. mgei*mKKsq * ( 4*t2*c22 + 4*t*u*c12 + 14*t*u*c22 + 4*u2*c22 )+
. mgei * ( 6*t2*u*c22 + 6*t*u2*c22 )+

```

$$\begin{aligned}
& \cdot \text{mgssi} * \text{mKKfo} * (- 8*t^2*c_{12} - 16*t^2*c_{22} - 2*t*u*c_{11} - \\
& \cdot 28*t*u*c_{12} - 40*t*u*c_{22} - 8*u^2*c_{12} - 16*u^2*c_{22}) + \\
& \cdot \text{mgssi} * \text{mKKsq} * (- 12*t^3*c_{22} - 12*t^2*u*c_{12} - 48*t^2*u*c_{22} - 12*t*u^2 \\
& \cdot \quad *c_{12} - 48*t*u^2*c_{22} - 12*u^3*c_{22}) + \\
& \cdot \text{mgssi} * (- 10*t^3*u*c_{22} - 20*t^2*u^2*c_{22} - 10*t*u^3*c_{22}) + \\
& \cdot \text{mgfo} * \text{mKKsi} * (4*t^2*c_{11} + 32*t^2*c_{12} + 24*t^2*c_{22} + 14*t*u*c_{11} + \\
& \cdot 80*t*u*c_{12} + 56*t*u*c_{22} + 4*u^2*c_{11} + 32*u^2*c_{12} + 24*u^2*c_{22}) + \\
& \cdot \text{mgfo} * \text{mKKfo} * (24*t^3*c_{12} + 36*t^3*c_{22} + 6*t^2*u*c_{11} + 96*t^2*u*c_{12} \\
& \cdot \quad + 120*t^2*u*c_{22} + 6*t*u^2*c_{11} + 96*t*u^2*c_{12} + 120*t*u^2*c_{22} + \\
& \cdot 24*u^3*c_{12} + 36*u^3*c_{22}) + \\
& \cdot \text{mgfo} * \text{mKKsq} * (14*t^4*c_{22} + 20*t^3*u*c_{12} + 70*t^3*u*c_{22} + 40*t^2*u^2* \\
& \cdot c_{12} + 116*t^2*u^2*c_{22} + 20*t*u^3*c_{12} + 70*t*u^3*c_{22} + 14*u^4*c_{22}) + \\
& \cdot \text{mgfo} * (10*t^4*u*c_{22} + 30*t^3*u^2*c_{22} + 30*t^2*u^3*c_{22} + 10*t*u^4* \\
& \cdot \quad c_{22}) + \\
& \cdot \text{mgsq} * \text{mKKei} * (- 16*t^2*c_{11} - 48*t^2*c_{12} - 16*t^2*c_{22} - 40*t*u*c_{11} \\
& \cdot - 112*t*u*c_{12} - 38*t*u*c_{22} - 16*u^2*c_{11} - 48*u^2*c_{12} - 16*u^2*c_{22}) + \\
& \cdot \text{mgsq} * \text{mKKsi} * (- 12*t^3*c_{11} - 72*t^3*c_{12} - 36*t^3*c_{22} - 48*t^2*u*c_{11} \\
& \cdot - 240*t^2*u*c_{12} - 120*t^2*u*c_{22} - 48*t*u^2*c_{11} - 240*t*u^2*c_{12} - 120 \\
& \cdot \quad *t*u^2*c_{22} - 12*u^3*c_{11} - 72*u^3*c_{12} - 36*u^3*c_{22}) + \\
& \cdot \text{mgsq} * \text{mKKfo} * (- 28*t^4*c_{12} - 28*t^4*c_{22} - 10*t^3*u*c_{11} - 140*t^3*u* \\
& \cdot c_{12} - 122*t^3*u*c_{22} - 20*t^2*u^2*c_{11} - 232*t^2*u^2*c_{12} - 196*t^2*u^2* \\
& \cdot c_{22} - 10*t*u^3*c_{11} - 140*t*u^3*c_{12} - 122*t*u^3*c_{22} - 28*u^4*c_{12} - 28* \\
& \cdot \quad u^4*c_{22}) + \\
& \cdot \text{mgsq} * \text{mKKsq} * (- 8*t^5*c_{22} - 20*t^4*u*c_{12} - 48*t^4*u*c_{22} - 60*t^3* \\
& \cdot u^2*c_{12} - 112*t^3*u^2*c_{22} - 60*t^2*u^3*c_{12} - 112*t^2*u^3*c_{22} - 20*t* \\
& \cdot \quad u^4*c_{12} - 48*t*u^4*c_{22} - 8*u^5*c_{22}) +
\end{aligned}$$

$$\begin{aligned}
& \cdot \text{mgsq} * (- 6*t^5*u*c22 - 20*t^4*u^2*c22 - 30*t^3*u^3*c22 - 20*t^2* \\
& \cdot \quad u^4*c22 - 6*t*u^5*c22)+ \\
& \cdot \text{mKKtw/mgsq} * (- 16*t^2*c11 - 8*t^2*c12 - 38*t*u*c11 - 20*t*u*c12 \\
& \cdot \quad - 16*u^2*c11 - 8*u^2*c12)+ \\
& \cdot \text{mKKte/mgsq} * (- 36*t^3*c11 - 24*t^3*c12 - 120*t^2*u*c11 - 84*t^2* \\
& \cdot \quad u*c12 - 120*t*u^2*c11 - 84*t*u^2*c12 - 36*u^3*c11 - 24*u^3*c12)+ \\
& \cdot \text{mKKei/mgsq} * (- 28*t^4*c11 - 28*t^4*c12 - 122*t^3*u*c11 - 124*t^3* \\
& \cdot \quad u*c12 - 196*t^2*u^2*c11 - 200*t^2*u^2*c12 - 122*t*u^3*c11 - 124*t*u^3 \\
& \cdot \quad *c12 - 28*u^4*c11 - 28*u^4*c12)+ \\
& \cdot \text{mKKsi/mgsq} * (- 8*t^5*c11 - 16*t^5*c12 - 48*t^4*u*c11 - 84*t^4*u* \\
& \cdot \quad c12 - 112*t^3*u^2*c11 - 188*t^3*u^2*c12 - 112*t^2*u^3*c11 - 188*t^2* \\
& \cdot \quad u^3*c12 - 48*t*u^4*c11 - 84*t*u^4*c12 - 8*u^5*c11 - 16*u^5*c12)+ \\
& \cdot \text{mKKfo/mgsq} * (- 4*t^6*c12 - 6*t^5*u*c11 - 28*t^5*u*c12 - 20*t^4* \\
& \cdot \quad u^2*c11 - 76*t^4*u^2*c12 - 30*t^3*u^3*c11 - 108*t^3*u^3*c12 - 20*t^2* \\
& \cdot \quad u^4*c11 - 76*t^2*u^4*c12 - 6*t*u^5*c11 - 28*t*u^5*c12 - 4*u^6*c12)+ \\
& \cdot \text{mKKsq/mgsq} * (- 4*t^6*u*c12 - 12*t^5*u^2*c12 - 20*t^4*u^3*c12 - 20 \\
& \cdot \quad *t^3*u^4*c12 - 12*t^2*u^5*c12 - 4*t*u^6*c12)+ \\
& \cdot \text{mKKft/mgfo} * (4*t^2*c11 + 10*t*u*c11 + 4*u^2*c11)+ \\
& \cdot \text{mKKtw/mgfo} * (12*t^3*c11 + 42*t^2*u*c11 + 42*t*u^2*c11 + 12*u^3* \\
& \cdot \quad c11)+ \\
& \cdot \text{mKKte/mgfo} * (14*t^4*c11 + 62*t^3*u*c11 + 100*t^2*u^2*c11 + 62*t* \\
& \cdot \quad u^3*c11 + 14*u^4*c11)+ \\
& \cdot \text{mKKei/mgfo} * (8*t^5*c11 + 42*t^4*u*c11 + 94*t^3*u^2*c11 + 94*t^2* \\
& \cdot \quad u^3*c11 + 42*t*u^4*c11 + 8*u^5*c11)+ \\
& \cdot \text{mKKsi/mgfo} * (2*t^6*c11 + 14*t^5*u*c11 + 38*t^4*u^2*c11 + 54*t^3* \\
& \cdot \quad u^3*c11 + 38*t^2*u^4*c11 + 14*t*u^5*c11 + 2*u^6*c11)+
\end{aligned}$$

$$\begin{aligned}
& \cdot \text{mKKfo/mgfo} * (2*t^6*u*c_{11} + 6*t^5*u^2*c_{11} + 10*t^4*u^3*c_{11} + 10*t^3 \\
& \cdot \quad *u^4*c_{11} + 6*t^2*u^5*c_{11} + 2*t*u^6*c_{11})+ \\
& \cdot \text{mKKte} * (24*t^2*c_{11} + 32*t^2*c_{12} + 4*t^2*c_{22} + 56*t*u*c_{11} + \\
& \cdot \quad 76*t*u* \\
& \cdot \quad c_{12} + 10*t*u*c_{22} + 24*u^2*c_{11} + 32*u^2*c_{12} + 4*u^2*c_{22})+ \\
& \cdot \text{mKKei} * (36*t^3*c_{11} + 72*t^3*c_{12} + 12*t^3*c_{22} + 120*t^2*u*c_{11} + \\
& \cdot \quad 240* \\
& \cdot \quad t^2*u*c_{12} + 42*t^2*u*c_{22} + 120*t*u^2*c_{11} + 240*t*u^2*c_{12} + 42*t*u^2* \\
& \cdot \quad c_{22} + 36*u^3*c_{11} + 72*u^3*c_{12} + 12*u^3*c_{22})+ \\
& \cdot \text{mKKsi} * (14*t^4*c_{11} + 56*t^4*c_{12} + 14*t^4*c_{22} + 70*t^3*u*c_{11} + 244* \\
& \cdot \quad t^3*u*c_{12} + 62*t^3*u*c_{22} + 116*t^2*u^2*c_{11} + 392*t^2*u^2*c_{12} + 100* \\
& \cdot \quad t^2*u^2*c_{22} + 70*t*u^3*c_{11} + 244*t*u^3*c_{12} + 62*t*u^3*c_{22} + 14*u^4* \\
& \cdot \quad c_{11} + 56*u^4*c_{12} + 14*u^4*c_{22})+ \\
& \cdot \text{mKKfo} * (16*t^5*c_{12} + 8*t^5*c_{22} + 10*t^4*u*c_{11} + 96*t^4*u*c_{12} + \\
& \cdot \quad 42* \\
& \cdot \quad t^4*u*c_{22} + 30*t^3*u^2*c_{11} + 224*t^3*u^2*c_{12} + 94*t^3*u^2*c_{22} + 30* \\
& \cdot \quad t^2*u^3*c_{11} + 224*t^2*u^3*c_{12} + 94*t^2*u^3*c_{22} + 10*t*u^4*c_{11} + 96*t* \\
& \cdot \quad u^4*c_{12} + 42*t*u^4*c_{22} + 16*u^5*c_{12} + 8*u^5*c_{22})+ \\
& \cdot \text{mKKsq} * (2*t^6*c_{22} + 12*t^5*u*c_{12} + 14*t^5*u*c_{22} + 40*t^4*u^2*c_{12}+ \\
& \cdot \quad 38*t^4*u^2*c_{22} + 60*t^3*u^3*c_{12} + 54*t^3*u^3*c_{22} + 40*t^2*u^4*c_{12} + \\
& \cdot \quad 38*t^2*u^4*c_{22} + 12*t*u^5*c_{12} + 14*t*u^5*c_{22} + 2*u^6*c_{22})+ \\
& \cdot \quad 2*t^6*u*c_{22} + 6*t^5*u^2*c_{22} + 10*t^4*u^3*c_{22} + 10*t^3*u^4*c_{22} + 6*t^2 \\
& \cdot \quad *u^5*c_{22} + 2*t*u^6*c_{22}
\end{aligned}$$

$$\text{Msq_gg} = -\text{Msq_gg}/t^2/u^2/s^2 *3./16.$$

VITA

Corneliu Marius Rujoiu

Candidate for the Degree of

Doctor of Philosophy

Thesis: PHENOMENOLOGY OF EXTRA DIMENSIONS

Major Field: Physics

Date Of Birth: September 4, 1973

Education and Scientific Degrees

Ph.D. (July 2006)	Physics Oklahoma State University Stillwater, USA
M.Sc. (1998)	Physics Bucharest University, Bucharest, Romania
B.Sc. (1997)	Physics Bucharest University, Bucharest, Romania

Scholarships

- "Broken Symmetries ", March 1998, Schladming, Austria
- Summer school in particle physics, June 1999, Trieste, Italy
- "TASI 2006", June 2006, Boulder, Colorado, USA

Name: Corneliu M. Rujoiu

Date of Degree: July, 2006

Institution: Oklahoma State University

Location: Stillwater, Oklahoma

Title of Study: PHENOMENOLOGY OF EXTRA DIMENSIONS

Pages in Study: 85

Candidate for the Degree of Doctor of Philosophy

Major Field: Physics

Scope and Method of Study: In this thesis, we propose three different methods to look for the existence of extra dimensions as predicted by the Universal Extra Dimensions (UED) with fat brane scenario. After a brief introduction, in the second chapter we give background on the Standard Model (SM) of particles and on the relevant theory describing the extra dimensions. Chapters three and four detail our proposed methods. Last chapter is reserved for conclusions.

Findings and Conclusions: The existence of extra dimensions is a very exciting idea not excluded by the present experimental results. We show that the future experiments at Large Hadron Collider have the potential to discover signature of extra dimensions in events involving production of jets plus missing energy. While the production of two jets plus missing energy gives an optimistic signal, the monojet plus missing energy channel can lead to the discovery of extra dimensions only when corroborated with a corresponding signal in the single photon plus missing energy channel. When taken into account, the idea of extra dimensions can also produce small, almost degenerate neutrino masses and naturally large mixing angles among them, with a bonus relation between the masses of the neutrinos and the charged leptons.

ADVISOR'S APPROVAL:
